U.S. DEPARTMENT OF COMMERCE
National Technical Information Service
PB-274 485

High Temperature Particulate Control with Ceramic Filters

Westinghouse Research Labs, Pittsburgh, Pa

Prepared for

Industrial Environmental Research Lab, Research Triangle Park, N C

Oct 77

TECHNICAL REPORT DATA

(Please read Instructions on the reverse before completing)

1. REPORT NO.
EPA-600/2-77-207

2\.

3. RECIPIENT'S ACCESSION NO.
PB274485

4. TITLE AND SUBTITLE
High Temperature Particulate Control with Ceramic Filters

5. REPORT DATE
October 1977

6. PERFORMING ORGANIZATION CODE

7. AUTHOR(S)
D. F. Ciliberti

8. PERFORMING ORGANIZATION REPORT NO.

9. PERFORMING ORGANIZATION NAME AND ADDRESS
Westinghouse Research Laboratory
Pittsburgh, Pennsylvania 15235

10. PROGRAM ELEMENT NO.
1AB012; ROAP 21ADL-029

11. CONTRACT/GRANT NO.
68-02-1887

12. SPONSORING AGENCY NAME AND ADDRESS
Industrial Environmental Research Laboratory
Office of Research and Development
U.S. Environmental Protection Agency
Research Triangle, Park, NC 27711

13. TYPE OF REPORT AND PERIOD COVERED
Final; 7/75-8/77

14. SPONSORING AGENCY CODE
EPA/600/13

15. SUPPLEMENTARY NOTES IERL-RTP project officer for this report is Dennis C. Drehmel, Mail Drop 61, 919/541-2925.

16. ABSTRACT The report gives results of an assessment of using ceramic materials as filters for fine particulate removal at high temperatures. The program was in two phases. Phase I, directed toward the development of a porous alumina membrane filter, had limited success because of the fragility of the membranes formed, and the difficulty in controlling the pore size distribution of the filters. The major objective of Phase II, concentrating on screening other available materials, was to identify materials with good filtration potential, select one or two of the most promising, and (as rapidly as possible) demonstrate them as hot gas fine particle filters in a several hundred cu m/hr hot test. Initial screening indicated that the most promising was a thin-walled, ceramic, cross-flow monolith, originally produced as a catalyst support for automotive exhaust systems. Screening tests indicated the possibility of virtually 100% removal of even submicron limestone test dust at face velocities and pressure drops not dissimilar from those typical of fabric filtration. Later bench scale tests at around 1000 K confirmed the material's ability to perform well at high temperatures. Final testing, at a larger facility where flows of 4.8 cu m/min at 950 K were achieved, indicated that this ceramic configuration offers great potential as a hot gas filter.

17. KEY WORDS AND DOCUMENT ANALYSIS

a. DESCRIPTORS		b. IDENTIFIERS/OPEN ENDED TERMS	c. COSATI Field/Group	
Air Pollution	Thermal Resistance	Air Pollution Control	13B	20M
Dust	Aluminum Oxide	Stationary Sources	11G	07B
Ceramics		Particulate	11B	
Filtration		Hot Gases	07D	
Dust Filters			13K	
High Temperature Tests			14B	

18. DISTRIBUTION STATEMENT
Unlimited

19. SECURITY CLASS (This Report)
Unclassified

20. SECURITY CLASS (This page)
Unclassified

21. NO. OF PAGES
174

22. PRICE
PC A08 | MF A01

EPA Form 2220-1 (9-73)

PB 274 485

EPA-600/2-77-207
October 1977

Environmental Protection Technology Series

HIGH [illegible]
CONTROL [illegible]

[illegible]
[illegible]
[illegible]
Research Triangle Park, North Carolina 27711

REPRODUCED BY
NATIONAL TECHNICAL
INFORMATION SERVICE
U. S. DEPARTMENT OF COMMERCE
SPRINGFIELD, VA. 22161

RESEARCH REPORTING SERIES

Research reports of the Office of Research and Development, U.S. Environmental Protection Agency, have been grouped into nine series. These nine broad categories were established to facilitate further development and application of environmental technology. Elimination of traditional grouping was consciously planned to foster technology transfer and a maximum interface in related fields. The nine series are:

1. Environmental Health Effects Research
2. Environmental Protection Technology
3. Ecological Research
4. Environmental Monitoring
5. Socioeconomic Environmental Studies
6. Scientific and Technical Assessment Reports (STAR)
7. Interagency Energy-Environment Research and Development
8. "Special" Reports
9. Miscellaneous Reports

This report has been assigned to the ENVIRONMENTAL PROTECTION TECHNOLOGY series. This series describes research performed to develop and demonstrate instrumentation, equipment, and methodology to repair or prevent environmental degradation from point and non-point sources of pollution. This work provides the new or improved technology required for the control and treatment of pollution sources to meet environmental quality standards.

REVIEW NOTICE

This report has been reviewed by the participating Federal Agencies, and approved for publication. Approval does not signify that the contents necessarily reflect the views and policies of the Government, nor does mention of trade names or commercial products constitute endorsement or recommendation for use.

This document is available to the public through the National Technical Information Service, Springfield, Virginia 22161.

EPA-600/2-77-207
October 1977

HIGH TEMPERATURE PARTICULATE CONTROL WITH CERAMIC FILTERS

by

D.F. Ciliberti

Westinghouse Research Laboratory
Pittsburgh, Pennsylvania 15235

Contract No. 68-02-1887
ROAP No. 21ADL-029
Program Element No. 1AB012

EPA Project Officer: Dennis C. Drehmel

Industrial Environmental Research Laboratory
Office of Energy, Minerals, and Industry
Research Triangle Park, N.C. 27711

Prepared for

U.S. ENVIRONMENTAL PROTECTION AGENCY
Office of Research and Development
Washington, D.C. 20460

DISCLAIMER

This report has been reviewed by the Office of Research and Development, U. S. Environmental Protection Agency, and approved for publication. Mention of trade names or commercial products does not constitute endorement or recommendation for use.

CONTENTS

Page

Abstract iv

Figures vi

Tables ix

1. Introduction 1
2. Conclusions 3
3. Recommendations 5
4. Discussion 6

Phase I

4.1 Theoretical Assessment 7
4.2 Materials Fabrication and Testing 32

Phase II

4.3 Procurement of Materials 57
4.4 Screening Tests 63
4.5 Low Flow High Temperature Tests 91
4.6 High Flow High Temperature Tests 118
4.7 Conceptual Design and Cost Comparison 153

ABSTRACT

This research project was intended to assess the possibility of using ceramic materials as filters for fine particulate removal in high temperature applications. The program has evolved into a two phase effort with the first phase effort directed toward the development of a porous alumina membrane filter. This effort was limited in success due to the fragile nature of the membranes formed and because it proved to be difficult to control the pore size distribution of the filters.

Phase II abandoned the concept of developing an entirely new filter media and concentrated on screening available materials. The major objective of this second phase was to identify materials with the good filtration potential, select one or two of the most promising candidates, and as rapidly as possible demonstrate them as hot gas fine particle filters on a several hundred m^3/hr hot test.

The initial screening of materials revealed that the most promising candidate was a thin walled ceramic, cross flow monolith, which was originally produced as a catylist support for automotive exhaust systems. Screening tests indicated that it was possible to achieve virtually 100% removal of even submicron limestone test dust at face velocities and pressure drops not dissimilar from those typical of fabric filtration. Subsequent bench scale tests at temperatures around 1000°K confirmed the ability of the material to perform well at elevated temperatures. The final stages of experimentation were conducted in a larger facility where flows of 4.8 m^3/min at 950°K were achieved. Although time limitations did not allow optimization of the system, these larger scale tests indicate that this configuration of ceramic filter offers great potential as a hot gas filter.

An economic assessment of this filter system was carried out by costing out a conceptual design for a commercial scale unit and comparing costs with a comparable granular bed filter. This calculation indicated that the ceramic filter system could have a capital cost approximately one-third that of a granular bed system.

This report was submitted in partial fulfilment of contract number 68-02-1887 to the Westinghouse Research Laboratories under the sponsorship of the Environmental Protection Agency. The work covers the period from July 1975 to August 1977.

LIST OF FIGURES

Number Page

1 Process Steps in Production of Ceramic Filters 9

2 Ceramic Filter Production Facility 11

3 Filter Plant Layout. 20

4 Westinghouse-ERDA Gasification Plant 27

5 Porous Aluminum Oxide Geometry. (Showing the oxide thickness or channel length ℓ, pore diameter d, barrier layer thickness b, and cell size, c) 33

6 High Voltage Anodizing Cell 34

7 Edge View Showing Channels of Sample W-66 at 1250X (1 cm=8 microns). This sample section is 65 microns thick. 50

8 Sample W-61A. Barrier Layer Side of Oxide Formed at 800 V. Cell size ∿ 1.3 μ; Pore Diameter 0.84 μ (5200X) . 51

9 Structural Shapes for 3M ThermaComb 61

10 3M Crossflow Ceramic Monolith 62

11 Size Distribution of Test Dust 64

12 Element Low Temperature Holder 66

13 3M Element and Holder Mounted Inside Pipe 67

14 Face Velocity Vs. Pressure Drop for Thick Walled Filters . 68

15 ΔP Vs. U for Zircar 135C Material 70

16 Flow Vs. Pressure Drop for 3M ThermaComb 71

17 Pressure Drop Vs. Flow for Clean 15.25 cm ThermaComb Cube. 72

18 ΔP Vs. Time for Selas-XFF. 73

19 ΔP Vs. Time for Selas-01 74

20 ΔP Vs. Time for Selas-10 75

21 ΔP Vs. Time for FMI Material 77

22 ΔP Vs. Time for Zircar Alumina Board (ZAL-15) 78

23 ΔP Vs. Flow for Zircar Alumina Board (ZAL-15) 79

24 ΔP Vs. Time for Zircar 135C Material 80

25 Pressure Drop Vs. Time for ThermaComb 83

List of Figures

Number Page

26 Pressure Drop Vs. Time for ThermaComb 84
27 Determination of Filter Cake Constant 86
28 Before and After 103 kPa Pulse. 87
29 Before and After 17 m^3/hr Flush for 2 Sec. 88
30 Pulsed Purge=137.9 kPa 3.0 Seconds Duration 90
31 Hot ThermaComb Test Jig 92
32 Flow Schematic and Cleaning Sequence for Low Flow-High Temperature System. 93
33 High Temperature Ceramic Test Facility 96
34 High Temperature Ceramic Filter Assembly 97
35 Pressure Drop Vs. Time at (1090°K) 99
36 Hot ThermaComb Test 101
37 Ambient Temperature Test (ThermaComb) 102
38 Hot ThermaComb Test 104
39 Hot ThermaComb Test 105
40 ThermaComb Filter Test-Constant Flow 107
41 ThermaComb Filter Test-Constant Flow 108
42 ThermaComb Filter Test-Constant Flow 109
43 Hot ThermaComb Test (High Dust Loading) 111
44 Hot ThermaComb Test Variation of Filter Pulse Purge 112
45 Hot ThermaComb Test Variation of Pulsed Purge 113
46 Hot ThermaComb Test Variation of Pulsed Purge 114
47 ThermaComb Filter Test-Pulse Times 115
48 Hot-Low Flow Test of W. R. Grace & Co. Ceramic Filter . . . 116
49 High Flow Test Facility 119
50 6 Inch ThermaComb Test Assembly 121
51 Schematic of Pulsing Modification 122
52 High Temperature High Flow Test Facility 124
53 High Temperature Ceramic Test Facility 125
54 Detail of Ceramic Filter Assembly 126
55 High Flow Test Starting with Clean Filters 129

List of Figures

Number Page

56 Pulse Intensity Tests 130

57 Pulse Intensity Tests 131

58 Filters and Vessel Precleaned 133

59 Initial Tests with ThermaComb Cut in Half 135

60 Manual Dirty Side Pulse Test 136

61 Hot Test with Initial Dirty Side Pulse 138

62 Hot Test with Initial Dirty Side Pulsed Continued 139

63 Hot High Flow Test After Individual Dirty and Clean Pulses. 140

64 Cold Test with Modified Pulse 141

65 Hot Test with Modified Pulse 142

66 Hot ThermaComb Test with Cleaning Pulse to Clean and Dirty Sides 143

67 Hot ThermaComb Test with Cleaning Pulse to Clean and Dirty Sides 145

68 Hot ThermaComb Test with Combined Pulse 146

69 Hot ThermaComb Test with Pulse Variations 147

70 Hot ThermaComb Test with Pulse Variation 148

71 Final Hot Test with ThermaComb 150

72 Initial Hot Test with 15cm Cube of W. R. Grace Material . . 151

73 Hot Test with 15cm Cube of W. R. Grace Material 152

74 Sketch of Possible Arrangement of Commercial Use of Ceramic Filters 155

LIST OF TABLES

Number		Page
1	Capital Costs for Ceramic Filter Production Facility	12
2	Materials and Power Per M^2 of Oxide Filter	13
3	Operating Costs in Thousands of Dollars for Producing 2000 M^2/Year of Cylindrical Oxide Membranes 2.5 cm x 100 cm	15
4	Labor Force for Ceramic Filter Production	16
5	Production Costs - Ceramic Membrane Filters	17
6	Filter Element Costs	19
7	Cost Data for Ceramic Membrane Filter Plant	22
8	Capital Charges	23
9	Costs for Granular Bed Filter - Bag Filter Plant	25
10	Coal Gasification-Combined Cycle Plant Costs $/kW, 250 MW Plant	28
11	Capital Costs for 635 MW Coal Fired Steam Plant	30
12	Annual Costs for Power Plants Per kW of Capacity	31
13	Average Cell Size and (pore diameter) in A/V for Various Fabrication Conditions	36
14	Pressure Pore Enlargement	39
15	Summary of Pressurized Etched Oxide Samples	41
16	Pressure Etched Samples	45
17	Pressure Etched Samples, Barrier Layer Up	47
18	Mechanical Testing Results	53
19	Survey Results	58
20	Ceramic Filter and Granular Bed Filter Costs	160

SECTION 1

INTRODUCTION

During the next two decades, the use of coal for the generation of electrical energy in the United States will triple. New coal-fired power plants will be built whose total capacity will almost equal that of plants currently installed. There is a real need for a lower cost, higher efficiency, less polluting means of generating power from coal. Gasification coupled with combined gas and steam turbine generation is one promising technique. But if coal gasification with combined cycle generation is to be completely successful, a system of cleaning and burning hot fuel gases is needed to meet emission standards on particulates, and to protect high temperature turbine blading.

Another promising coal conversion technology that is currently under investigation is that of pressurized fluidized bed combustion. This process has particle removal requirements that are essentially the same as those required by the gasification scheme with the exception that the gas to be cleaned is a flue gas rather than a reducing fuel gas. This may allow a wider choice of materials of construction since it is anticipated that flue gas will be less corrosive to standard materials.

Current experimentation with inertial collectors indicates that they will not give adequate cleaning to meet either environmental or turbine requirements on a mass loading or size distribution basis. Consequently it appears that some novel, final stage of positive filtration will be required.

Two methods of filtering hot corrosive gases that have received attention recently are granular bed filtration and ceramic filters. There are several schemes for granular bed filtration which exist in varying degrees of commercialization. The work carried out here was intended to advance ceramic filtration technology to the stage where some reasonable comparisons of performance and economics could be made between the systems.

This study has identified some promising ceramic filter media, and both the economic and performance comparisons with granular bed filtration look promising.

SECTION 2

CONCLUSIONS

This experimental work has been carried out in two phases, the first investigating the development and use of membrane type ceramic filters and the second phase focusing on screening and testing available porous ceramic materials as hot gas filters.

Some conclusions that can be drawn from the Phase I effort are listed below:

- The economics of ceramic membration filtration appear to be favorable when compared with other hot gas filtration concepts.
- The delicate nature of the ceramic membrane filters makes commercial use of them unlikely in large electric power generating applications.
- No suitable means for supporting the membranes was discovered although this does not seem to be an insoluble problem.
- The most troublesome technical problem was the lack of control of pore size and size distribution resulting from the electrolytic pore forming process.

Phase II examined several commercially available types of ceramic materials which can be broadly grouped into two categories: porous thick walled filters and thin walled monolithic honeycomb structures.

Some conclusions drawn from this work apply to both categories of materials:

- Filters of this nature are suitable for operation at temperatures exceeding any current coal conversion process requirements.
- The filters exhibit good resistance to corrosion with the possible exception of alkali metal attack.

- The materials withstand thermal cycling well.
- The filters generally exhibit virtually 100% effective particle removal of a submicron test dust.
- Cleaning methods can be devised to allow continuous operation.

Conclusions with regard to the thick walled filters tested are as follows:

- These filters generally had a relatively high resistance to flow.
- They were relatively difficult to clean, although most of them could be cleaned by vigorous back washing.
- The physical embodiment of these filters generally did not lend itself to easy, efficient incorporation into a viable commercial unit.

Conclusions reached concerning the thin walled monolithic structures are as follows:

- Effective cleaning for continuous can be achieved relatively easily with back washing pulses.
- The filters have relatively low pressure drops at moderate face velocities.
- The filters have very high surface area to volume ratios which makes efficient use of pressure vessel containments.
- The preliminary economic analysis of a commercial module of using this type of ceramic filter indicates capital costs could be as low as one-third those of a similar granular bed system.
- A system based on the use of this type of filter material appears to be as viable as a hot gas cleaning system.

SECTION 3

RECOMMENDATIONS

The work conducted under Phase I of this effort was successful to only a limited extent. Since the probability of developing a commercially viable system based on the electrolytic oxidation of alumina membrane filters is remote, it is recommended that no further work be carried out in this direction.

The effort in Phase II of this project has in large part been successful in that it has been possible to demonstrate continuous high temperature filtration of fine particulates on a fairly large scale. These encouraging results have been obtained using filter materials that have not been designed specifically for use as filters, and in spite of the fact that the high flow facility was not originally designed to accommodate these materials. The following suggestions can therefore be strongly recommended.

- An effort should be made to explore filter fabrication options in an attempt to optimize parameters such as porosity, pore size, cell size, wall thickness, etc.
- This effort should be conducted in parallel with a bench scale hot filtration test facility so that the effects on filter performance can be quickly measured and correlated.
- A third effort should focus on the design problems associated with the incorporation of this type of filter into a viable piece of equipment. This effort should have as its goal the design and fabrication of a pilot unit capable of operation at 1000°C and at 10 atm with flows in the range of 750-1000 m^3/hr.

SECTION 4

DISCUSSION

SUMMARY - PHASE I

In the initial phase of this program we have attempted to develop and test ceramic filter elements suitable for high temperature high pressure use. The work has concentrated specifically on alumina membranes fabricated by Horizons, Inc. using their electrolytic oxidation technology.

Success has been limited. Two problems have proven unsurmountable within the time frame available for this development effort. The fragile nature of the membranes has made handling and testing of the material difficult. No commercially viable support techniques could be devised. Additionally, wide variations in pore size from specimen to specimen were not brought under control. Consequently it was not possible to reliably reproduce filter elements with the required pressure drop/flow rate/filtration characteristics.

4.1 THEORETICAL ASSESSMENT

Objective. The objective was to establish the technical and economic feasibility of using a porous ceramic membrane for fine particle control in advanced power systems.

Collection Efficiency. Techniques for predicting collection efficiency of ceramic filters by impaction and interception mechanisms have been considered. In general, these techniques may only be applied to simplified models of the flow through a clean filter, and do not account for the effect of deposited particulate. An examination of the literature failed to furnish any satisfactory technique for predicting the efficiency of filtration on an established filter cake.

Experimental information on devices with similar operating characteristics to the proposed ceramic membrane showed essentially complete particle retention for particle sizes down to 0.1 μm diameter.

A simplified method of calculating Brownian deposition was used to predict the extent to which particles entering the filter pores would be collected on the pore walls. This showed deposition to be complete when

$$\sqrt{\frac{8Dt}{\pi}} \geq \frac{d-dp}{2}$$

where

D is Brownian diffusivity
t is residence time of flow through the pore
d is pore diameter
dp is particle diameter

For a ceramic filter element which would have 1 μm pores and a thickness of 250 μm, complete collection is predicted at all gas velocities up to 30 cm/sec.

Based on these considerations, a porous ceramic membrane filter should be capable of achieving 90% collection of the submicron particles produced in advanced power systems.

Assessment of Filter Costs. We have assessed filter fabrication costs, and filter operating costs as a function of filter characteristics such as thickness, pore size, free cross-section and operating pressure loss. The results indicate that the porous ceramic filter can be competitive with alternate fine particle control systems on a cost-effectiveness basis.

Production of Filter Elements. Filter element production requires four major processing steps.

- Electrolysis of aluminum to form porous alumina
- Stripping of the formed alumina from the base metal
- Chemical processing to remove barrier layers and to etch pores
- Firing to convert the alumina to the stable α form

In addition several service functions are required. A flow sheet of the steps involved in the commercial production of ceramic membrane filters is shown in Figure 1.

Aluminum stock is mechanically formed as required (cut to size, swaged, etc.) and assembled into racks for electrolysis. The racks pass to the electrolysis cells where the oxide is formed. From the cells, the assemblies are sent, after washing, to an aluminum stripping bath. Here the elements are immersed in a bromine-methanol solution which strips the oxide from the metal.

Individual elements are removed, washed and immersed in an etch solution which removes barrier layers and enlarges pore diameters. The elements are then dried, fired to convert the alumina to the α form, inspected and packed for dispatch.

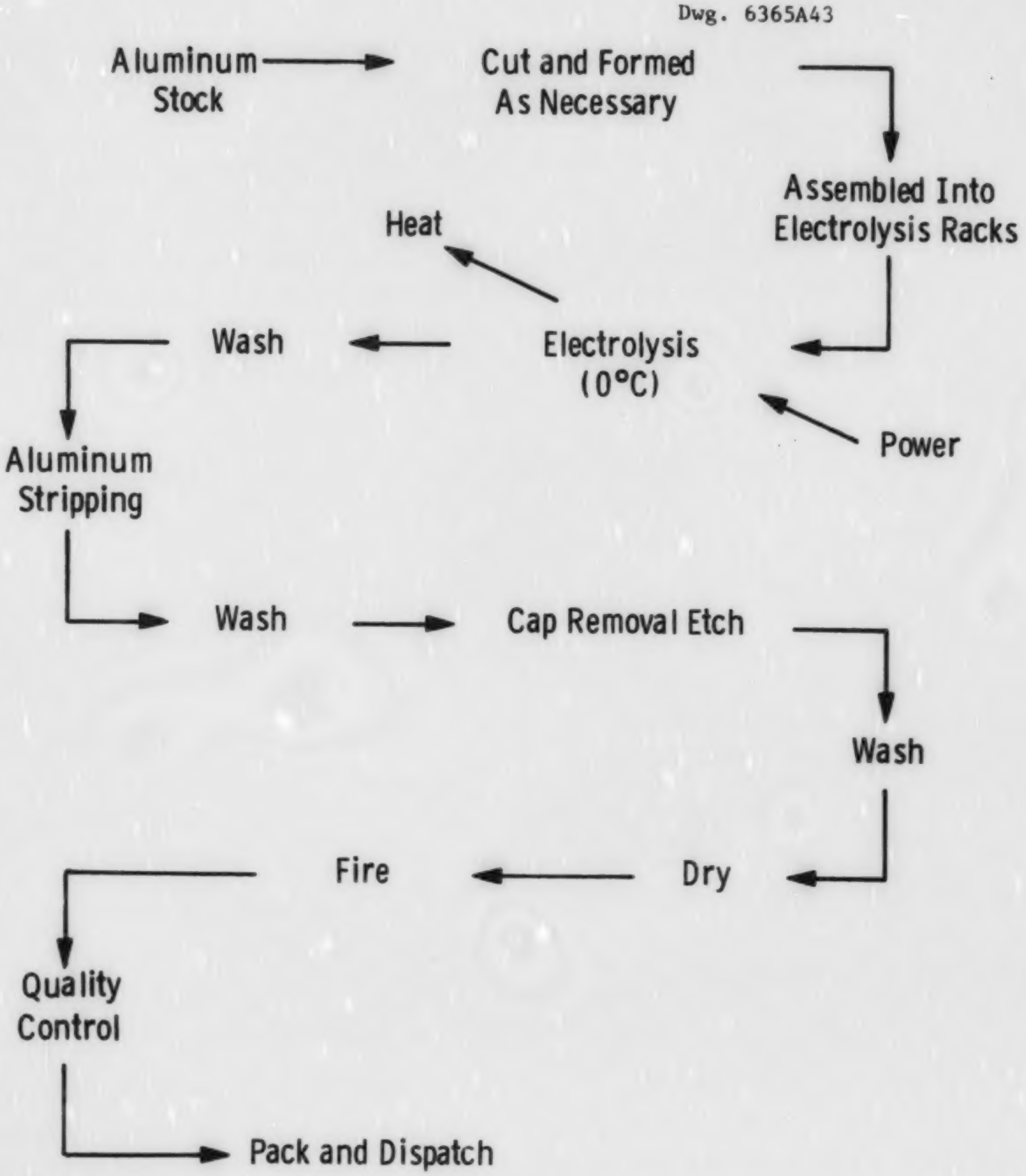
Dwg. 6365A43
Aluminum Stock
Cut and Formed As Necessary
Assembled Into Electrolysis Racks
Heat
Electrolysis (0°C)
Power
Wash
Aluminum Stripping
Wash
Cap Removal Etch
Wash
Dry
Fire
Quality Control
Pack and Dispatch

Fig. 1 — Process steps in production of ceramic filters

Capital Equipment. An estimate of capital equipment requirements and capital equipment costs has been made for a production facility with the capacity to produce 1 M^2/hr of filter surface. This plant would have a nominal capacity of 2000 M^2 per year when operating on a one shift basis, or 8000 M^2 per year when operating on a continuous (4 shift) basis.

For the purposes of this exercise, a base case has been assumed for filter characteristics so that equipment sizes can be estimated. The assumptions are that the filter elements have a thickness of 250 μm, and a pore size of 1 μm. Estimates for filters with differing characteristics have been obtained by applying factors to the base case.

A plant layout showing the major items of capital equipment is shown in Figure 2; while Table 1 lists the costs of the individual items and of the completed facility.

Operating Costs, Annual Costs

Raw Materials. Raw materials costs for the fabrication of ceramic membrane filter elements have been estimated by Horizons, Inc. Their estimates indicate a materials cost of approximately $17.50 per M^2 (Tables 2 and 3).

Power. Power for electrolysis and auxiliary use has been costed at the rate of 3¢ per kW hr.

Labor. Labor estimates provided by Horizons have been used as a basis for establishing a minimum labor force for a production facility (Table 4).

Capital Charges. Capital costs are estimated at 25% P.A.

Combining these cost estimates for the two production rates previously cited (2000 M^2 P.A. and 8000 M^2 P.A.) establishes a cost range for ceramic membrane filters of $150 per M^2 to $250 per M^2 (Table 5). The major costs are power, labor and capital charges.

Dwg. 6365A42

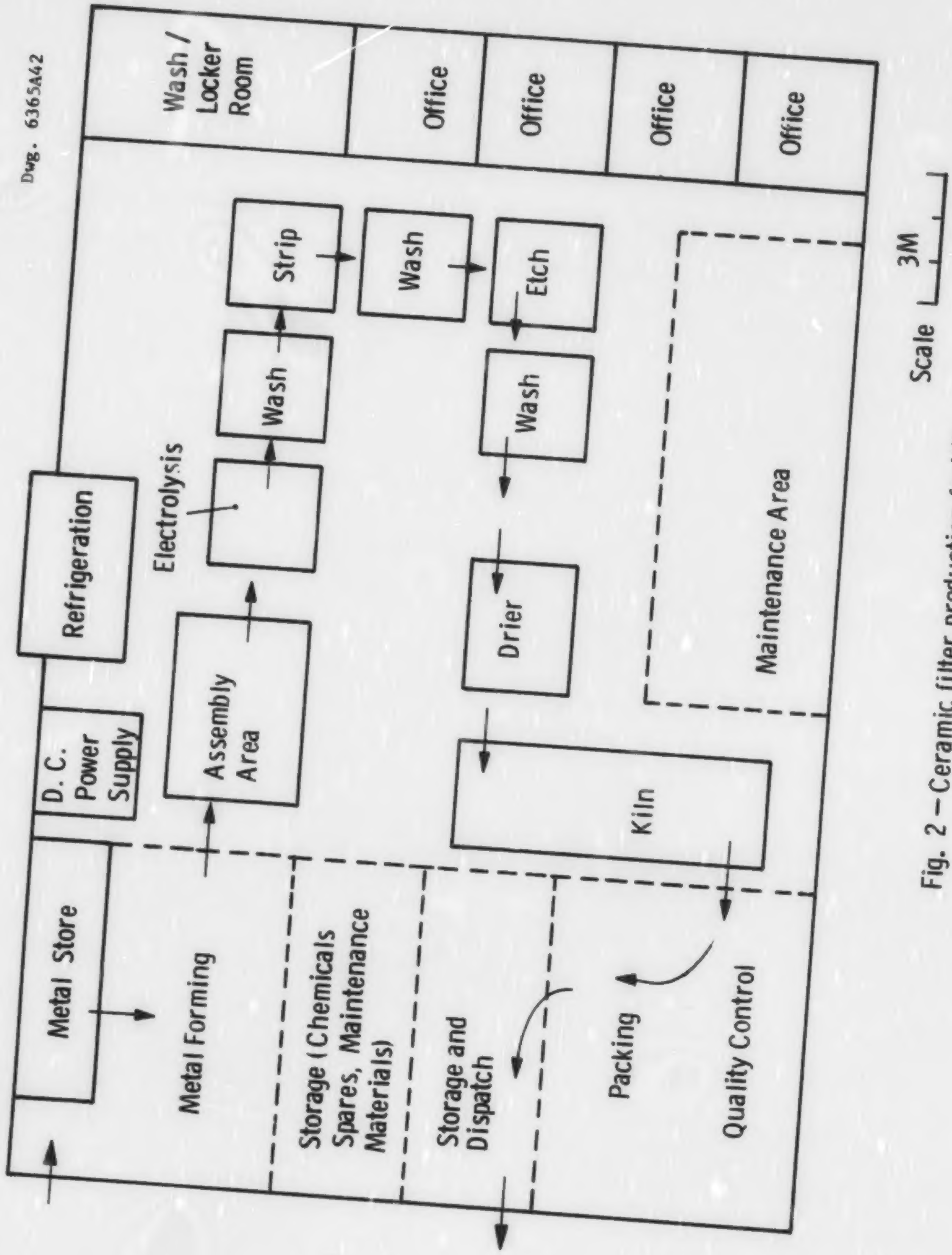
Wash / Locker Room
Office
Office
Office
Office
Refrigeration
D. C. Power Supply
Metal Store
Metal Forming
Assembly Area
Electrolysis
Wash
Strip
Wash
Etch
Wash
Drier
Kiln
Maintenance Area
Storage (Chemicals Spares, Maintenance Materials)
Storage and Dispatch
Packing
Quality Control
Scale
3M

Fig. 2 – Ceramic filter production facility

Table 1

Capital Costs for Ceramic Filter Production Facility
Base Case - 1 M^2/Hr., 250 μm Thick, 1 μm Pores

Equipment	Installed Cost
Metal Forming Equipment (Budget Estimate)	$ 20,000
Power Supply (G.E. Rectiformer, 2000 kW)	85,000
Drier	10,000
Kiln	25,000
Tanks, Racks, Mechanical Transfer	50,000
Building 540 M^2 @ $200/$M^2$	108,000
SUBTOTAL	$298,000
Engineering	40,000
Contingency	40,000
Interest During Construction	25,000
TOTAL	$403,000

Table 2

Materials and Power Per M^2 of Oxide Filter

Materials

(1) + (2) Aluminum 1199 formed to proper shape and anodizing chemicals

Membrane Thickness (µm)	Membrane Thickness (mils)	Aluminum Thickness (µm)	Aluminum Thickness (mils)	Aluminum Weight Kg	Min. Cost* ($)	Anodizing Chemicals ($)
125	5	100	4	0.3	1.2	2.70
250	10	200	8	0.6	2.4	5.40

(3) Chemicals for removal of unused aluminum

Bromine 0.25 Kg (~\$1.10/Kg) = \$0.275

Methanol 8.0 litra (~\$0.10/litre) = \$0.80

(4) Chemicals for removal of barrier layer and pore enlargment \$2.50

(5) Materials for supports - estimate at < \$10.00

Power for Anodizing for Pore Diameters to 0.8 µm

Membrane Thickness (µm)	Average Amperes at 600V D.C.	Approximate Hours	Total Ampere-Hours at 600V D.C.	Approximate Power Costs for Anodizing and Cooling (\$0.03/KW-hr)
125	31	20	620	16.60

---

*1199 Al formed to cylindrical units 2.5 cm x 100 cm will probably cost at least \$4/Kg.

Table 2 (continued)

Membrane Thickness (μm)	Average Amperes at 600V D.C.	Approximate Hours	Total Ampere-hours at 600V D.C.	Approximate Joule Heating (KW) Requiring Cooling	Approximate Power Costs for Anodizing and Cooling ($0.03/KW-hr)
250	31	40	1240	11	35.50

Power for Converting to Alpha Form

High temperature furnace capable of holding 1200°C for 15 minutes.
This may not be needed if conversion is effected in the hot gas stream.

Table 3

Operating Costs in Thousands of Dollars for Producing
2000 M^2/Year of Cylindrical Oxide Membranes 2.5 cm x 100 cm

Membrane Thickness (μm)	Materials	Power	Direct Labor*	Total
125 $\leq$ 0.8 μm diameter	15.0 (+<20)	33.2	12.0 (+<20)	60.2 (+<40)
250 $\leq$ 0.8 μm diameter	22.8 (+<20)	71	16.0 (+<20)	93.8 (+<40)

*Labor

Direct labor for producing at rate of 100 2.5 cm x 100 cm cylindrical elements 250 μm thick per day.

2 Men at \$4/hour = \$64/day/8 M^2 = \$8/M^2.

Estimate 125 μm thick at \$6/M^2 and 500 μm thick at \$10/M^2.

Estimate labor for supports at <\$10/M^2.

Table 4

Labor Force for Ceramic Filter Production

Function	One Shift Number	Operation Cost($)	Four Shift Number	Operation Cost($)
Engineering	1	20,000	1	20,000
Supervision	1	15,000	4	65,000
Process Work	3	27,000	9	90,000
Maintenance	1	11,000	1	11,000
Metal Forming	1	9,000	2	18,000
Quality Control	1	9,000	2	18,000
Packing & Storage	1	9,000	2	18,000
TOTAL ($)		100,000		240,000
With Overheads @ 100%		200,000		480,000

Table 5

Production Costs - Ceramic Membrane Filters

	Production 2000 M^2/Year	Production 8000 M^2/Year
Raw Materials	35,000	140,000
Power		
Electrolysis	120,000	480,000
Driers, Kilns, Etc.	1,000	5,000
Labor	200,000	480,000
Capital Charges @ 25% P.A.	100,000	100,000
TOTAL ANNUAL COST	456,000	1,205,000
Cost per M^2	228	151

Two areas of uncertainty exist - labor costs and capital costs. The labor force estimates could be significantly lower than actual requirements in an operating plant, while capital cost estimates are at best speculative. If labor costs were double our estimate, filter costs would increase by \$60 to \$100 per M^2. In addition, if capital costs were twice our estimates, filter costs would increase by \$15 to \$60 per M^2.

If these escalators are added to the original estimates to give a worst case, the estimated range for the cost of ceramic filters becomes \$230 to \$400 per M^2.

Projections of filter costs for membranes 125 μm thick and 500 μm thick are listed in Table 4.6. The costs range from \$112 per M^2 for 125 μm material produced at a rate of 8000 M^2 P.A. to \$350 per M^2 for 500 μm material produced at a rate of 2000 M^2 P.A. If capital and labor charges are doubled to give worst case estimates, these limits are adjusted to \$182/M^2 and \$536/M^2 respectively.

Filter Plant. Ceramic membrane filters will efficiently remove submicron particles from gas streams. However, due to the small pore diameter, flow rates must be relatively low and pressure drops will be relatively high. Consequently they cannot be economically employed in conventional gas cleaning applications.

In high pressure processes (such as coal gasification) where gas volumes are kept low by pressurized operation and pressure drops up to 100 kPa may be tolerated, the ceramic membrane has possible applications. The resistance of the filters to high temperature chemical attack make them well suited for use under extreme conditions.

A typical plant would consist of several pressure vessels containing manifolded ceramic membrane filter candles. The vessels would be arranged so that they could be sequentially removed from the filtration cycle and cleaned by a reverse flow of clean gas. A schematic layout of a complete plant consisting of four vessels is shown in Figure 3. Three vessels are shown filtering the raw gas while the fourth vessel (#4) is cleaned by a reverse gas flow.

Table 6

Filter Element Costs

Thickness	125 μm		500 μm	
Production Rate	2000 M^2 PA	8000 M^2 PA	2000 M^2 PA	8000 M^2 PA
Basic Estimate $/$M^2$	184	112	349	232
Escalated Estimate (Capital & Labor Charges Increased by 2x)	321	182	536	314

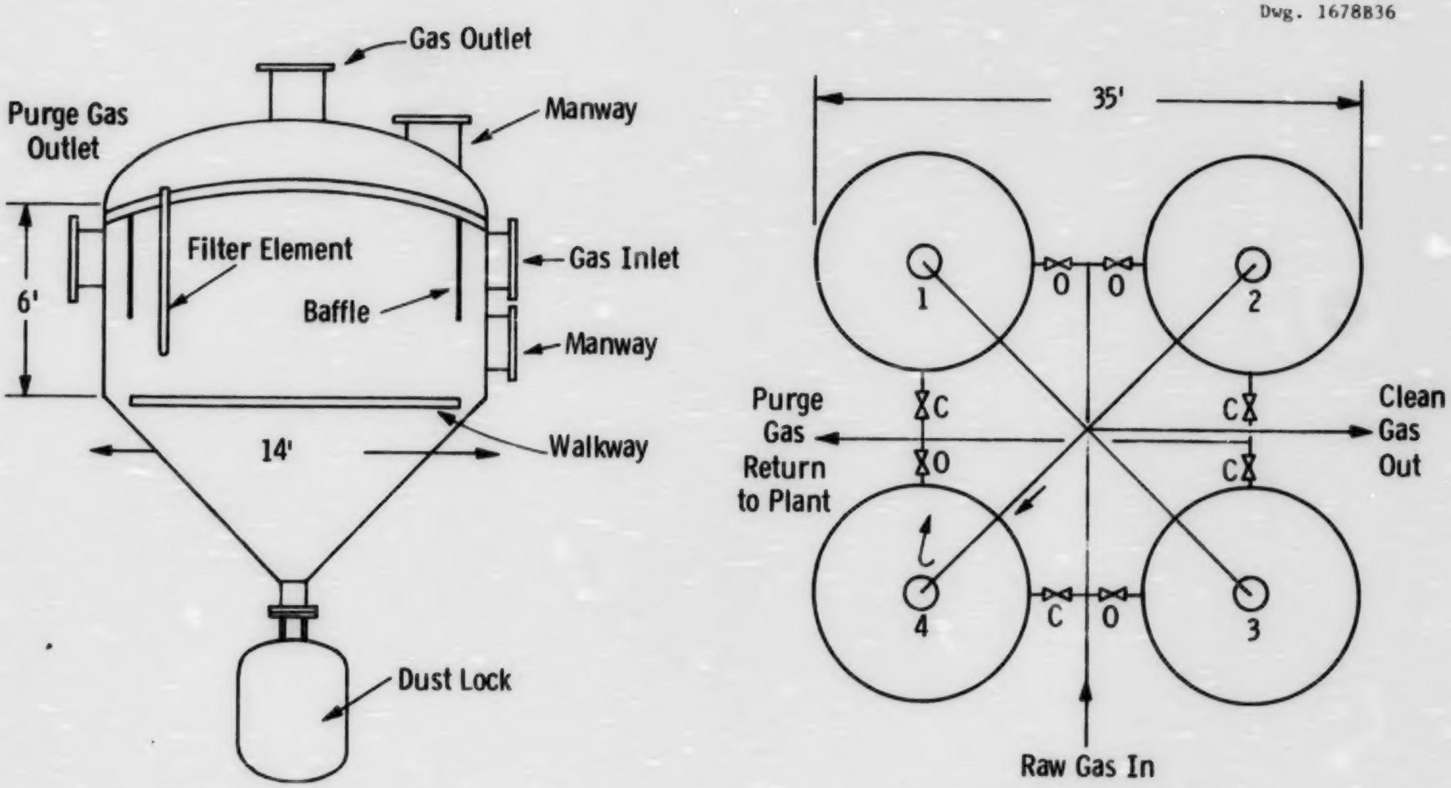
Dwg. 1678B36
Gas Outlet
Purge Gas Outlet
Manway
Filter Element
Gas Inlet
6'
Baffle
Manway
Walkway
14'
Dust Lock
35'
1
2
3
4
O
O
C
O
C
C
C
O
Purge Gas Return to Plant
Clean Gas Out
Raw Gas In

Filter Vessel (Conceptual)

Plant Layout Plan (Conceptual)
C - Closed O - Open
Vessel #4 in Cleanup Mode

Fig. 3 —Filter plant layout

A filter plant of the size shown would accommodate approximately 200 M^2 of filter surface, assuming filter candles 1 M long by 2.5 cm diameter.

Filter Plant Costs. Capital costs for a filter plant can be assessed once the required filter area is established. This will determine the cost of the filter elements required, and also the size and cost of the containing vessels. To establish operating costs it is additionally necessary to know the operating pressure loss through the filters.

For the purpose of this evaluation we have estimated costs for a filter plant which treats approximately 30 M^3/S of gas at 870°C and 1620 kPa. This is equivalent to the output of a gasifier which supplies fuel to a 250 MW combined cycle plant.

The estimates have been made for various filter characteristics - pore diameter, thickness and free cross-section. In addition, gas velocity/pressure drop effects have been estimated. Typical results are shown in Table 7.

Referring to the table, filter costs are estimated at two levels; the normal level (N) based on the filter production cost estimates and the maximum level (M) based on the "worst case" estimates.

Vessel costs were estimated for a 200 M^2 filter plant based on a four vessel arrangement, and costs for other installations were factored by a 0.7 power law.

Annual costs for owning the filter plant are also tabulated at the normal and maximum level. For this estimate, the plant life has been assumed to be 20 years, while the filters are assumed to have a 5 year life. The breakdown of capital charges is given in Table 8.

Table 7

Cost Data For Ceramic Membrane Filter Plant

Pore Diameter µm	Membrane Thickness µm	Pore Gas Velocity cm/s	Free Cross Section %	Superficial Velocity cm/s	ΔP KPa	Filter Area M^2	Filter Cost \$ x 10^6 N	Filter Cost \$ x 10^6 M	Vessel Cost (Installed) \$ x 10^6	Filter Cost Installed \$ x 10^6 (N)	Filter Cost Installed \$ x 10^6 (M)	Total Filter Plant Cost \$ x 10^6 (N)	Total Filter Plant Cost \$ x 10^6 (M)	Annual Cost \$ x 10^6 (N)	Annual Cost \$ x 10^6 (M)
0.5	125	3	12	0.375	20	9866	1.697	3.058	9.168	3.394	6.116	12.562	15.284	3.097	4.066
			25	0.75		4933	0.849	1.529	5.643	1.698	3.058	7.341	8.701	1.766	2.251
			50	1.5		2467	0.424	0.765	3.474	0.848	1.530	4.322	7.173	1.017	1.260
		6	12	0.75	40	4933	0.849	1.529	5.643	1.698	3.058	7.341	8.701	1.766	2.251
			25	1.5		2467	0.424	0.765	3.474	0.848	1.530	4.322	5.004	1.017	1.260
			50	3.0		1233	0.212	0.382	2.139	0.424	0.764	2.563	2.903	0.542	0.713
		9	12	1.12	60	3304	0.568	1.024	4.261	1.136	2.048	5.397	6.308	1.282	1.607
			25	2.25		1644	0.283	0.510	2.615	0.566	1.020	3.181	3.635	0.740	0.902
			50	4.5		822	0.141	0.255	1.610	0.282	0.510	1.892	2.120	0.432	0.513
	250	3	12	0.375	40	9866	2.170	3.749	9.168	4.340	7.498	13.508	16.666	3.434	4.558
			25	0.75		4933	1.085	1.875	5.643	2.170	3.750	7.813	9.393	1.935	2.497
			50	1.5		2467	0.542	0.937	3.474	1.084	1.874	4.558	5.348	1.101	1.382
		6	12	0.75	80	4933	1.085	1.875	5.643	2.170	3.750	7.813	9.393	1.935	2.477
			25	1.5		2467	0.542	0.937	3.474	1.084	1.874	4.558	5.348	1.101	1.382
			50	3.0		1233	0.271	0.469	2.139	0.542	0.938	2.681	3.077	0.634	0.775
	500	3	12	0.375	80	9466	3.068	4.913	9.168	6.136	9.826	15.304	18.994	4.073	5.387
			25	0.75		4933	1.534	2.456	5.643	3.068	4.912	8.711	10.555	2.254	2.911
			50	1.5		2467	0.767	1.228	3.474	1.534	2.456	5.008	5.930	1.261	1.589
1.0	125	9	12	1.12	15	3303	0.607	1.060	4.262	1.214	2.120	5.478	6.382	1.310	1.632
			25	2.25		1644	0.304	0.530	2.615	0.608	1.060	3.223	3.675	0.755	0.916
			50	4.5		822	0.152	0.265	1.610	0.304	0.530	1.914	2.140	0.440	0.521
		18	12	2.25	30	1644	0.304	0.530	2.615	0.608	1.060	3.223	3.675	0.755	0.916
			25	4.5		822	0.152	0.265	1.610	0.304	0.530	1.914	2.140	0.440	0.521
			50	9.0		411	0.076	0.132	0.992	0.152	0.264	1.144	1.256	0.258	0.298
		36	12	4.5	60	822	0.152	0.265	1.610	0.304	0.530	1.914	2.140	0.440	0.521
			25	9		411	0.076	0.132	0.992	0.152	0.264	1.144	1.256	0.258	0.298
			50	18		206	0.038	0.066	0.611	0.076	0.132	0.687	0.743	0.153	0.173
	250	9	12	1.12	30	3303	0.789	1.321	4.262	1.578	2.642	5.840	6.904	1.439	1.819
			25	2.25		644	0.395	0.660	2.615	0.790	1.320	3.405	3.935	0.820	1.009
			50	4.5		822	0.197	0.330	1.610	0.394	0.660	2.004	2.270	0.472	0.567
		18	12	2.25	60	1644	0.395	0.660	2.615	0.790	1.320	3.405	3.935	0.820	1.009
			25	4.5		822	0.197	0.330	1.610	0.394	0.660	2.004	2.270	0.472	0.567
			50	9		411	0.099	0.165	0.992	0.198	0.330	1.190	1.322	0.274	0.321
	500	9	12	1.12	60	3303	1.552	1.770	4.262	2.304	3.540	6.566	7.802	1.698	2.137
			25	2.25		1644	0.576	0.885	2.615	1.152	1.770	3.767	4.385	0.949	1.169
			50	4.5		822	0.288	0.443	1 610	0.576	0.886	2.186	2.496	0.537	0.647

Table 8

Capital Charges

Taxes and Insurance	2.0%
Interest on 65% Borrowed Capital @ 6-3/4%	4.4%
Profit on 35% Equity @ 7-1/2%	2.6%
Federal Income Tax	2.6%
Maintenance	4.0%
Depreciation	
Plant - 20 Year Linear	5.0%
Filters - 5 Year Linear	20.0%

Alternative Gas Cleaning Plant

Granular Bed Filter Plant. An alternative gas cleaning system for fine particulate control in a coal gasification combined cycle system would, based on available data, require two particle collection units to achieve the same efficiency as the ceramic membrane plant. One unit, a granular bed filter, would be installed in the high pressure gas line for turbine protection, while a second unit would be required to remove submicron particles from the exhaust gases.

To establish the comparative costs of this system, capital and operating cost estimates have been made for comparison with those of a ceramic membrane plant.

Granular bed filter costs have been factored from estimates made by the Ducon Co. On this basis the installed cost for a 250 MW filter unit is \$16.20 per kW. Budget estimates by baghouse manufacturers suggest that an installed baghouse for the control of fine particle emissions will cost \$16.80 per kW. Consequently a particle control system based on conventional collection equipment will have an installed capital cost of approximately \$33 per kW, or $\$8.25 \times 10^6$ for a 250 MW plant.

Annual costs for owning and operating this plant are $\$1.786 \times 10^6$ (Table 9).

Consider now an equivalent ceramic membrane plant which operates with a maximum pressure loss of 100 kPa. The operating cost for this unit would be \$428,000 based on a power cost of 2¢/kWhr. Consequently, for the ceramic membrane plant to be competitive with the more conventional unit, the annual capital charges must be less than $\$1.3 \times 10^6$.

Reference to Table 7 indicates that this target can be achieved, provided filters of the required characteristics can be fabricated. For example, a 125 μm membrane with 0.5 μm pores and a free cross-section of 25% would be satisfactory provided the superficial gas velocity was 1.5 cm per second or greater.

Table 9

Costs for Granular Bed Filter - Bag Filter Plant

Installed Capital Cost - $\$8.25 \times 10^6$

Annual Costs

Fixed Costs	$957,000
Depreciation (20 Year Linear)	412,500
Maintenance	330,000
Power (@ 2¢ per kWhr)	86,000
TOTAL	$1,785,000

Conventional Power Plant. A second alternative to the ceramic membrane-combined cycle power plant would be a conventional coal-fired power plant.

Such a plant would have to incorporate sulfur and particulate control processes. For the purposes of this evaluation, it will be assumed that limestone-wet scrubbing is sufficient for adequate emission control.

To make a comparative evaluation it is necessary to establish complete costs for both the coal gasification-combined cycle plant, and for the conventional steam plant. The coal gasification-combined cycle system is evaluated on the basis of a 250 MW Westinghouse-ERDA coal gasification unit (Fig. 4) while for the conventional plant, a 635 MW unit is considered.

In evaluating the comparative costs for owning and operating these systems, it is necessary to assume costs for capital, fuel, power, and sulfur sorbents. For this purpose capital charges have been set at 20.6% (Table 9); power is charged at 2¢ per kWhr; coal costs have been set at 80¢/10^6 Btu; while limestone or dolomite for sulfur removal is assumed to cost \$7 per ton.

All costs are for the last quarter of 1974 to maintain a common basis for comparison.

Capital Costs. Cost accounts for a 250 MW coal gasification-combined cycle power plant have been prepared from recent estimates for a Westinghouse-ERDA system. Gasification-desulfurization plant with ancillary equipment will have an installed cost of \$135 per kW, while the packaged combined cycle plant adds an additional \$180 per kW. Land, electric plant, first stage dust collectors, and miscellaneous plant equipment account for an additional \$33 per kW, and interest during construction is \$50 per kW. This results in a total capital cost of \$398 per kW for a plant without fine particle collection equipment (Table 10). The heat rate for this plant is estimated to be 8750 Btu/kWhr.

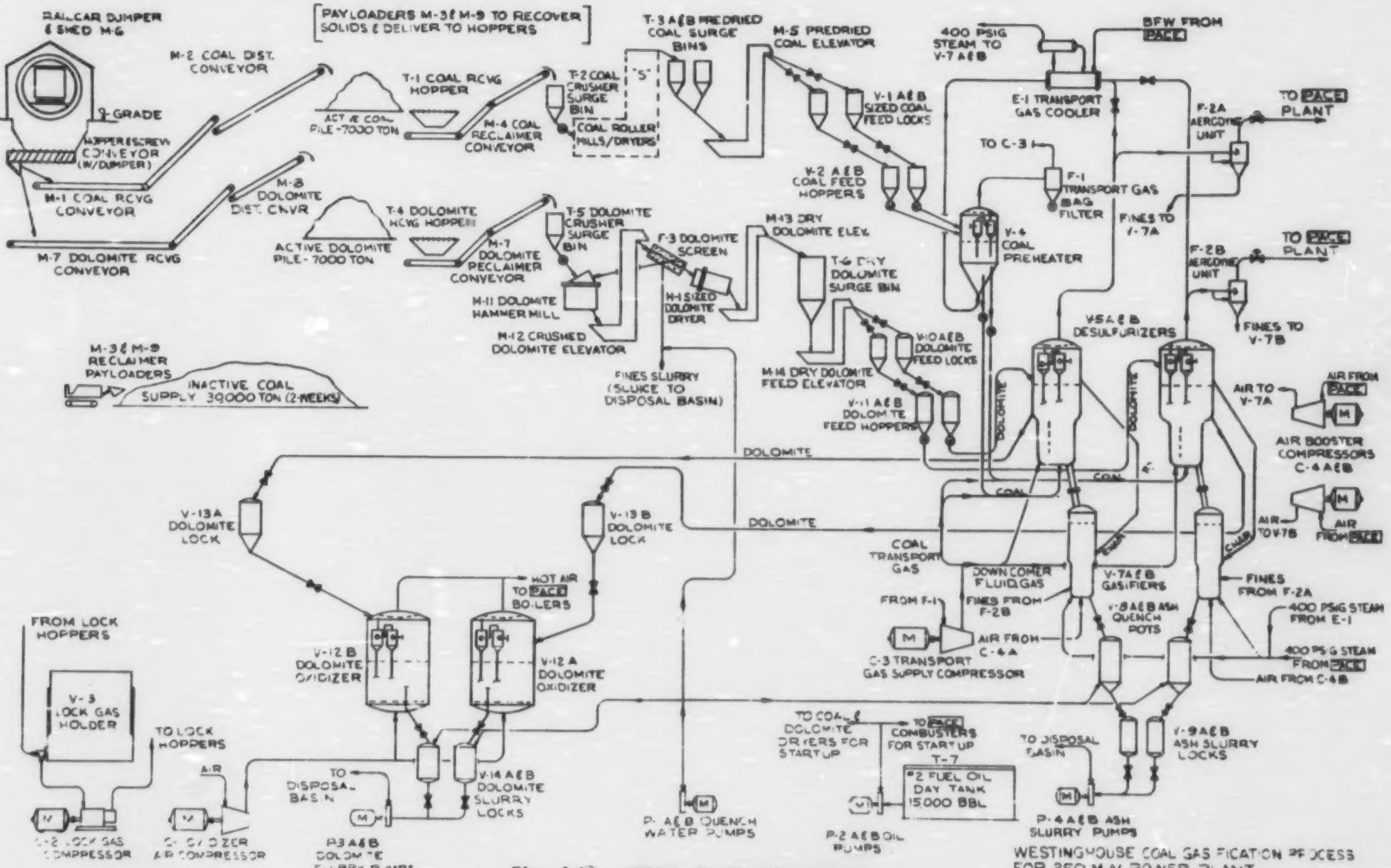
RAILCAR DUMPER & SHED M-6
GRADE
HOPPER & SCREW CONVEYOR (W/DUMPER)
M-1 COAL RCVG CONVEYOR
M-2 COAL DIST. CONVEYOR
M-7 DOLOMITE RCVG CONVEYOR
M-8 DOLOMITE DIST. CNVR
PAYLOADERS M-3 & M-9 TO RECOVER SOLIDS & DELIVER TO HOPPERS
ACTIVE COAL PILE-7000 TON
T-1 COAL RCVG HOPPER
M-4 COAL RECLAIMER CONVEYOR
T-2 COAL CRUSHER SURGE BIN
"S"
COAL ROLLER MILLS/DRYERS
T-3 A & B PREDRIED COAL SURGE BINS
M-5 PREDRIED COAL ELEVATOR
V-1 A & B SIZED COAL FEED LOCKS
V-2 A & B COAL FEED HOPPERS
ACTIVE DOLOMITE PILE-7000 TON
T-4 DOLOMITE RCVG HOPPER
M-7 DOLOMITE RECLAIMER CONVEYOR
T-5 DOLOMITE CRUSHER SURGE BIN
M-11 DOLOMITE HAMMER MILL
M-12 CRUSHED DOLOMITE ELEVATOR
F-3 DOLOMITE SCREEN
H-1 SIZED DOLOMITE DRYER
FINES SLURRY (SLUICE TO DISPOSAL BASIN)
M-13 DRY DOLOMITE ELEV.
T-6 DRY DOLOMITE SURGE BIN
M-14 DRY DOLOMITE FEED ELEVATOR
V-10 A & B DOLOMITE FEED LOCKS
V-11 A & B DOLOMITE FEED HOPPERS
M-3 & M-9 RECLAIMER PAYLOADERS
INACTIVE COAL SUPPLY 39000 TON (2-WEEKS)
400 PSIG STEAM TO V-7 A & B
E-1 TRANSPORT GAS COOLER
BFW FROM PACE
TO C-3
F-1 TRANSPORT GAS BAG FILTER
V-4 COAL PREHEATER
F-2A AERODYNE UNIT
TO PACE PLANT
FINES TO V-7A
F-2B AERODYNE UNIT
TO PACE PLANT
FINES TO V-7B
V-5 A & B DESULFURIZERS
AIR TO V-7A
AIR FROM PACE
AIR BOOSTER COMPRESSORS C-4 A & B
AIR TO V-7B
AIR FROM PACE
DOLOMITE
DOLOMITE
COAL
COAL
CHAR
CHAR
COAL TRANSPORT GAS
DOWN COMER FLUID GAS
FROM F-1
FINES FROM F-2B
AIR FROM C-4A
C-3 TRANSPORT GAS SUPPLY COMPRESSOR
V-7 A & B GASIFIERS
V-8 A & B ASH QUENCH POTS
FINES FROM F-2A
400 PSIG STEAM FROM E-1
400 PSIG STEAM FROM PACE
AIR FROM C-4B
V-9 A & B ASH SLURRY LOCKS
TO DISPOSAL BASIN
P-4 A & B ASH SLURRY PUMPS
TO COAL & DOLOMITE DRYERS FOR STARTUP
TO PACE COMBUSTERS FOR START UP
T-7
#2 FUEL OIL DAY TANK 15,000 BBL
P-2 A & B OIL PUMPS
P-1 A & B QUENCH WATER PUMPS
V-13A DOLOMITE LOCK
V-13 B DOLOMITE LOCK
HOT AIR TO PACE BOILERS
V-12 B DOLOMITE OXIDIZER
V-12 A DOLOMITE OXIDIZER
V-14 A & B DOLOMITE SLURRY LOCKS
TO DISPOSAL BASIN
P-3 A & B DOLOMITE SLURRY PUMPS
FROM LOCK HOPPERS
V-3 LOCK GAS HOLDER
TO LOCK HOPPERS
AIR
C-2 LOCK GAS COMPRESSOR
C-1 OXIDIZER AIR COMPRESSOR
M
WESTINGHOUSE COAL GASIFICATION PROCESS FOR 250 MW POWER PLANT
WCS 11-1-72

Fig. 4 Ⓦ — ERDA Gasification Plant

Reproduced from best available copy.

Table 10

Coal Gasification - Combined Cycle Plant Costs
$/kW, 250 MW Plant

Coal Gasification Plant and Auxiliaries	$135
Combined Cycle Plant	180
Land	1
Electric Plant	15
Cyclone Dust Collectors	12
Misc. Plant Equipment	5
Interest During Construction	50
TOTAL ($/kW)	$398

A cost account for a conventional 635 MW power plant is listed in Table 11. This is based on a published 1971 cost account and has been factored by the M&S index to update the costs to late 1974. An additional $50 per kW is added to cover the capital costs associated with a limestone-wet scrubbing system for particle and sulfur removal. The final cost is $475 per kW. The heat rate for the plant is 9122 Btu/kWhr (based on Hammond #4 station of Georgia Power and Light).

Annual Costs. Annual costs for owning and operating these two plants have been assessed per kW of installed capacity to give numbers which may be readily compared. The results (Table 12) show the combined cycle plant to be approximately $15 per kW per year cheaper, before fine particle control equipment is accounted for.

If $10 per kW per year is committed to fine particle collection, the combined cycle plant maintains its competitive position. This allows a total annual expenditure of $\$2.5 \times 10^6$ on a ceramic membrane filter plant.

Reference to Table 7 indicates that a ceramic membrane filter plant can be operated for less than this $\$2.5 \times 10^6$ annual total.

Discussion. This preliminary estimate of ceramic filter costs and of filter plant costs indicates that such units can be economically competitive with alternative systems for fine particle control in power plant applications. Indications are that the required filter properties are well within the scope of available and developing technology.

The review of filter costs indicates some minimum requirements for filter properties, based purely on economic considerations. With additional information on allowable pressure drop-membrane thickness limits (i.e., mechanical properties) the field of acceptable filter characteristics may be further defined. This will allow clear objectives for filter development to be established.

Table 11

Capital Costs for 635 MW Coal Fired Steam Plant

	$/kW
Land and Land Rights	1.51
Structures and Improvements	36.59
Boiler Plant Equipment	83.57
Turbine-Generator	74.79
Electric Plant	20.10
Misc. Plant Equipment	5.65
Undistributed Costs	40.26
Other Plant Costs	3.90
Contingency	17.58
Escalation	69.91
Interest During Construction	64.23
General Items, Engineering	7.38
	425.47
Limestone/Wet Scrubbing System	50.00
TOTAL ($/kW)	475.47

Table 12

Annual Costs for Power Plants Per kW of Capacity Load Factor 0.7

	Conventional	Combined Cycle (No Fine Particle Collection)
Fixed Costs (11.6%	$55.10	$46.05
Depreciation (5%)	23.75	19.85
Maintenance (4%)	19.00	15.88
Dolomite/Limestone	2.40	4.20
Power (for gas cleaning)	0.34	1.70
Fuel	43.98	42.20
TOTAL	$144.57	$129.88

4.2 MATERIALS FABRICATION AND TESTING

Objectives. To develop, fabricate, and test small, flat aluminum oxide filter membranes having satisfactory pore size, open area, strength, and filtration characteristics.

Fabrication Approach and Results

Fabrication Summary. Gamma aluminum oxide was electrochemically fabricated as flat 4.5 cm diameter discs 100 to 250 microns thick, chemically treated for barrier layer removal and pore enlargement, and fired to 1200°C for conversion to the alpha form. The oxide was examined for structural integrity, internal geometry, and bend strength. Over 150 samples were fabricated to varying stages of completion, with 43 samples between about 60 and 190 microns thick sent to Westinghouse for filter testing. The better samples had average pore diameters near each surface of generally 0.7 to 0.9 micron with internal pore diameters probably closer to 0.4 to 0.6 micron, particularly for the thicker samples.

Formation of Oxide. Electrochemical oxidation of aluminum under controlled conditions will form an oxide with parallel channels extending through its thickness. These channels are open at one end and capped at the other by a removable continuous oxide layer called the barrier layer. Figure 5 shows the oxide's structure. When electrochemically fabricated, the oxide is in the gamma form.

The aluminum oxide was fabricated in 4.5 cm diameter discs, 100 to 250 microns thick, from high purity aluminum 1199 (99.99%) in an oxalic acid electrolyte. The fabrication cell is shown in Figure 6. In operation, the cell is tilted so that the electrolyte covers the specimen even with the circulation pumps off. The pumps deliver fresh, cooled electrolyte to the face of the oxide specimen at the rate of 600 gph, and cooled glycol to the back aluminum side of the specimen at the rate of 350 gph. The 1/2 ton heat exchanger

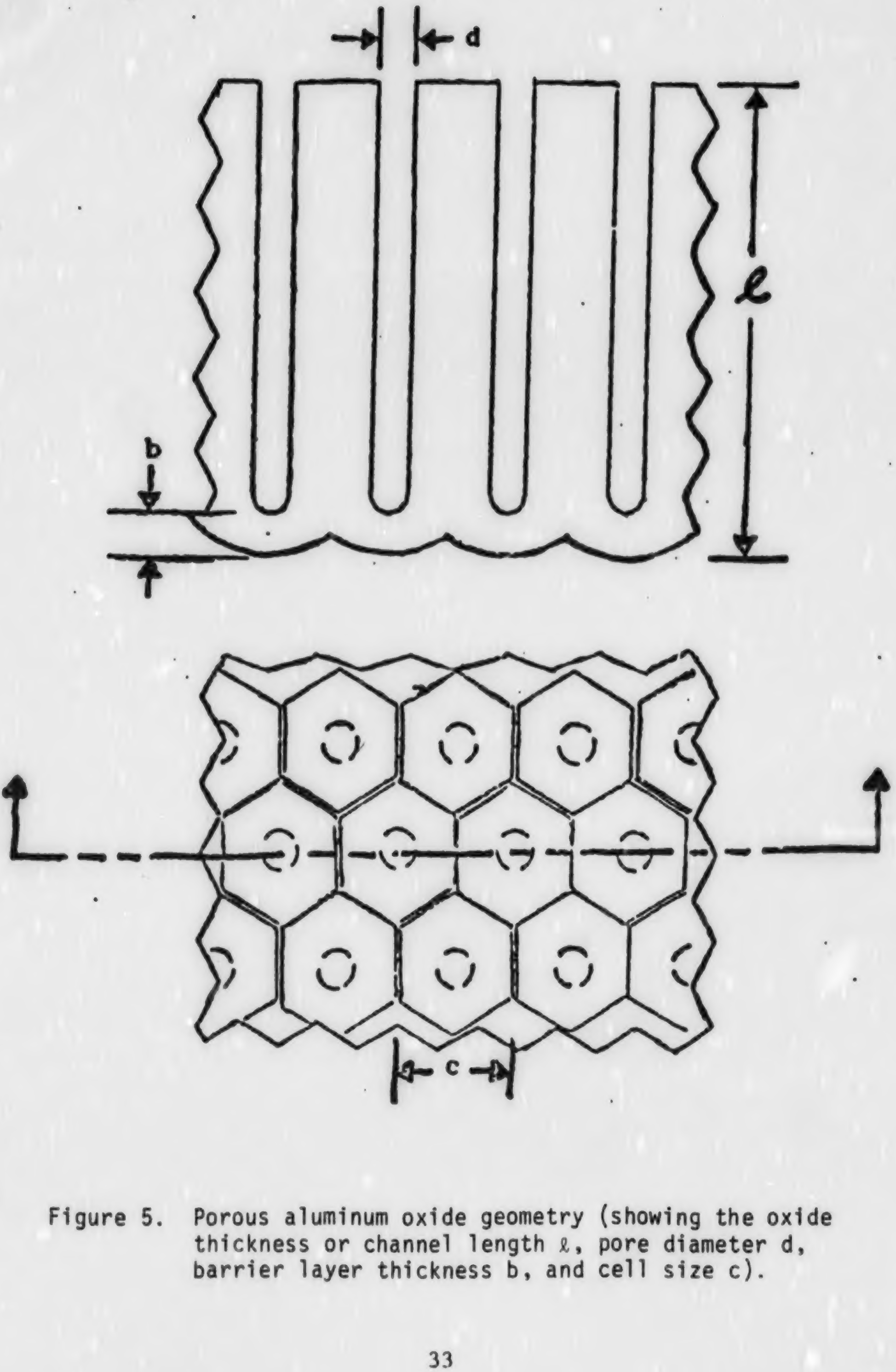

Figure 5. Porous aluminum oxide geometry (showing the oxide thickness or channel length ℓ, pore diameter d, barrier layer thickness b, and cell size c).

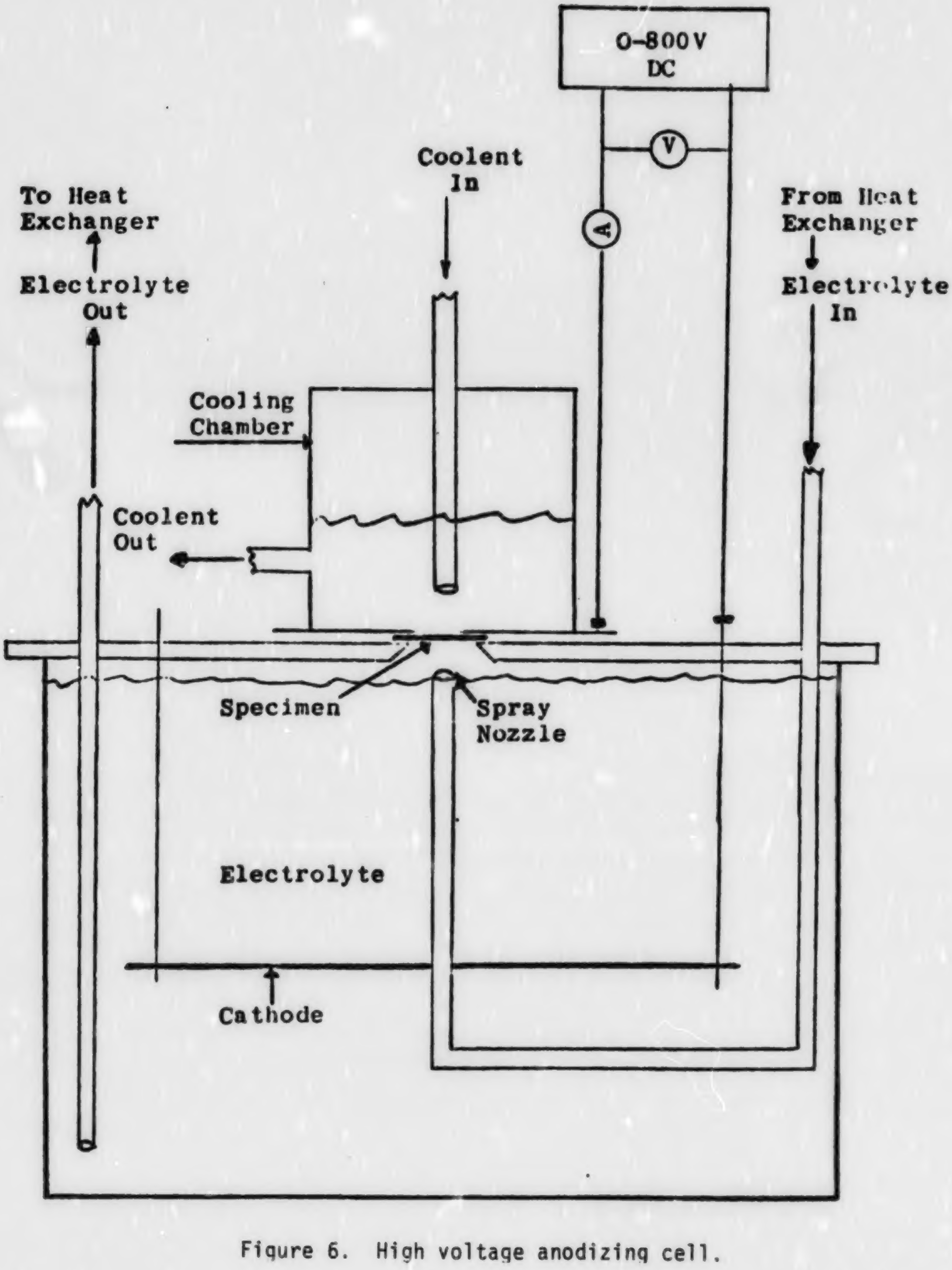
0-800V
DC
V
A
Coolent
In
To Heat
Exchanger
Electrolyte
Out
From Heat
Exchanger
Electrolyte
In
Cooling
Chamber
Coolent
Out
Specimen
Spray
Nozzle
Electrolyte
Cathode

Figure 6. High voltage anodizing cell.

is capable of maintaining electrolyte temperature to within 0.5°C at 2°C when both fabrication cells are in operation. The equipment is capable of providing up to 800 V D.C., with appropriate current, voltage, and temperature monitoring.

Initially the electrolyte used was 0.5, 1.0, or 1.5% oxalic acid containing 0.1% titanium (IV) oxalate at 3°C. The resulting cell size and pore diameters are given in Table 13.

Since a titanium (IV) salt is needed only to minimize the lower voltage section thickness and to achieve the higher voltages necessary to produce large pores, but is not appropriate for a reasonable oxide growth rate, the titanium (IV) salt containing solution should be used initially for the first part of the anodizing when the voltage is increased to 600 V or 800 V, with a non-titanium (IV) salt containing oxalic acid used for the remainder of the run. The simplest approach is to have two cells, one containing each electrolyte, and to move the sample from one cell to another at the appropriate time. However, since the sample could never be placed in the second cell identical to its positioning in the first cell, thus allowing for uniform oxide growth, it was necessary to arrange for a change of electrolyte in each cell with the sample remaining in position. Consequently, the plumbing for each of two fabrication cells was modified to permit the following operation.

- Fabrication of the oxide in an aqueous solution containing 1% oxalic acid and 0.1% titanium (IV) salt while the voltage is being increased from 0 to 600 or 800 V;
- Power turned off;
- Titanium containing solution pumped out of cell; cell and lines rinsed with deionized water;
- 5% oxalic acid solution pumped into cell;
- Power turned on and desired high voltage section grown;
- Power turned off, sample removed, and new sample put on;
- 5% oxalic acid solution pumped out, cell and lines rinsed with deionized water, and titanium containing solution returned to cell for a new run.

Table 13

Average Cell Size and (pore diameter)
in A/V for Various Fabrication Conditions

Oxalic Acid Concentration (%)	400V	500V	600V	800V
0.5	16.5 (8.3)	14.0 (7.8)	15.3 (6.8)	-
1.0	16.2 (7.0)	-	13.0 (7.5)	13.7 (8.1)
1.5	15.8 (8.0)	-	12.9 (7.4)	-

To increase the current density more, the electrolyte temperature was raised to 27°C for the entire fabrication process. An anticipated favorable consequence of increasing electrolyte concentration and temperature was the growth of larger pores within larger oxide cells. With the 5% oxalic acid solution at 27°C, the cell size is 27 Å/V. This means the as-formed pore diameters at 600 V will be up to 3000 Å or 0.3 micron.

Barrier Layer and Low Voltage Section Removal. After the excess aluminum attached to the oxide is removed by a 5% bromine in methanol solution, the barrier layer on one side of the membrane and the low voltage section (formed as the voltage was increased from 0 to 600 or 800 V) on the opposite side of the membrane were removed by simple treatment with an aqueous nitric acid-hydrofluoric acid solution. Successful removal of these two unwanted oxide sections was verified by scanning electron microscope examination. As an additional check that the unwanted sections had been removed, the calculated thickness of the high voltage section (determined from time-current-efficiency data) was compared to the final oxide thickness.

The decrease in oxide thickness after removal of the unwanted sections was generally about 50 to 75 microns.

Pore Enlargement. This aspect of the program received considerable attention. Both alkaline and acid etching solutions which had shown some success in the past were systematically studied using different procedures for exposing the oxide to the etchant. These procedures included simple immersion of the oxide in the etchant, forcing the etchant with mild pressure through the oxide pores, and vacuum impregnating of the oxide with the etchant. The same acid solution which was used to remove the barrier layer was found to be the most effective. This solution's effectiveness was further examined at various concentration strengths using combinations of the following procedures:

- Soaking of the oxide in the etchant for 1/2 to 11 minutes after a water presoak.
- Soaking of the oxide in the etchant for 1/4 to 5 minutes without a water presoak.

- Ultrasonic treatment of the oxide in the etchant for 1/2 to 4 minutes after a water soak.
- Ultrasonic treatment of the oxide in the etchant for 1/2 to 3 minutes without a water presoak.
- Treatment of the unstripped oxide with the etchant for 1/2 to 3 minutes.
- Treatment of the oxide with etchant under filtration pressure.

After the oxide samples were thinned by ion milling to permit SEM examination of the interior geometry, only two of the pore enlargement techniques were partially effective for the interior of the oxide. These techniques were ultrasonic treatment of the oxide in the etchant after the oxide has been dried at about 100°C, and treatment of the oxide with the etchant under filtration pressure. Both techniques needed improvement because the interior section pore diameters were not as large as the exterior section pore diameters. Tables 14 to 17 show how the pore etching evolved to a final procedure of multiple pressure etchings, generally with a 25%, 10%, 5% etchant concentration sequence and the loss of about 12 to 20 microns of oxide thickness. Samples treated in this manner had larger internal pores than their predecessors, particularly if they were less than 4 mils thick. A brief study was made of an acetone based etchant, but no significant advantage was gained by its use.

Even after many months of examining pore enlargement, the pore diameters at the center of the membrane were probably no larger than 0.4-0.6 micron, even though the diameters closer to the two surfaces were frequently 0.8 micron of greater. Figure 7 is a cross-section micrograph of an etched sample and Figure 8 is a surface micrograph of an etched sample.

Samples returned from Westinghouse were examined with the SEM. Some showed structural irregularities which could have aided in their fracturing. Some of the samples which broke in processing prior to being sent to Westinghouse had the same irregularities, but others which broke in processing had no apparent irregularities. Consequently, with such inconclusive data, no fabrication procedural changes were made.

Table 14

Pressure Pore Enlargement

Sample	Thickness (μ)	Support	Etchant Conc. (%)	Pressure (psi)	Time at Pressure (min.)	Etchant Flow Rate (drops/sec.)	Observations
W-43B-2	163	None	5	Electrolyte side up		0.18	small effect
						0.22 increasing to 0.4	
				4	5		
				5.5	12		
				Barrier side up			
				4	2.5	2.9	no effect
W-60-1	150	None	5	Electrolyte side up			
				4	5	1.1	
				5	1		
				Barrier side up		liquid poured out	no effect
				4	<1		
W-6	73	None	5	1	3	0	sample broke
				1.5	5	1.3 decreasing to 0.16	
W-1-1	100	Yes*	5	One side			
				4	21	0.28 decreasing to 0.13	sample gouged
				Other side			
				8	33	0.03	

Table 14 (continued)

Sample	Thickness (μ)	Support	Etchant Conc. (%)	Pressure (psi)	Time at Pressure (min.)	Etchant Flow Rate (drops/sec.)	Observations
W-1-2	100	Yes	5	One side			
				4	25	0.29 decreasing to 0.5	small effect
				Other side			
				4	12.5	0.67	
W-19-1	112	Yes	25	4 to 6	6	0	Interior pores about 0.35-0.4 μ; etching severe
				7	2	0.28	
W-23-1	65	Yes	10	4	5	0	
				5	20	0.28 decreasing to 0.22	too severe
W-32-1	133	Yes	10	electrolyte side up			
				4	5	0	
				5	7.5	0.28	
				barrier side up			
				4	7.5	1 decreasing to 0.67	slight effect
W-33-1	160	Yes	25	One side only			
				4	8	0.06 increasing to 0.14	interior pores about 0.4 μ
W-34-1	120	Yes	25	One side only			
				4 to 9	6	0	interior pores about 0.4 μ
				10	4	0.67	

*Milipore filter used as support

Table 15

Summary of Pressurized Etched Oxide Samples

Sample	Calculated High Voltage Thickness (μ)	Oxide Side Up	Etching Pressure (psi)	Etching Time (min.)	Final Thickness (μ)	Observations
W-65-1	160	electro. barrier	4-10 4-7	11 8	103	Holes in center
W-66-1	160	electro.	4-6	6	98	Perimeter damaged. Holes in center. Channels opened to $\geq$ 0.5 μ
W-69	157	electro. barrier	4 4-5	4 7	135	Few holes at perimeter. Channels opened to $\geq$ 0.5 μ
*W-70	154	electro.	4-5	3.5	127	Good appearance except for chip at perimeter. Diameters at surface ∿0.6 μ
W-71	153	electro.	4	4	100	Broke, Pores ∿0.6 μ
*W-73	160	electro. barrier	4-7 4-7	6 5	127	Good appearance. Diameters at surface ∿0.65 μ

Table 15 (continued)

Sample	Calculated High Voltage Thickness (μ)	Oxide Side Up	Etching Pressure (psi)	Etching Time (min.)	Final Thickness (μ)	Observations
W-74	irregular					Cracked upon etching
W-76	155	electro. barrier	4-7 6-8	6 6.5	132	Holes, Diameters at surface ∿0.55 μ. Interior fair
W-77	155 rough barrier	electro.	4-7	6		Holes
*W-78	157	electro. barrier	4-7 4-7	6 5	130	Good appearance
*W-81	155	electro. barrier	4-7 4-7	6 6	124	Good appearance
*W-82	149	electro. barrier	4-7 4-9	6 7.5	147	Good appearance
W-84	152	electro. barrier	4-7 4-8	6 6	125	Small holes in one section. Diameters at surface ∿0.55 μ. Internal looks good
*W-83	159	electro. barrier	4-7 4-9	6 7	127	Good appearance

Table 15 (continued)

Sample	Calculated High Voltage Thickness (μ)	Oxide Side Up	Etching Pressure (psi)	Etching Time (min.)	Final Thickness (μ)	Observations
*W-85	160	electro.	4-7	7	124	Good appearance. Diameters at surface ∿0.55 μ
*W-86		electro. barrier	4-7 4-7	7 7	122	Small holes
W-89	120	electro. barrier	4-7 4-7	6 6	112	Small holes and large holes in center
W-90	150	electro. barrier	4-6 4-7	6 6	124	Holes and crack in one area. Diameters at surface ∿0.8 μ
*W-92	160	electro. barrier	4-7 4-7	6 7	124	Holes around edge
*W-93	160	electro.	4-7	6	122	Good appearance
*W-94	170	electro.	4-7	6	124	Good appearance. Diameters at surface ∿0.54 μ
*W-95	170	electro. barrier	4-7 7	6 5.5	112	Many small holes

Table 15 (continued)

Sample	Calculated High Voltage Thickness (μ)	Oxide Side Up	Etching Pressure (psi)	Etching Time (min.)	Final Thickness (μ)	Observations
W-96	250	electro.	4	1	223	Good appearance
W-97	222	electro.	4-7	6		Many small holes
		barrier	4-7	5.5	129	
*W-98	165	electro.	4	2	113	Large and small holes
		barrier	4-7	7		
W-99	166	electro.	4-7	6	107	Hole where cracked after fabricated
*W-100	180	barrier	4	3	135	Good appearance Diameters at surface ∿0.5 μ
*W-101	245	barrier	4-5	4	157	Chip near edge Good appearance. Diameters at surface ∿0.6 μ
*W-102	160	barrier	4-6	4.5	102	Good appearance

Table 16

Pressure Etched Samples

Sample	Calculated High Voltage Thickness (μ)	Oxide Side Up	Etching Pressure (psi)	Etching Time (min.)	Final Thickness (μ)	Observations
W-103*	157	Barrier side	4-6	5	135	Good appearance
W-105	210	Barrier side	4-6	6	185	Cracked in center upon removal from etching apparatus; otherwise, good appearance
W-107*	185	Barrier side	4-5	6.5	150	Good appearance
W-108	217	Barrier side	4-6	6	100	Holes
W-109*	217	Barrier side	4-6	6.5	167	Good appearance
W-110*	125	Barrier side	4-6	5.5	100	One pinhole
W-112*	200	Barrier side	4-5	6	160	Good appearance
W-113*	195	Barrier side	4-5	5.5	150	Good appearance
W-114	120	Barrier side	4-5	3.5	85	Holes
W-115*	125	Barrier side	4-5	3	100	Good appearance
W-116	195	Barrier side	4	2.5	135	Broke

---

*Sent to Westinghouse

Table 16 (continued)

Sample	Calculated High Voltage Thickness (μ)	Oxide Side Up	Etching		Final Thickness (μ)	Observations
			Pressure (psi)	Time (min.)		
W-118*	177	Barrier side	4-6	6	150	Good appearance
W-120*	205	Barrier side	4-6	5.5	157	Good appearance
			4	2.5	155	Good appearance

Table 17

Pressure Etched Samples, Barrier Layer Up

Sample	25% Etching		10% Etching		Final Thickness (mils)	Observations
	Pressure (psi)	Time (min.)	Pressure (psi)	Time (min.)		
121	4	2.5			3.0	Has holes
122			4-5	3.5		
			4	2.5	3.5	Broke
123*	4	3.0	4	4.0	6.1	Good
124			4	2.5	2.8	Broke
125			(5%) 4	5.0	3.6	Good. Cracked with cermet support
126	4	3.0	4	4.0	7.3	Broke
127	4	4.0	4	5.5		
			(5%) 4	3.0	5.8	Hole in sample
128*			4-5	4.0		Good
129			4	1.5	4.2	
			(5%) 4	3.5		
			(5%) 4	6.5	5.1	Good. Cracked with cermet support
130	4	4.0	4	5.0	6.4	Good. Cracked with cermet support

Table 17 (continued)

Sample	25% Etching Pressure (psi)	25% Etching Time (min.)	10% Etching Pressure (psi)	10% Etching Time (min.)	Final Thickness (mils)	Observations
131	4	3.5	4	5.0	5.1	Pin holes
132*†	4	5.0	4	5.0	6.5	Good
134	5	4.5	4	2.5	5.1	Pin holes
135*†	4	4.0			4.7	Good
137*†	4	4.5	4	1.75	6.0	Good
138*†	4	5.0	4	5.0	6.7	Good
139*†	4	5.0	4	5.0	6.4	Good
140*†	5	5.0	4	5.0	6.3	Good
141*†	4	4.5	5	4.5	5.9	Good
142*†			4 4	2.5 1.5	3.7	Good
143*†	5	5.0	7	5.0	6.5	Good
144	7	6.0	5	5.0	5.3	Broke upon removal from apparatus
146*†	4	3.0	4	3.0	4.8	Good
149*†			4 (5%) 4	3.0 1	2.9	Good

Table 17 (continued)

Sample	25% Etching Pressure (psi)	25% Etching Time (min.)	10% Etching Pressure (psi)	10% Etching Time (min.)	Final Thickness (mils)	Observations
150	4	3				
151†					3.9	Pin holes
156*†			4 4	3.0 3.0	3.8	Good
157*†	4 4-6	5 6	4	3.0	3.7	Good
158*†			4-6	5.0	4.6	Good
168*†			4	3.0	3.3	Good
172*†			(5%) 4	0.5	2.7	Good
			0 (5%) 4	1.0 0.5	3.3	Good

*Sent to Westinghouse

†Ceramic disc supports

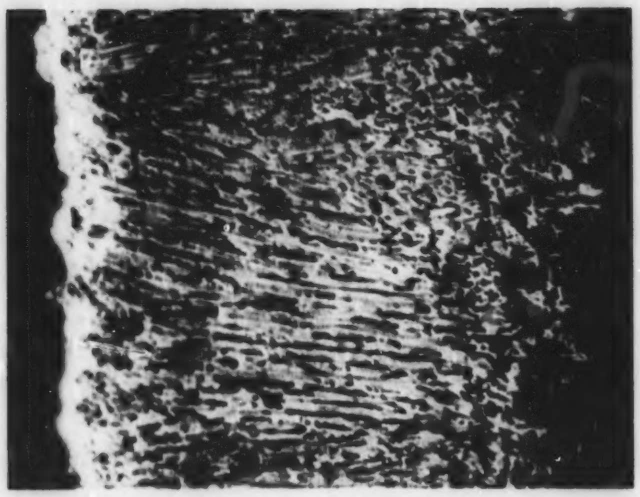

Figure 7. Edge view showing channels of sample W-66 at 1250X (1 cm = 8 microns). This sample section is 65 microns thick.

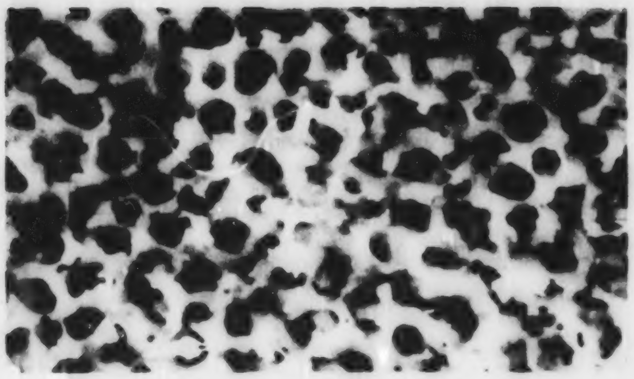

Figure 8. Sample W-61A. Barrier layer side of oxide formed at 800 V. Cell size ∿1.3 μ; pore diameter 0.84 μ (5200X).

Conversion to the Alpha Form. After removal of the barrier layer and low voltage section from the oxide and enlargement of the pores, the oxide was heated in air at 1200"C for 20-30 minutes in order to effect the change from the gamma to the alpha form. The membranes converted to the α-alumina form showed no damage to the channels from the treatment. The pore diameters were slightly larger as the pore walls shrank. The membrane thickness also shrank about 3%. The alpha form seemed less compliable than the gamma. Since the oxide tended to curl during heating, a confining pressure to keep the oxide flat was applied by use of thin zircon slabs. Applying this confining pressure is an art. However, bend strength measurements on the pore enlarged alpha and gamma forms showed them to be comparable in strength, as reported in Table 18.

Sample 2267-11 was not pore enlarged, as indicated by the low porosity. The 7.3 mil thick sample was about 5 times stronger than the 5.3 mil thick samples and 3 times stronger than the 6.3 mil thick sample. Measurements were done as described by T. R. Wilshaw's(1) method for measuring fracture stress. Wilshaw's method is a symmetrical central bending test in which the disc shaped sample is placed on a support ring which is approximately half the diameter of the sample. The load is put onto the top of the sample by a loading ball which is approximately half the diameter of the support ring. The fracture stress σ_F is then given by

$$\sigma_F = \frac{3P}{2\pi t^2} \quad (1-\nu) \quad \frac{a^2 - \Gamma_o^2}{2b^2} + (1+\nu) \ \ell n \frac{a}{\Gamma_o}$$

where P is the load, t the sample thickness, ν Poisson's ratio, a the support ring radius to its inner diameter, Γ_o the loading ball flat section radius, and b the sample radius.

Table 18

Mechanical Testing Results

Sample	Thickness (mils)	Porosity (%)	Form	Bend Strength (10^3 psi)
W-94	4.9	15	Alpha	11
2267-11	5.0	3	Gamma	350
W-99	4.2	15	Gamma Alpha	7.3 7.3
W-100	5.3	15	Gamma	8.7
W-101	6.3	16	Gamma	15.1
W-116	5.2	15	Gamma	9.3
W-126	7.3	15	Gamma	47

Data acquired some years ago indicated that at 800°C the approximate temperature of the gasifier gas stream, the gamma oxide would convert to the alpha in about 20 hours. Since it appeared possible that the oxide could be mounted in the gamma form, to facilitate sample production, samples in the gamma form were used for the pressure testing.

Supports for the Filter Membranes. During the filter testing, it became apparent that the membranes needed to be supported. The rationale in designing the supports was to make them mechanically sufficient to permit room temperature filter testing of the membranes, and to optimize their design for high temperature application in Phase II. Two different mechanical supports were examined. The first consisted of a mullite ring around the circumference on each side of the membrane with a reinforcing lattice on one side of the membrane of an alumina cermet. The second consisted of a highly porous solid ceramic disc about 2 mm thick placed on one side of the filter membrane with a 6 mm hole latticed 2 mm thick disc of the same ceramic material placed on the other side of the filter membrane, and the entire assembly held together at the circumference with a silicone rubber, sufficient for room temperature testing.

The mullite ring-cermet lattice support was used for 4 samples. The first was tested at Westinghouse, the remaining 3 never left Horizons, as it was found that the alumina cermet shrank upon curing and cracked the membranes attached to it.

The second mounting procedure - backing each side of the membrane with a porous ceramic disc - was most successful in enabling testing of the membranes to 10 psi.

Filter Tests. The filter test program had three major objectives:

- To establish the gas flow/pressure drop characteristics of the membrane filter.

- To establish that the filters could achieve high (>90%) collection efficiency on a polydisperse submicron dust.
- To demonstrate an operable cleanup technique which would allow the filters to be used in a cyclic manner for an indefinite period of time.

To achieve any of these ends it was first necessary to mount and seal the test specimens in a holder. This proved to be difficult.

Initial specimens had been fired to convert the alumina to the α form. This distorted the filters, producing a "wrinkled" edge which was virtually impossible to seal, without cracking the specimen. By avoiding the firing (i.e., leaving the specimens in the as fabricated γ form) this problem was overcome.

From the economic analysis, an acceptable flow rate/pressure drop criteria of >750 cc/min flow at a pressure drop of 100 kPa was adopted. Initial tests showed that the filter specimens would break under test before this criteria could be met. Several support systems were used without success.

Finally, the filters were sandwiched between two heavy porous ceramic discs to provide support while flow characteristics were determined. Of twelve samples tested in this manner, only two showed acceptable flow rates, and one of those two broke in spite of the heavy supports.

Two filtration tests were performed at reduced flow rates using filters with 0.5 μm pores. Filtration efficiency was greater than 90% for submicron particles, but both samples were broken before any definitive tests could be made.

Because of the poor mechanical properties of the material, the poor reproducibility of the specimens, and the lack of any practical support system, no further filtration tests were attempted.

SUMMARY - PHASE II

In Phase II of this program the emphasis shifted from attempting to develop and test a new ceramic membrane filter, toward the identification and testing of existing forms of ceramic materials that held the possibility of being utilized as hot gas filters. The second phase effort evolved into several distinct tasks: procurement of materials, screening tests, hot bench scale tests, hot high flow tests and conceptual design with cost comparison.

4.3 PROCUREMENT OF MATERIALS

Objective. The goal of this task was to search for and identify existing ceramic materials that offered the possibility of being utilized as filters in application where elevated temperatures and corrosive atmospheres would be encountered.

Procedure. This task was an ongoing effort throughout the entire second phase, however, the most concerted activity occurred in the initial stage during the transition from Phase I to Phase II. Personnel from Horrizons Research, Inc., Acurex/Aerotherm and Westinghouse R&D participated in this effort. Personnel from Horrizons Research, Inc. identified several promising forms of zirconia and alumina papers, felts and boards. Samples of several forms of these materials were obtained from Zircar Products, Inc. through Horrizons.

Acurex Corporation/Aerotherm Division had just completed a project for the EPA under Contract 68-02-1318, and was in the process of completing a final report, "Evaluation of Ceramic Membrane Filters As a Controf for Fine Particulate."(2) Since one task included in this effort was an industry survey of possible materials, their input was most helpful. A summary of their survey results is presented in Table 19. Because of the close association of personnel at Aerotherm with this effort, a subcontract was negotiated with them in order that they might continue their efforts in the identification of new materials.

Through contact with the Ceramics Department at Westinghouse R&D a cross flow, honeycomb, silicon carbide material manufactured by Norton Company was identified. Finally, contacts made by Westinghouse at a jointly sponsored, EPA, ERDA Symposium on fine particulate control led to the identification of a cross-flow monolithic material produced by the W. R. Grace & Company.

Table 19

Survey Results

Company	Code*	
1. Babcock & Wilcox Co., Refractories Div. Augusta, Georgia	C	Did not think they had any materials that would work for the application.
2. Coors Poreclain Co. Golden, Colorado	c,f	Several small scale filters for this particle size. No high temperature filter experience. Samples sent to Aerotherm. Nominal wall thickness -6 mm (1/4").
3. Corning Glass Co.	f,s	Nothing for this application. Celcor cordierite monoliths a possibility.
4. Dollinger Corp. Rochester, New York	f	Some filter elements that would work for this application. Relatively thick wall, large pressure drop (-100 kPa (1 atm). Elements available for testing.
5. General Refractories Bala Cynwyd, Pa.	c,s	Nothing for this application. Versagrid cordierite honeycomb is a possibility; however geometrical constraints a problem.
6. Horizons, Inc. Cleveland, Ohio	c	This membrane (-0.25 mm thick) being developed for testing in this application under Westinghouse - EPA program.
7. 3-M Company Saint Paul, Minn.	c,s	AlSiMag 795 (cordierite) honeycomb structure should work for this application. Elements available for testing. Low Pressure drop. High surface area to volume ratio. Good process control over pore size, porosity and membrane thickness. Samples sent to Aerotherm.
8. Norton Company Worcester, Mass.	c,s	Two materials suitable for thick walled filters. Also Spectramic honeycomb is a possibility.
9. Selas Flotronics Springhouse, Pa.	f	Micro-porous porcelain element would be suitable. Pressure drop -50 kPa. Sample sent to Aerotherm.
10. Wisconsin Porcelain Sun Prairie, Wisconsin	c,f	Thick walled filter elements similar to 4 and 9. No membranes.

*c - ceramic manufacturer
f - filter supplier
s = catalyst support manufacturer

Results. In general the materials identified could be classified in two groups - thick walled elements and thin walled honeycomb structures. The materials that were screened as being representative of the spectrum of thick walled materials were: Zircar 135C, Zircar ZAL-15, Selas 01, 10, XFF and a FMI (Fiber Materials, Inc.) material. The Zircar 135C sample was an alumina paper tube 3.5 cm long by 2.5 cm inside diameter. The wall thickness was 0.47 cm. The tubular structure appeared to have been made by wrapping hundreds of layers of the alumina paper around a mandrel prior to firing. In this form the material was not brittle and could be handled and worked with ease. It is reasonable to expect that a much thinner walled form of the material could be successfully used as a filter. The Zircar ZAL-15 material and the FMI material physically resembled each other exactly. The specimens were flat boards approximately 1 cm thick. The materials are very low density, soft and porous. These materials could be shaped easily which facilitated the screening tests, but there was some tendency to crumble at compression seals. It is expected that mechanical problems with sealing might be experienced in a commercial device using this material because of its low strength. The samples of filter media from Selas Flotronics were flat discs with a diameter of 8.75 cm by 1.25 cm thick. The materials were a microporous porcelain with varying porosity. Two of the samples Selas 01 and 10 were much less permeable than the third, Selas XFF, although there were no easily discernable differences in appearance.

Of the three materials grouped in the thin walled cross flow honeycomb category samples of the 3M Thermacomb and W. R. Grace & Co. material were obtained for testing. Efforts to obtain samples of the Norton Company cross flow material were not successful. The 3M cross flow structure is made up of several layers in the following pattern: a thin (0.25-1.5 mm) porous cordierite sheet, a layer of cordierite corrugations similar in apperance to those used in cardboard, another flat of sheet of cordierite followed by another layer of corrugations oriented 90° from the corrugations below. The presently available forms of the material have 1.97, 3.15 or 4.72 corrugations per cm. The cross flow element is shown with other available configurations in Figure 9. The material obtained from W. R. Grace & Company is virtually the same with the exception that straight, perpendicular dividers are used giving rectangular holes rather than the triangular holes seen in the Thermacomb. The Grace material tested had approximately 8.5 holes per cm and an equal number of layers per cm. One suggested method of using these materials as filters is illustrated in Figure 10.

These materials have many properties that make them attractive as filters. Among these are (1) working temperature to 1200°C (2) very good mechanical strength despite thin separators (3) excellent resistance to thermal shock (4) excellent resistance to corrosive atmospheres and (5) very high surface area to volume ratios. It is estimated that the Thermacomb material tested had 3.27 cm^2 filter area per cm^3 of element while the W. R. Grace & Company material had approximately 6.52 cm^2 of usable area per cm^3 of element. One might expect a ratio on the order of 0.1 cm^2 filter area per cm^3 for a typical fabric filtration facility.

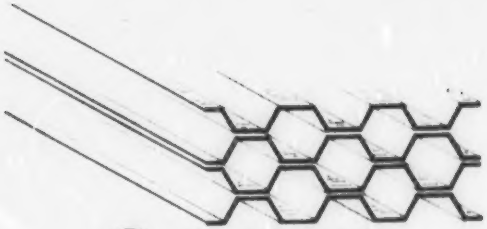

Ⓐ HC HONEYCOMB

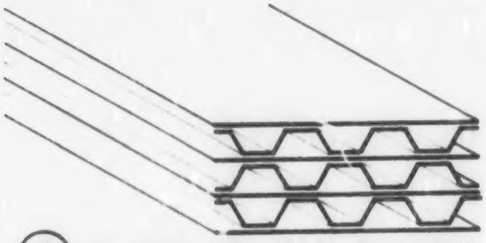

Ⓑ SC SPLIT CELL (Note Separator)

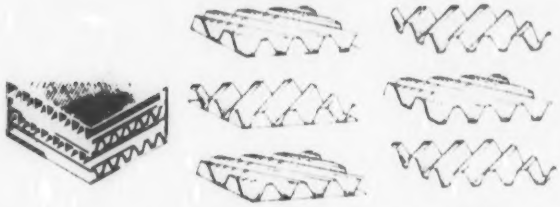

XFSC
CROSS-FLOW,
SPLIT CELL
Note separators
and corrugations
at 90°

XXSC
CRISS-CROSS,
SPLIT CELL
Note separators
and corrugations
at 45°

XXHC
CRISS-CROSS,
HONEYCOMB
with corrugations
at 45°
Note there is no
separator.

Figure 9. Structural shapes for 3M ThermaComb.

Reproduced from
best available copy.

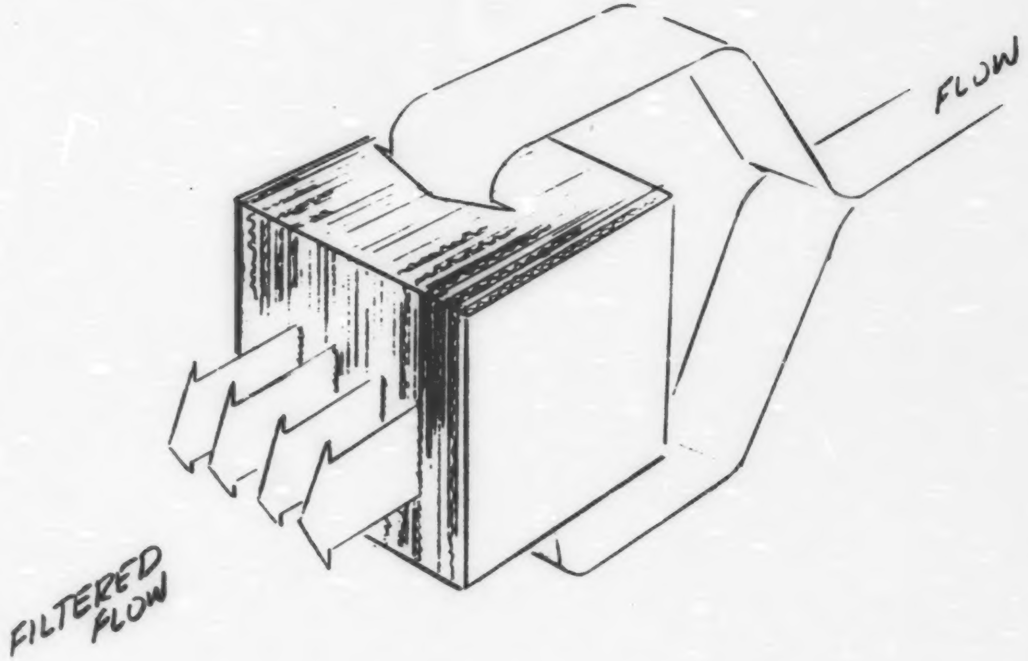
FLOW
FILTERED FLOW

Figure 10. 3M crossflow ceramic monolith.

4.4 SCREENING TESTS

Objective. Since the overall goal of the Phase II effort was to demonstrate successful hot gas filtration on a fairly large scale, it was decided to screen the materials identified and isolate one or two of the candidates that looked most promising. Once identified, virtually all further work would be confined to developing techniques for testing these materials and recording their filtration characteristics.

Procedure. The screening tests used consisted of two parts. First a measurement of pressure drop as a function of flow at ambient conditions was made. This was followed by actual filtration tests to determine overall particle removal efficiencies and possible techniques for on line cleaning of the filter.

Since the thick walled samples obtained varied greatly in size and shape it proved necessary to fabricate test jigs for each of the filters screened. In general these holders were of simple construction from plexiglass so that the inlet and outlet of the filter could be observed visually. Provisions for pressure drop taps and dust sampling were included.

The overall efficiency of the filters was measured by isokinetically sampling the dust laden stream from which the inlet to the filter was taken, and simultaneously filtering the entire outlet from the test specimen with either a milipore or a glass mat filter in the milipore filter holder. Dispersed dust was supplied to the test specimen by sampling either the inlet or outlet of a 3 m^3/min cyclone that had been in use. The test dust was fed to and dispersed in the cyclone system by a modified harvard dry dust disperser.(3) This dust was a ground limestone classified to be all less than 10μ. The size distribution of the cyclone inlet and outlet dust as measured by a Sierra Cascade impactor is given in Figure 11. Dust loadings at the inlet could be regulated in the range of 1 to 5 gm/m^3 while the finer outlet dust loadings were generally about one-tenth this range.

Curve 686415-B

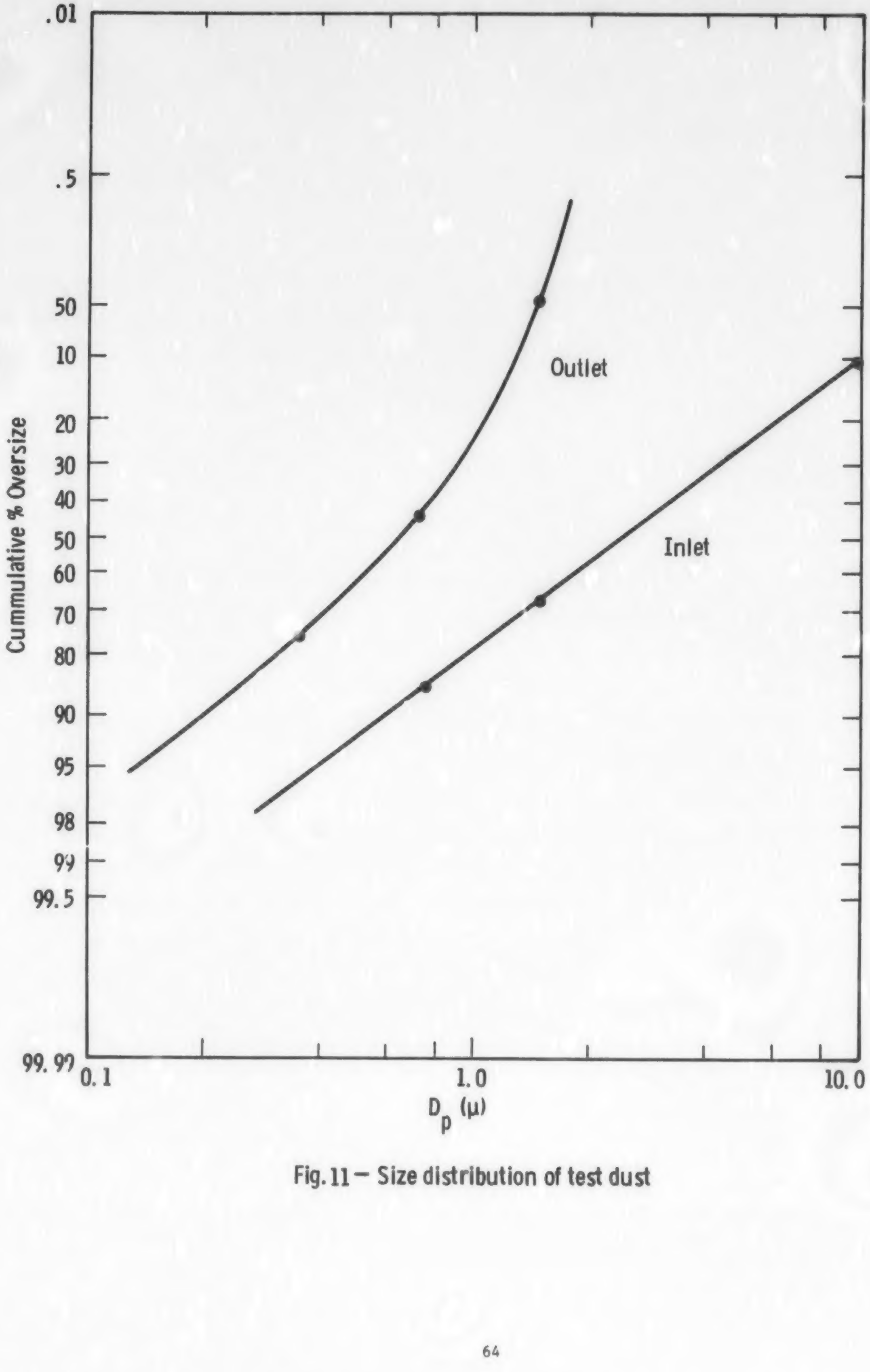

Fig. 11 — Size distribution of test dust

It has been assumed throughout this work that the cleaning technique used must allow continuous operation since methods that require cooling and removal of the filter media for cleaning are not thought to be practical for commercial applications. The cleaning method most frequently considered for such applications basically employs some form of back washing from the clean side of the filter. This flushing of the filter surface can be in the form of either a sharp pulse in the reverse direction or a gentler continuous flow for a longer period of time. In applications where the filter can physically withstand the pulse cleaning option, it is usually preferred since it is quick and requires less cleaning gas. For the screening tests, continuous flow cleaning was accomplished by simply isolating the filter outlet from the exit sampler and then allowing filtered house air to flow back through the filter from the clean side. The pulsed cleaning option was tested by charging a 0.385 ℓ vessel to the desired pressure and then venting this vessel to the clean side of the filter through a solenoid valve.

The system for mounting the 3M Thermacomb material was somewhat more complicated because of the unusual configuration of the material. Acurex/Aerotherm provided a mounting plate and top retainer similar to the one shown in Figure 12. A plexiglass enclosure was fabricated to mate with the support plate provided so the filtration process could be visually observed. The completed test jig is similar to the one shown in Figure 13. It was necessary to seal the Thermacomb to the retaining and support plate with RTV to prevent leaking.

Results. The pressure drop vs. flow characteristics for some of the thick walled elements is summarized in Figure 14. The most porous Selas filter and the FMI material had relatively low pressure drops (6.5 and 3.8 kPa) at face velocities of 20 m/min, while the two fine pore Selas materials had relatively high pressure drops in the range of 80-100 kPa at the same face velocity. The two Zircar materials were received and tested after these tests were completed. The

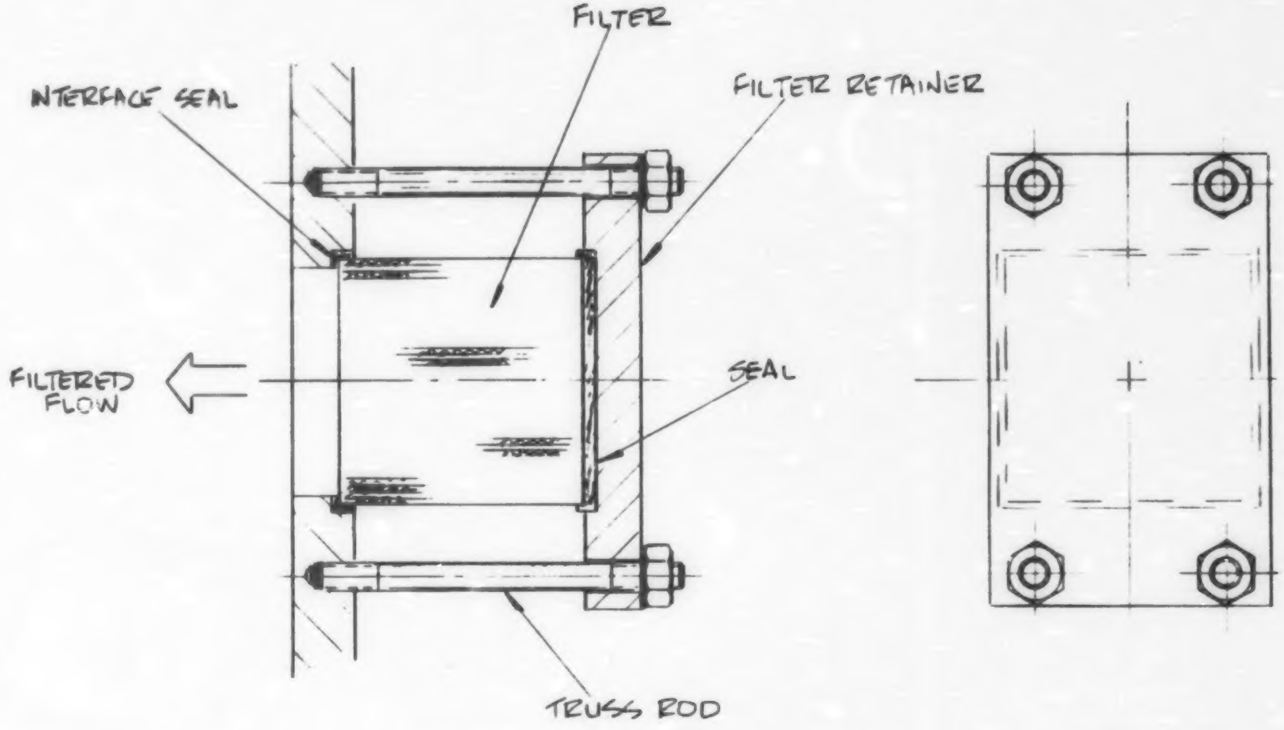
FILTER
INTERFACE SEAL
FILTER RETAINER
FILTERED FLOW
SEAL
TRUSS ROD

Figure 12. 3M element low temperature holder.

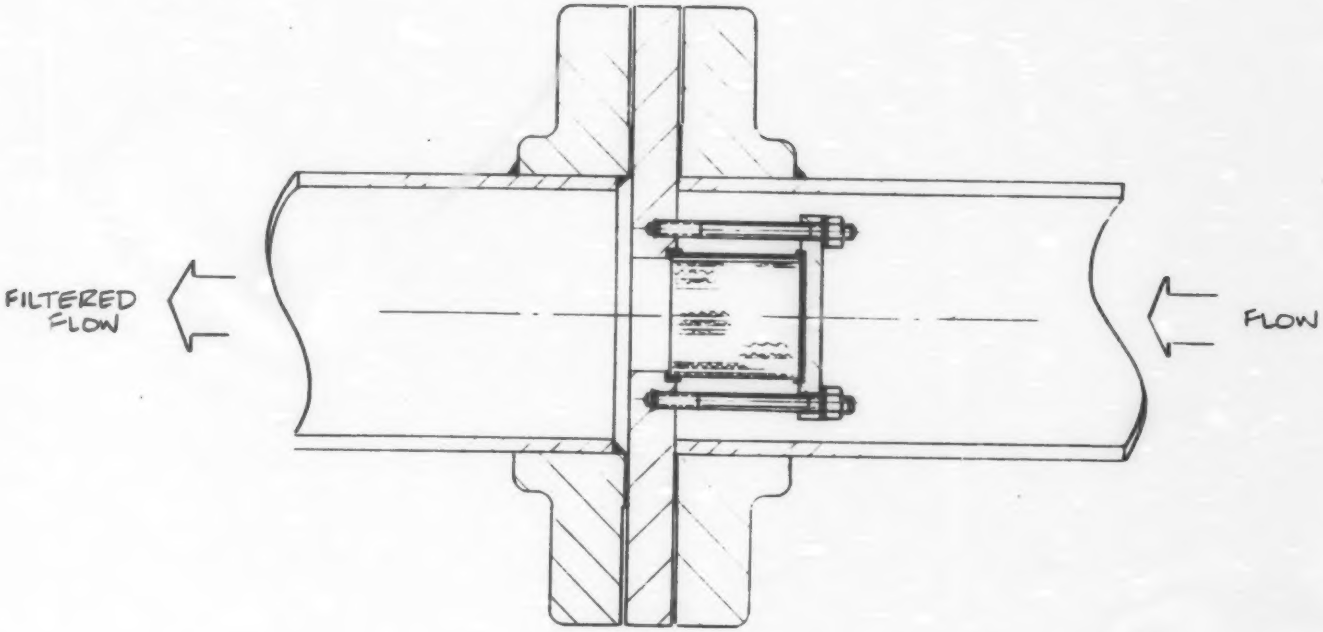
FILTERED
FLOW
FLOW

Figure 13. 3M element and holder mounted inside pipe.

Curve 686421-A

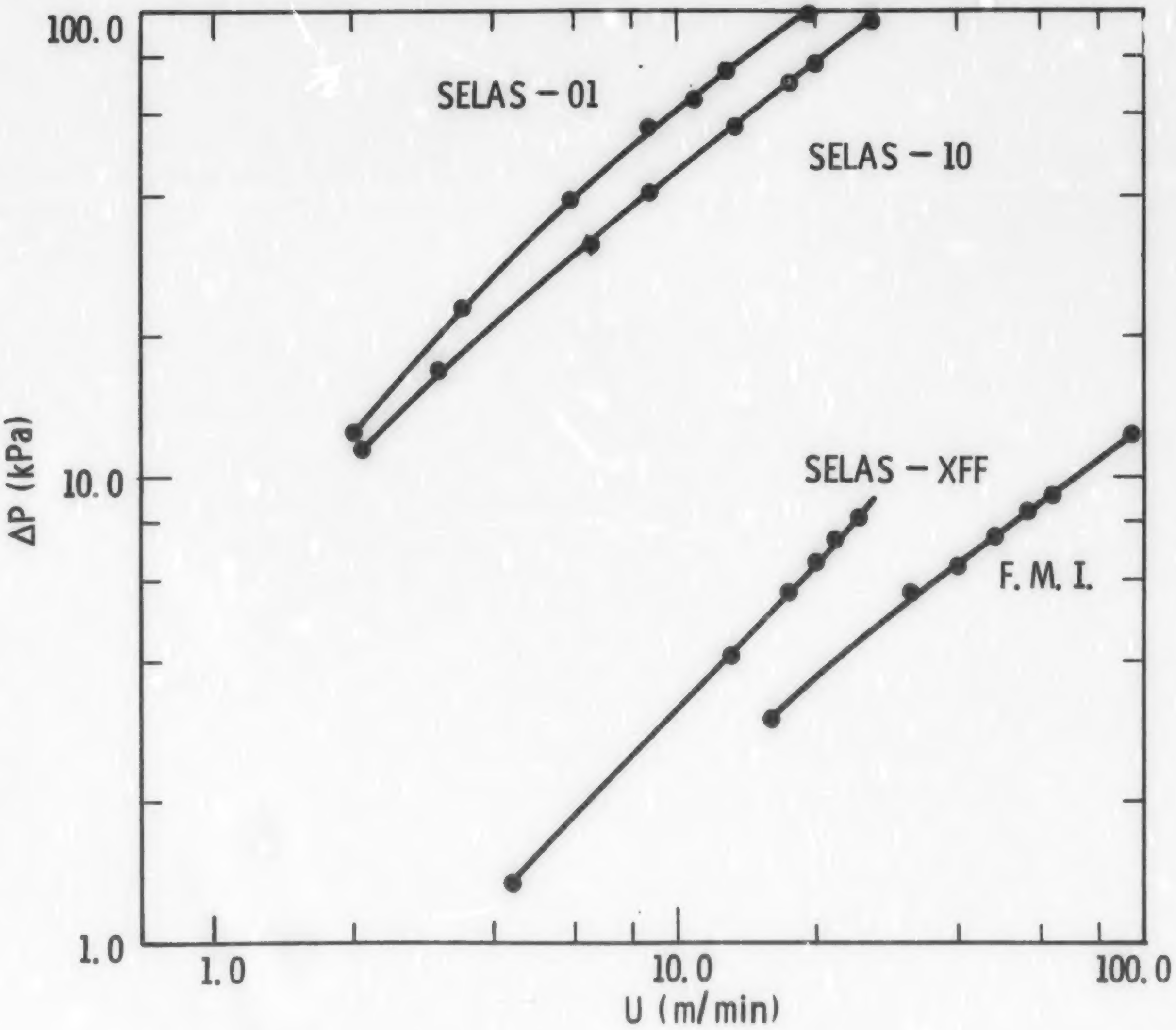

Fig. 14 – Face velocity vs pressure drop for thick walled filters

Zircar ZAL-15 proved to have virtually the same pressure drop-flow characteristics as the FMI material. The Zircar 135C alumina paper tube had a flow resistance slightly higher than the Selas XFF and the FMI material as is shown in Figure 15.

The screening tests with the 3M Thermacomb were carried out on a cube of that material roughly 5 cm on a side with approximately 0.029 m^2 of surface area for flow. The results of this test are shown in Figure 16. At a face velocity of 10 m/min the filter had a pressure drop of approximately 10 cm H_2O or 0.98 kPa which indicates a resistance to flow that is lower than the FMI material. Much later in the program, 15 cm cubes of Thermacomb were tested. These elements had an estimated filter area of 0.804 m^2. At a pressure drop of 4 kPa a flow of 8 m^3/min or nearly 10 m/min was measured. This is a slightly higher pressure drop than observed in the small cube and it corresponds to a flow resistance that is virtually the same as the FMI material (Figure 17). The W. R. Grace & Company samples were received late in the program and were not tested with clean flow.

Upon completion of pressure drop-flow measurements, experiments sampling the test dust were begun at ambient conditions to characterize filter efficiency and cleanability. The filtration runs with the thick walled elements were flow tests with typical inlet mass loadings in the range of 0.05 to 0.2 gm/m^3. The results from the tests of the three Selas materials are shown in Figures 18, 19 and 20. Experiments with the most porous Selas element (XFF) were carried out at two face velocities, 11.9 m/min and 3.0 m/min. During these runs no penetration of dust could be measured, and the pressure drop vs. time curves indicated that the filter could be cleaned repeatedly. The cleaning cycle consisted of a single pulse from the 0.385 ℓ vessel charged to 1 atm pressure. This element seemed to suffer a small irreversible increase in pressure drop after being exposed to the test dust, however, this increase in pressure drop did not appear to persist in subsequent cycles. The other two Selas materials were tested at a face velocity

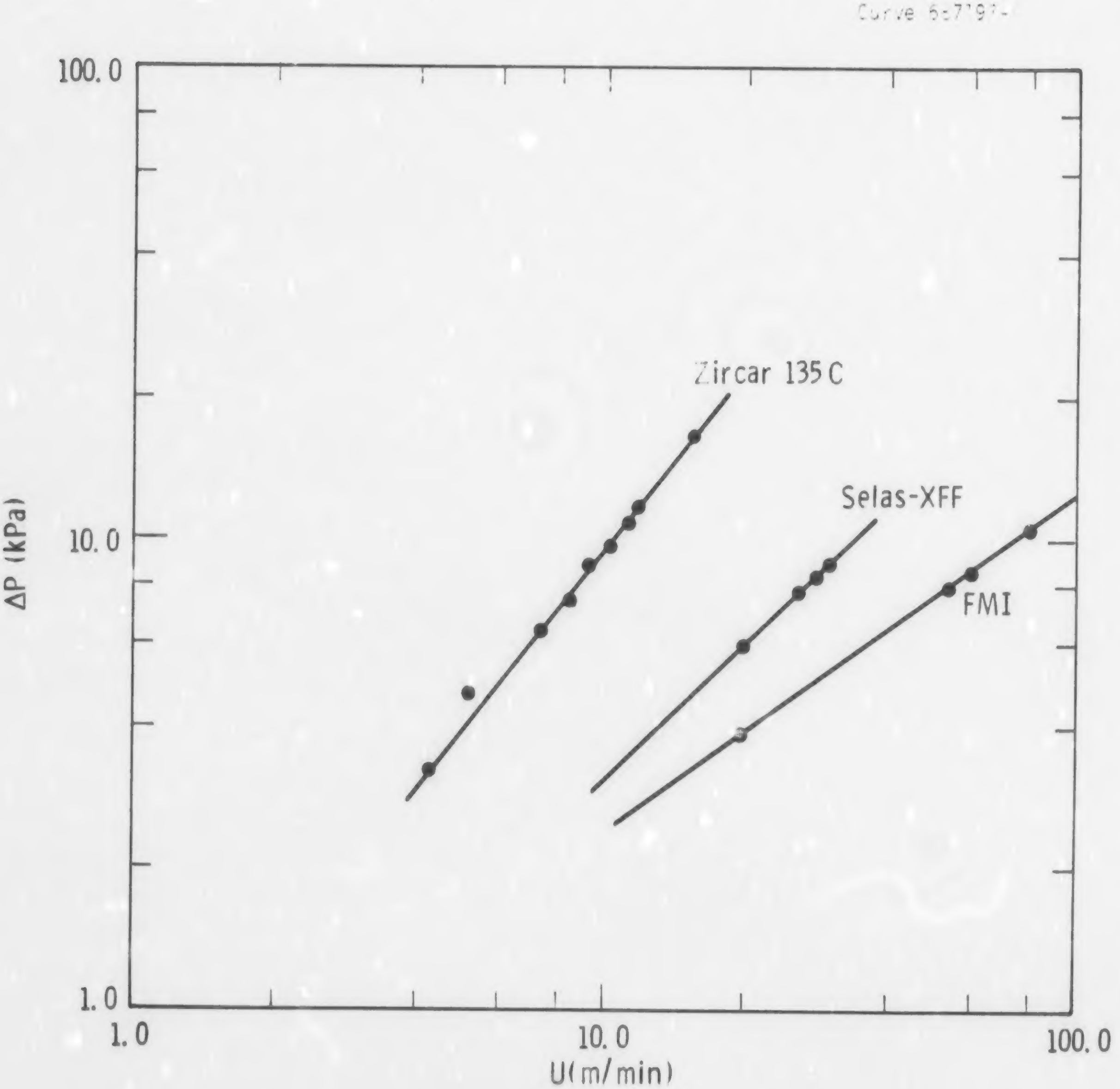

Fig. 15 — Δ P vs U for Zircar 135C material

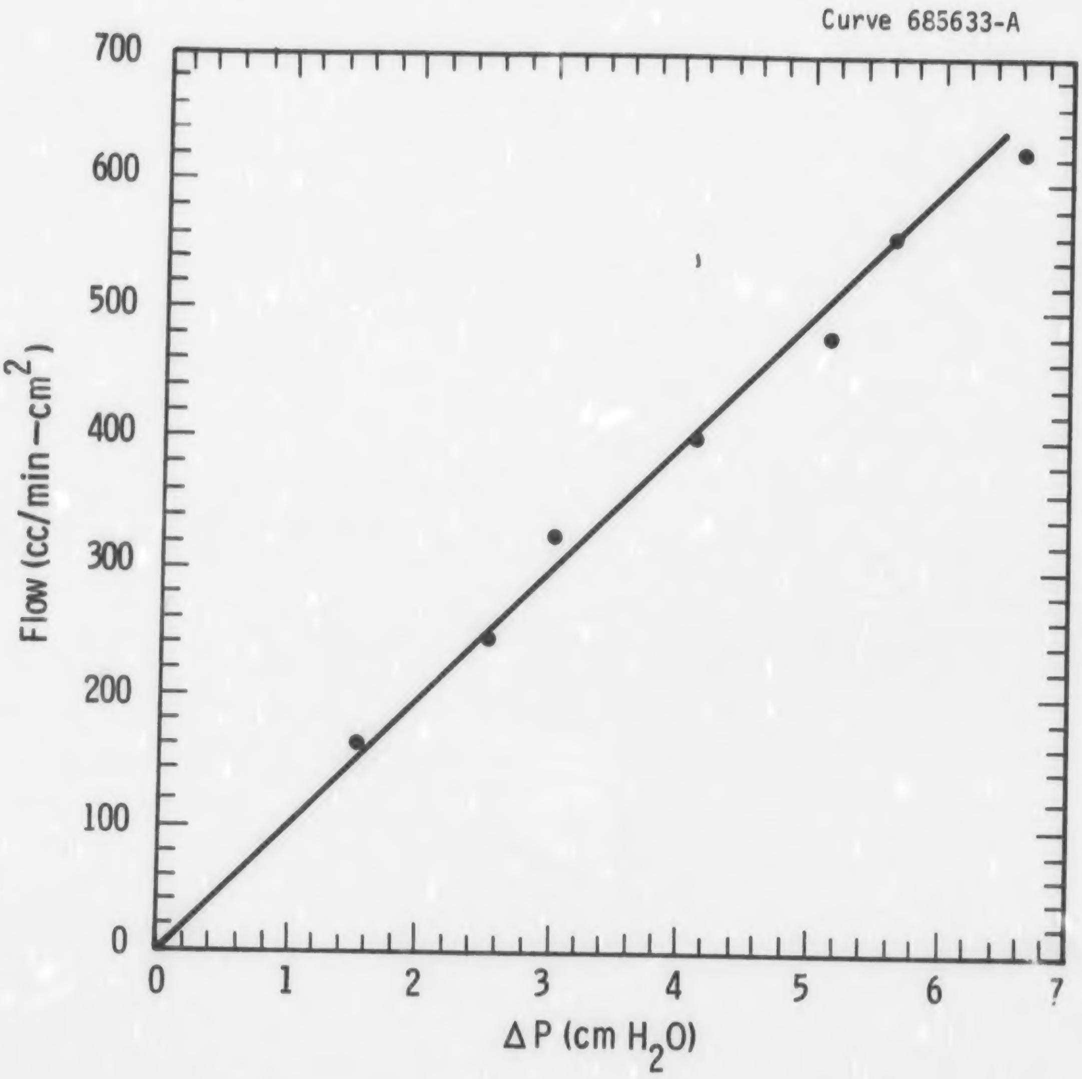

Fig. 16 – Flow vs. pressure drop for 3M thermacomb

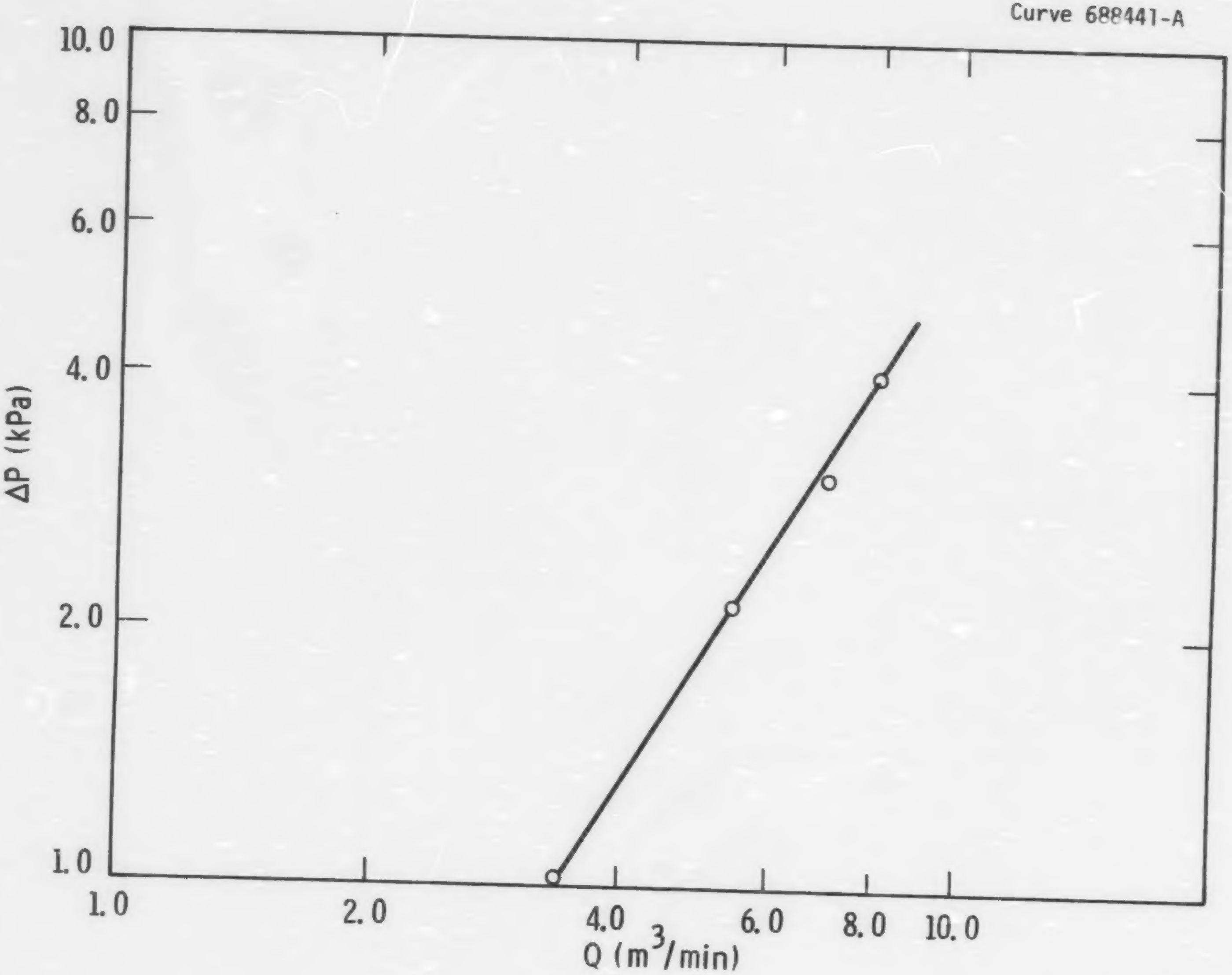

Fig. 17 — Pressure drop vs flow for clean 15.25 cm thermacomb cube

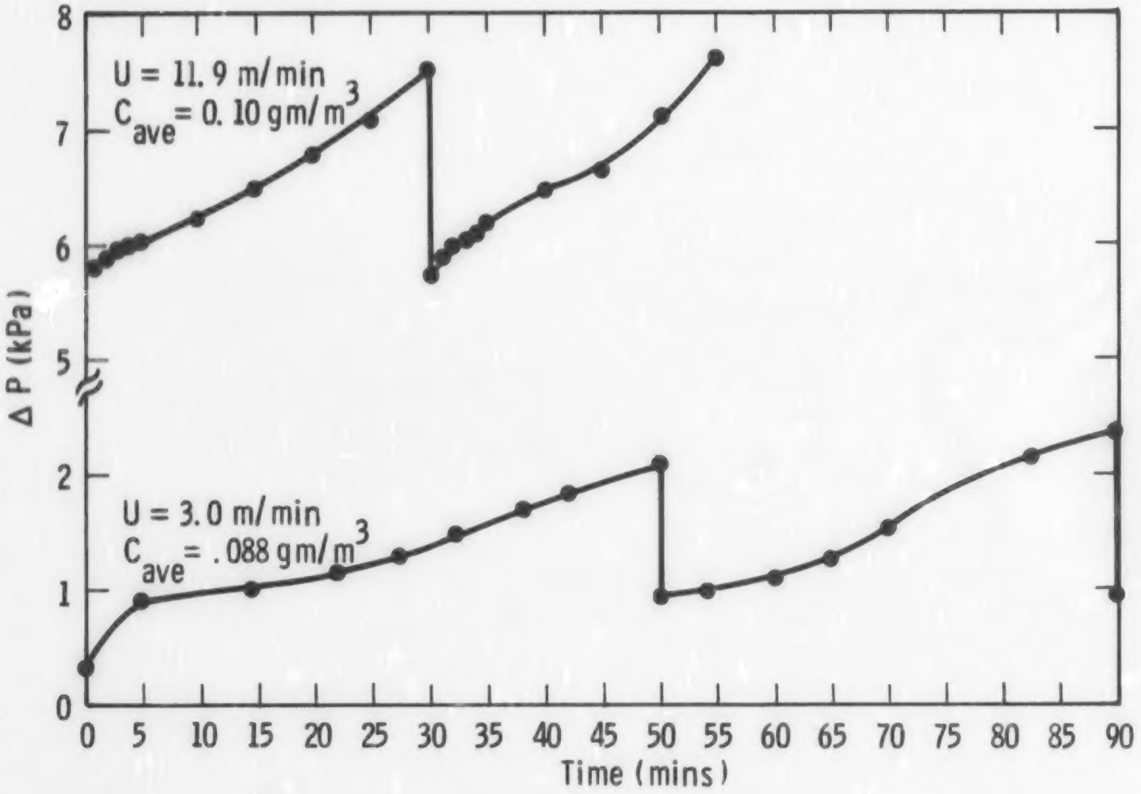

Curve 686422-A

Fig. 18 – Δ P vs time for SELAS – XFF

Curve 586419-A

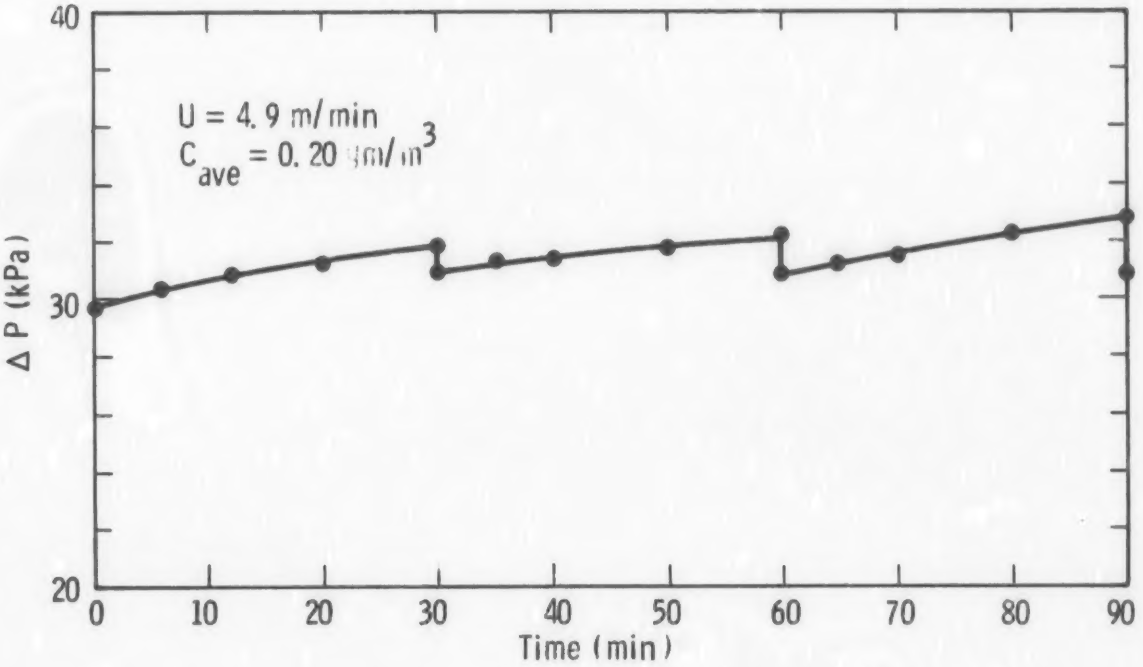

Fig. 19—Δ P vs time for SELAS – 01

Curve 686420-A

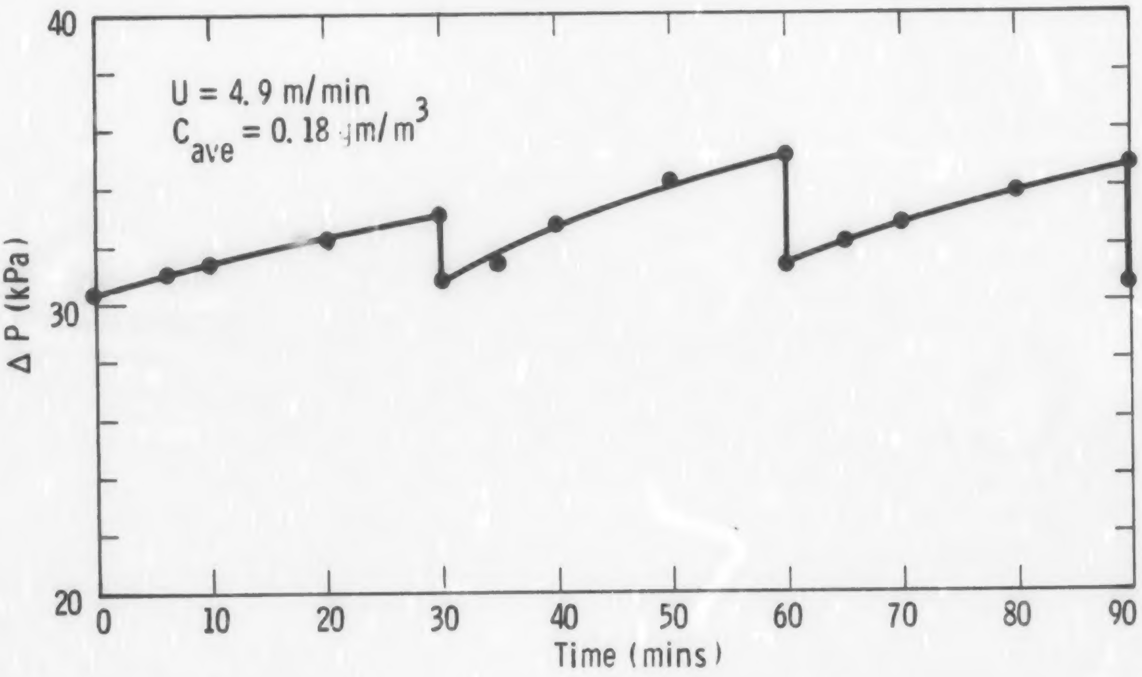

Fig. 20 – ΔP vs time for SELAS – 10

of 4.9 m/min and had substantially higher pressure drops. Again, no dust penetration could be measured, however, there was some difficulty in cleaning the filters and the pulse pressure had to be increased to 2 atm to obtain to maintain a stable cycle. It was noted that these less porous materials did not seem to suffer as much irreversible increase in flow resitance as did the more porous XFF sample. The data from tests with the FMI material are presented in Figure 21. As with the other materials virtually no penetration was measured during this test. This material experienced only a slight increase in flow resistance after having been exposed to the test dust. This material was readily cleaned to a repeatable degree by a one atm pulse. Tests with the Zircar ZAL-15 material gave the results presented in Figure 22. As can be seen there was a small increase in the initial pressure drop after the first cycle, but this increase leveled out after a few cycles. The magnitude of the increased resistance to flow is shown in Figure 23 where pressure drop vs. face velocity of the clean "as received" material is compared with the material after one cycle. The holder used in these tests did not allow the use of a high pressure pulse for cleaning so a continuous back flush at about 1 atm for 2-5 seconds was used to clean the filter. The tubular Zircar alumina paper (135C) was tested and found to be, like the other thick walled elements, 100% effective in removal of the test dust. The pressure drop vs. time data for this test are presented in Figure 24. The filter holder used did not allow a pulse type of cleaning so a continuous flow at about 0.7 atm for several seconds was used. Even without the pulse cleaning this material suffered virtually no irreversible increase in pressure drop over the few cycles examined. It is believed that this material could be formed with a wall thickness considerable less than the 0.47 cm used in these tests and not reduce its ability to remove particulates. This would reduce pressure drop and

Curve 686418-A

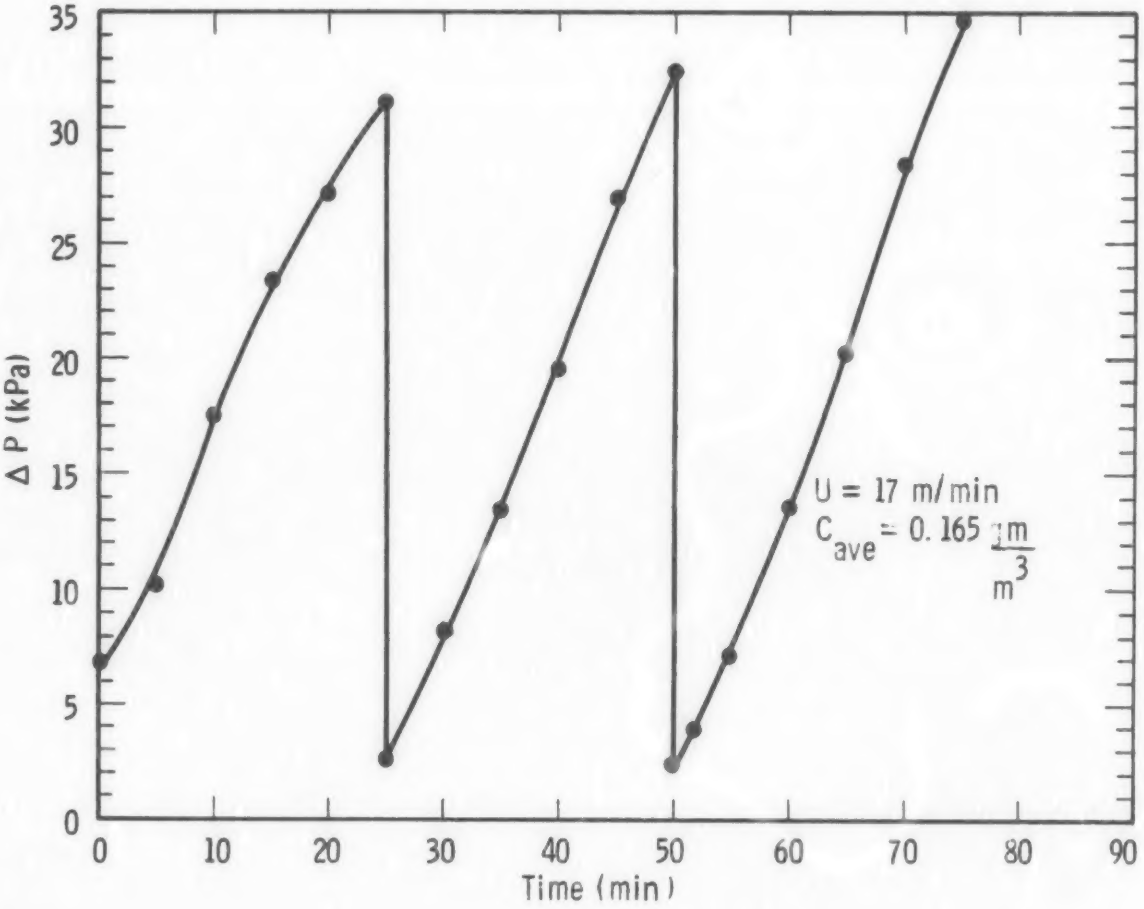

Fig. 21—Δ P vs time for FMI material

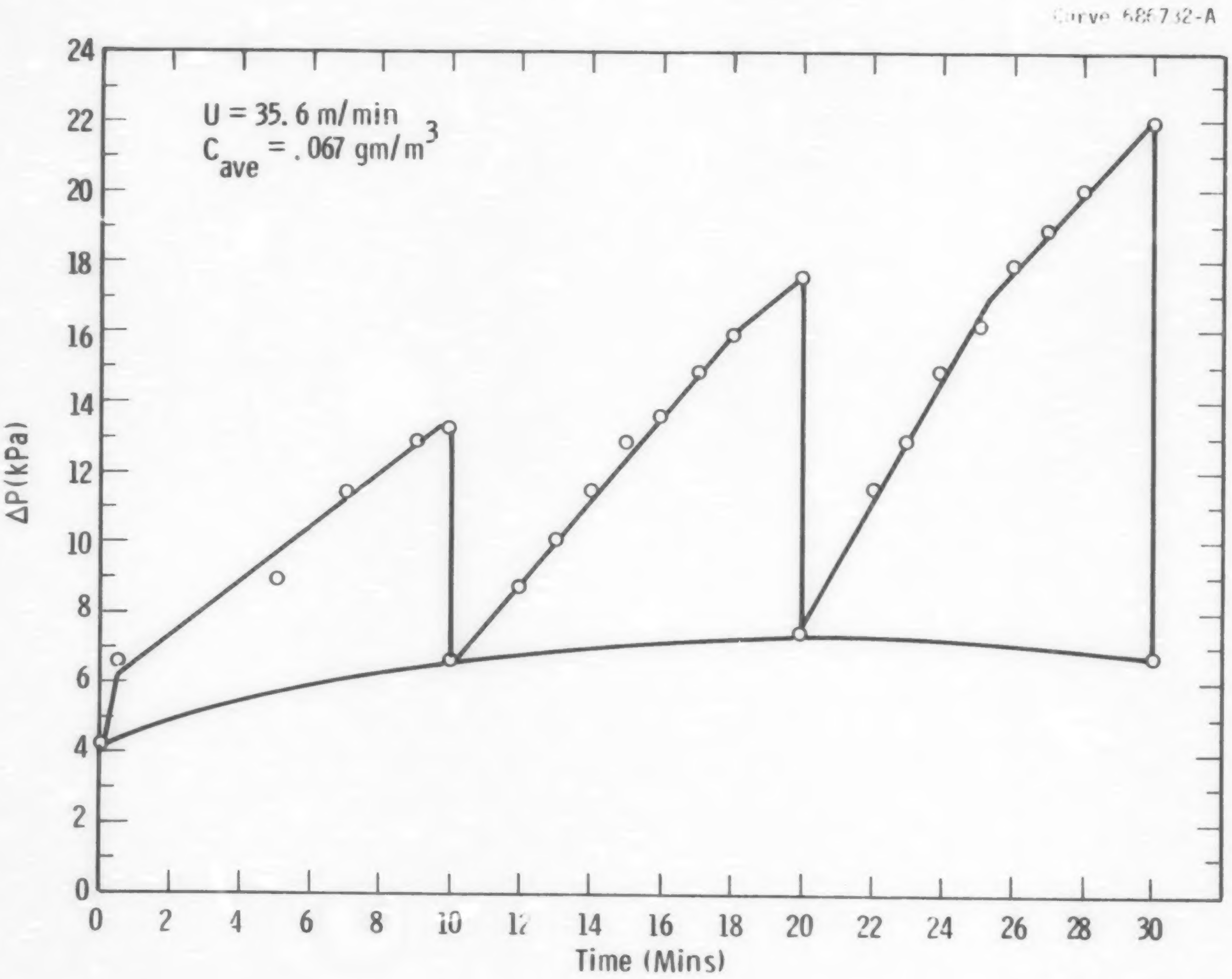

Fig. 22 — ΔP vs time for Zircar alumina board (ZAL-15)

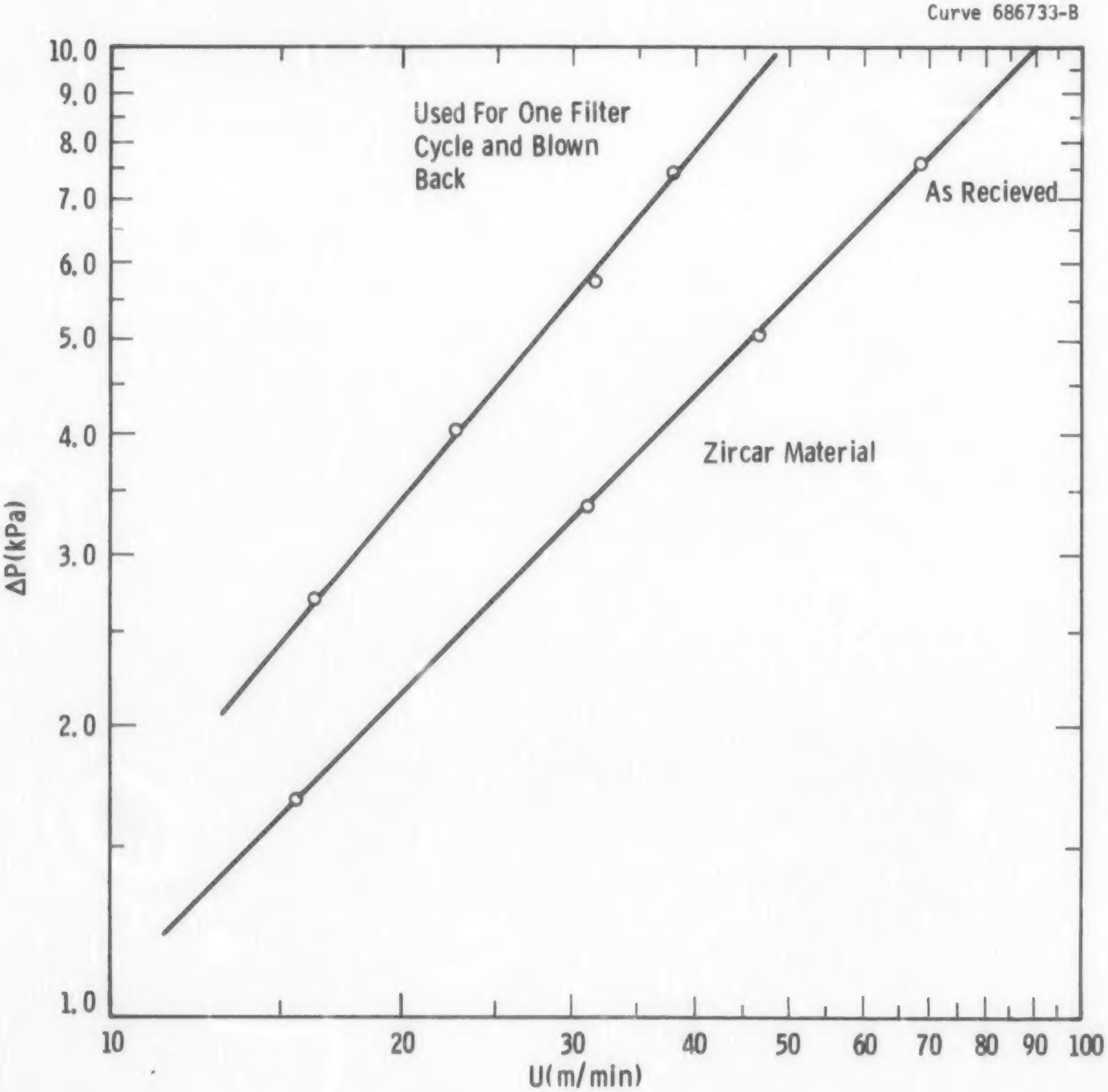

Fig. 23 — ΔP vs flow for Zircar alumina board (ZAL-15)

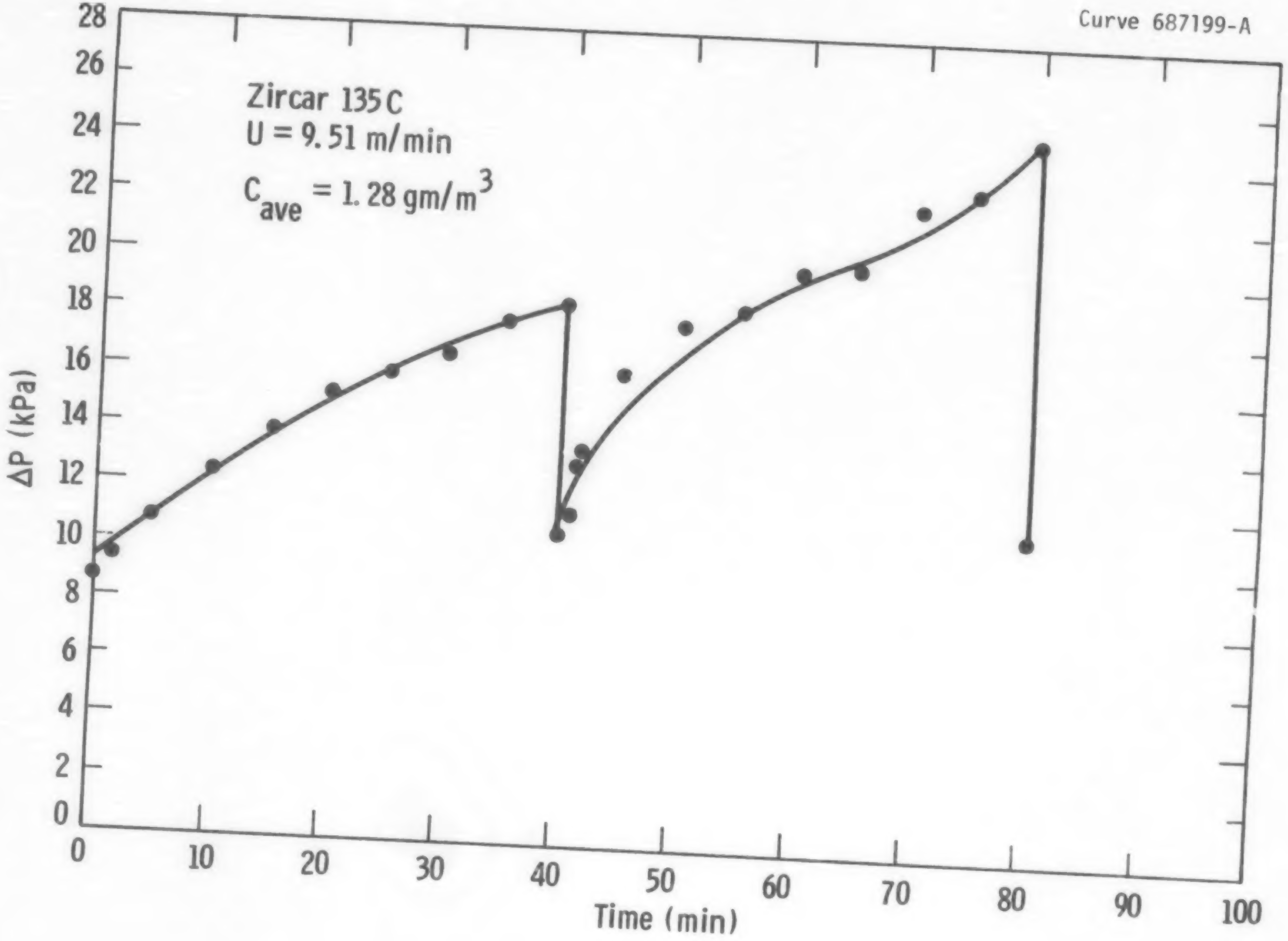

Fig. 24 — ΔP vs time for Zircar 135C material

make cleaning easier. Such a filter could be very attractive for hot gas filtration.

Filtering tests with the thin walled honeycomb structures was initially confined to samples of 3M Thermacomb since the W. R. Grace material was not received until late in the project. Tests with the Thermacomb material led to the following observations:

(1) Pressure drop rose rapidly during an initial transient period to a relatively steady pressure drop, from which it rose much more slowly at a constant rate.

(2) Some dust could be seen on the filter outlet walls but the amount did not increase after about a 5 minute period.

(3) Overall efficiencies based on typical sample times of 1 min. inlet and 20 min. outlet were around 98 to 99%.

(4) The size distributions obtained from inlet and outlet sampling with cascade impactors appeared to be the same, although there was considerable uncertainty in the outlet sample due to its small size.

(5) Reversing the flow of air removed considerable amounts of dust from the corrugations and returned the initial steady pressure drop to its previous value. Visual examination of the filter indicated that relatively few of the corrugations were swept entirely clean, but this apparently had little effect on the filter's performance.

Based on the observation that the inlet and outlet size distributions appeared to be identical it was concluded that relatively large holes existed in the filter. Finding the holes by examining the outlet side of the filter was not easy because the dust and filter material are virtually the same color. Eventually two corrugations were found to be leaking by probing each corrugation with a dark wire and checking for dust on the wire. Each leak was marked and a visual observation was made during a subsequent run. For the first several minutes a large amount of dust was passed through the leaks, but the leaks appeared to heal themselves in 3 or 4 minutes, after which no dust was seen to escape, for the remainder of the filtering cycle. This explained both the high overall efficiency observed, and the similar size distributions of the inlet and outlet. The corrugations that leaked were then plugged and a series of constant flow tests were run.

An attempt to set the dust loadings at 2.0 gm/m^3 was made, but problems with the dust dispensing apparatus did not allow good control of the feed rate. This necessitated the taking of several dust samples throughout the runs so that a reasonable average dust concentration could be recorded. At the beginning of each series of constant flow runs, the filter was removed and cleaned as completely as possible. At the end of subsequent cycles the filter was cleaned only by a pulse of back flush air. Figures 25 and 26 show the results of a series of runs carried out at flow rates of .085 and .057 m^3/min corresponding to face velocities of 2.92 and 1.95 m/min.

The behavior of the ceramic filter is remarkably similar to that of fabric filters, with a short transient of rapid increase in pressure drop followed by a steady, linear increase in ΔP with time. The data is consistent with filteration theory as indicated by the following analysis. The total pressure drop is considered to consist of a contribution due to the media ΔP_m, and due to the accumulated cake, ΔP_c.

$$\Delta P_{tot} = \Delta P_m + \Delta P_c$$

For given gas properties, the pressure drop across a filter media, ΔP_m, is proportional to the face velocity, U and filter thickness, L_m. The pressure drop across the cake is similarly proportional to the face velocity and cake thickness L_c. If a constant dust concentration, C, is assumed, the cake thickness is proportional to the produce of the measured variables, UCt, where t is time. The total pressure drop for a given gas, temperature and filter is given by:

$$\Delta P_{tot} = K'U + KU^2tc,$$

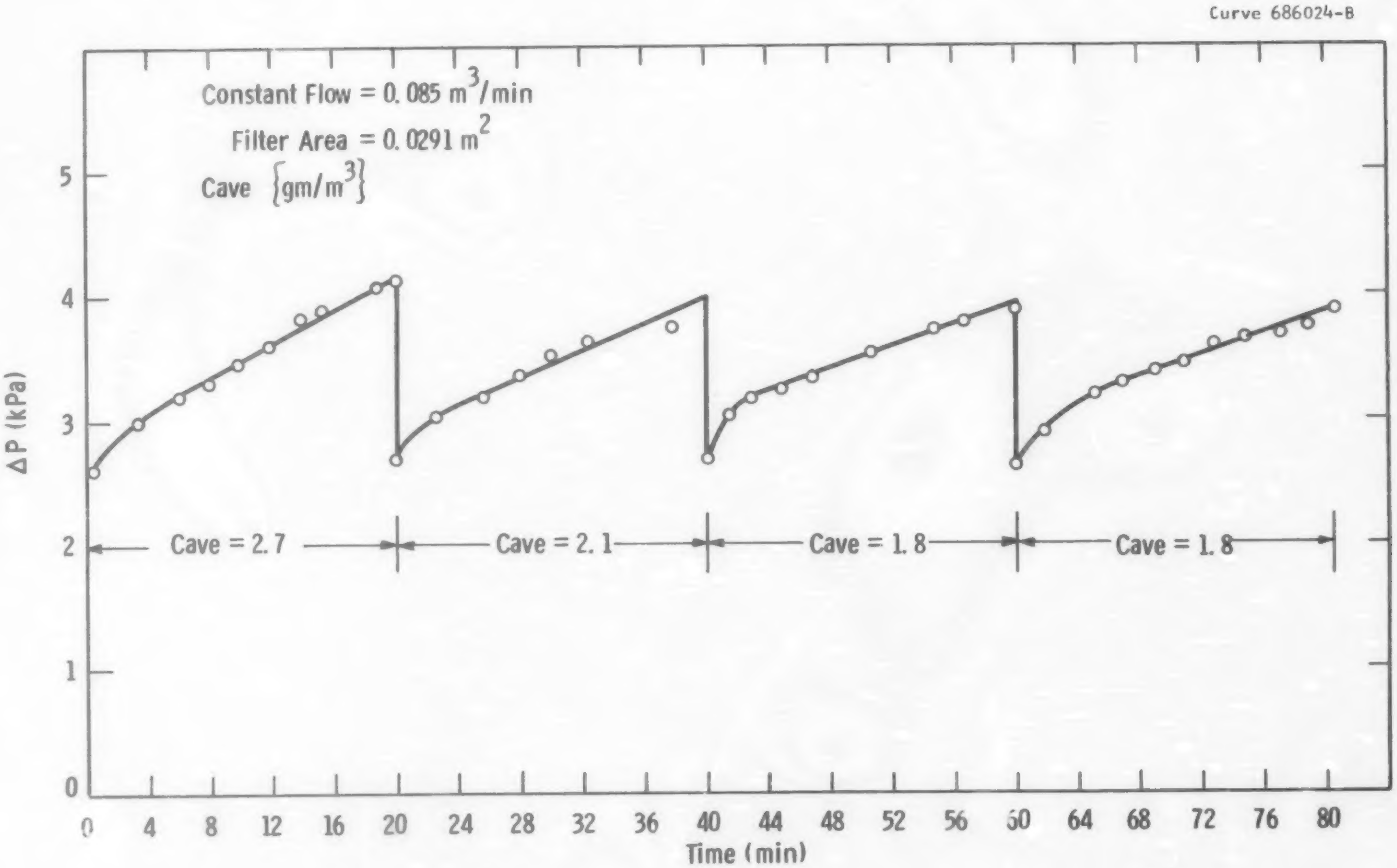

Fig. 25 — Pressure drop vs time for ThermaComb

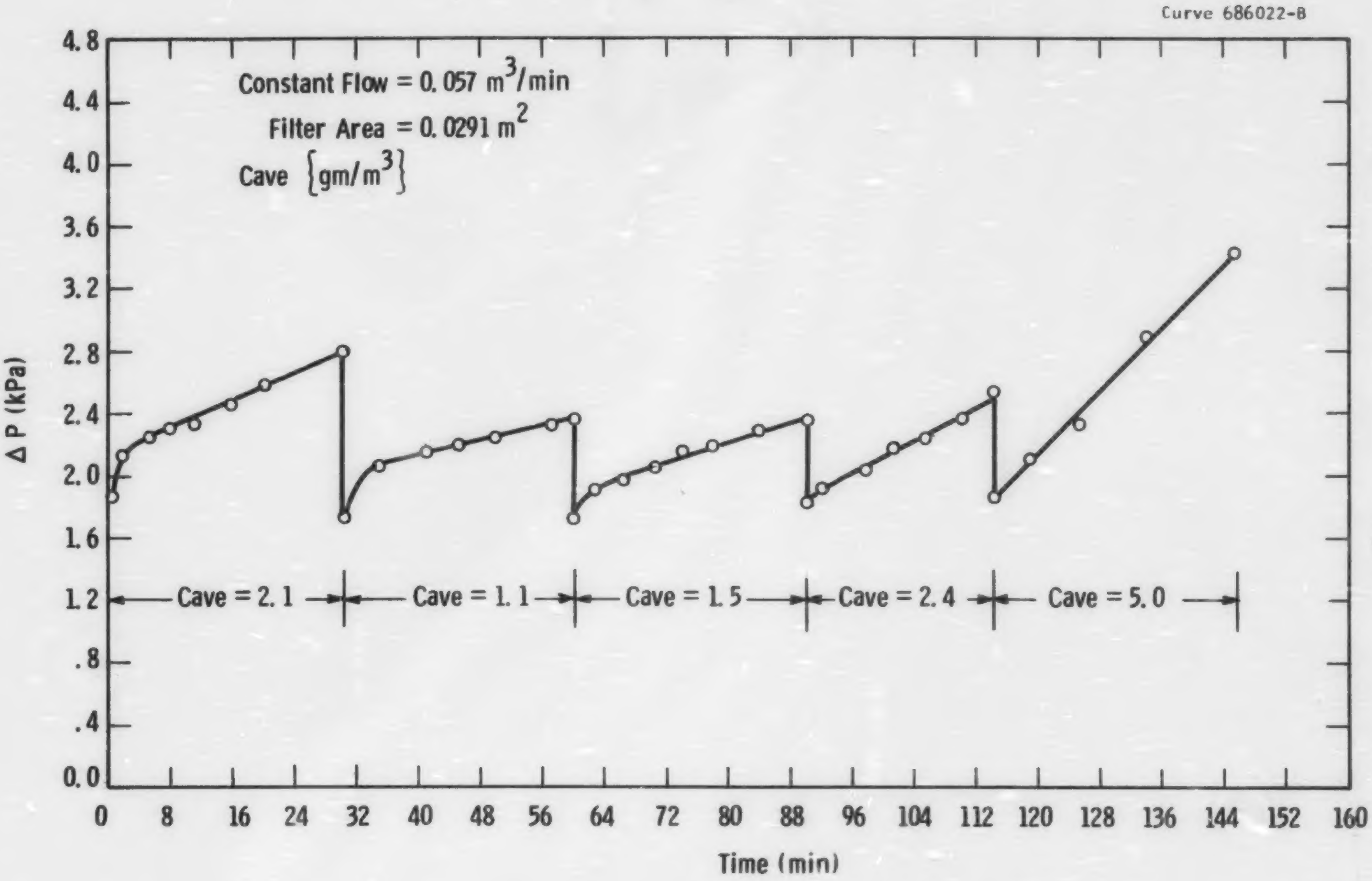

Fig. 26 — Pressure drop vs time for ThermaComb

where K' and K are constants for a given filter and incompressible cake. The linear dependence of ΔP_{tot} on time is substantiated by the steady part of the ΔP_{tot} vs t curves. Confirmation of the assumed form of dependence of the variables U and C can be achieved by plotting the slope of the ΔP_{tot} vs t curves, normalized by division by U^2 vs C. This plot should yield a straight line with a slope equal to K which is a property of the filter cake and gas viscosity only. Figure 27 presents these data and indicates that the assumed form of ΔP_c is confirmed by all the data.

Two further observations of major importance were made concerning the initial steady pressure drop.

(1) The magnitude of the initial steady pressure drop was not prohibitively high.

(2) The initial steady pressure drop remained constant with the adopted cleaning technique.

At the relatively high face velocity of 3.25 cm/sec this ceramic filter had an initial steady pressure drop of about 2 kPa. A typical fabric filter at this face velocity could be expected to have a pressure drop in the range of 1 to 1.75 kPa.

The fact that the initial steady pressure drop does not appear to increase as the filter is cycled is most important as it indicates that no discernable deterioration of performance had occurred due to irreversible pore blockage. Figures 28 and 29 show the filter before and after cleaning by a pulsed back flush and a back flush accomplished by a more gradual flow. The pulse was accomplished by pressurizing a .385 liter vessel to 2 atm total pressure, and subsequently venting this vessel using a solenoid valve. The more gradual flush was accomplished by manually opening a valve allowing a flow of approximately 0.25 m^3/min to flow for 2 sec. Both methods return the initial steady pressure drop to the level obtained when the filter has been removed and carefully vacuumed clean, although visual examination of the filter reveals that neither the pulse nor the gradual flush completely clean the corrugations.

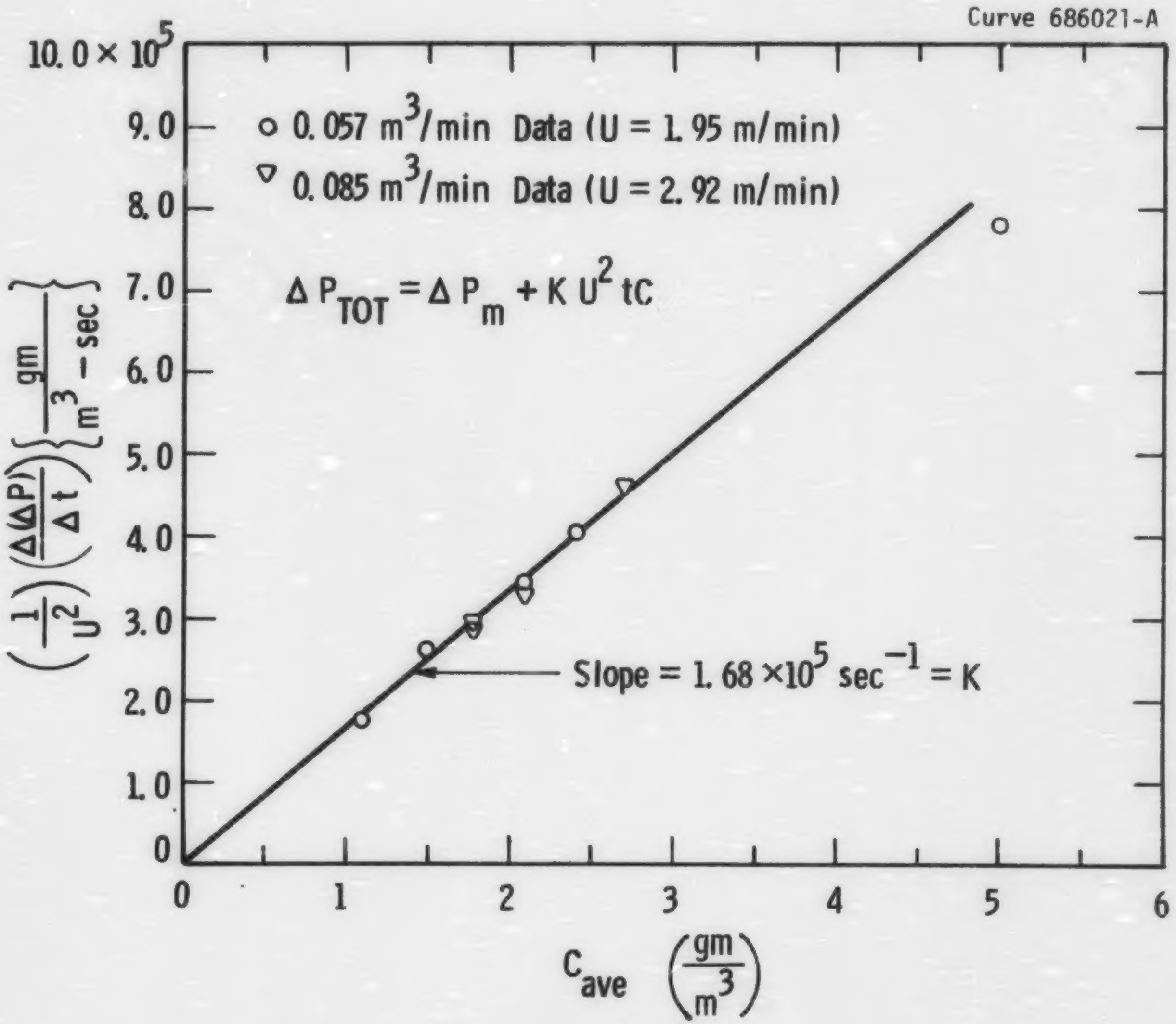

Fig. 27 — Determination of filter cake constant

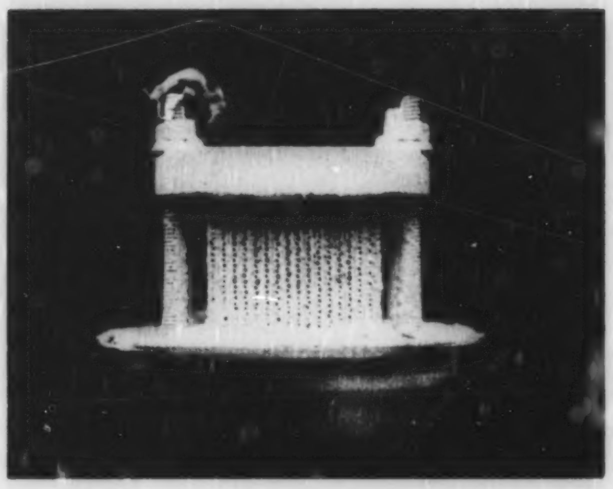

Before

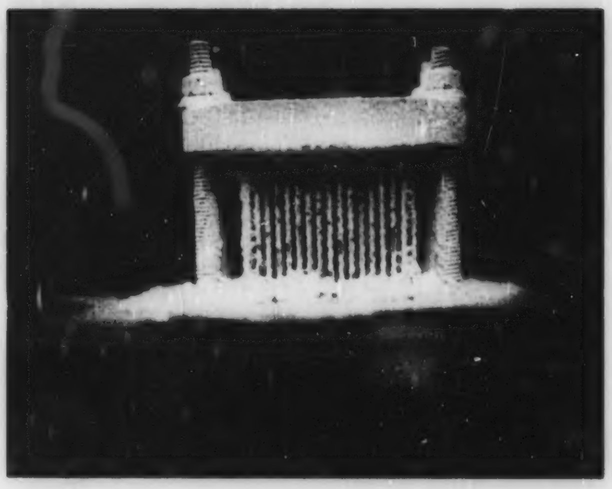

After

Figure 28. Before and after 103 kPa pulse.

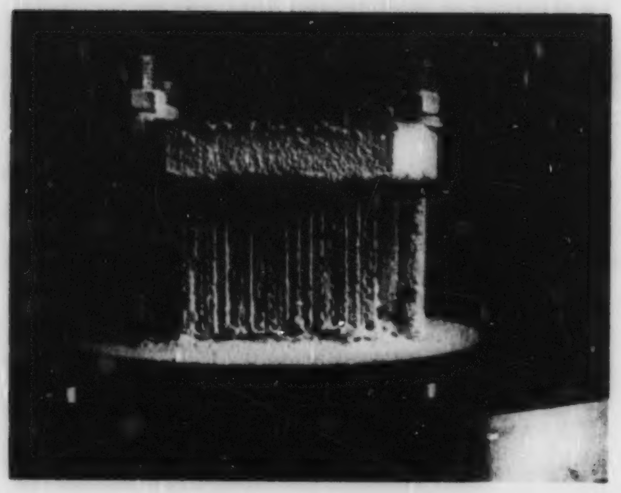

Before

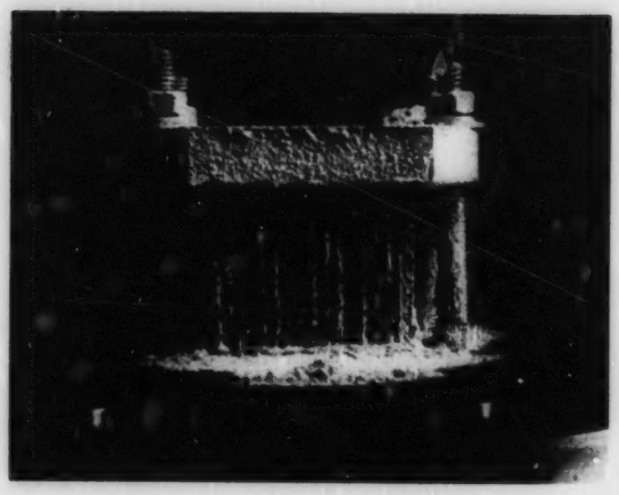

After

Figure 29. Before and after 17 m^3/hr flush for 2 sec.

Upon receipt of the W. R. Grace & Company materials a filtering test at ambient conditions was carried out. The data from this test are reported in Figure 30. At a face velocity of 0.483 m/min the initial pressure drop was about 1 kPa which is about twice that measured for the 3M Thermacomb material. The barrier thickness for the Grace material was measured at 0.38 mm or about twice that of the Thermacomb (0.2 mm) which explains the larger resistance to flow. In other respects the performance of this material quite similar to the Thermacomb, it being virtually 100% effective in dust removal and able to be cleaned to a constant level by a 1.36 atm pulse from a 0.385 ℓ container.

As can be seen from the data generated during the screening tests, several of the ceramic materials appear to have promise as hot gas filters. The decision to proceed to hot gas testing of the Thermacomb type materials was based on material's good performance as a filter and its unique configuration which allows large surface area to volume ratios.

Curve 689454-B

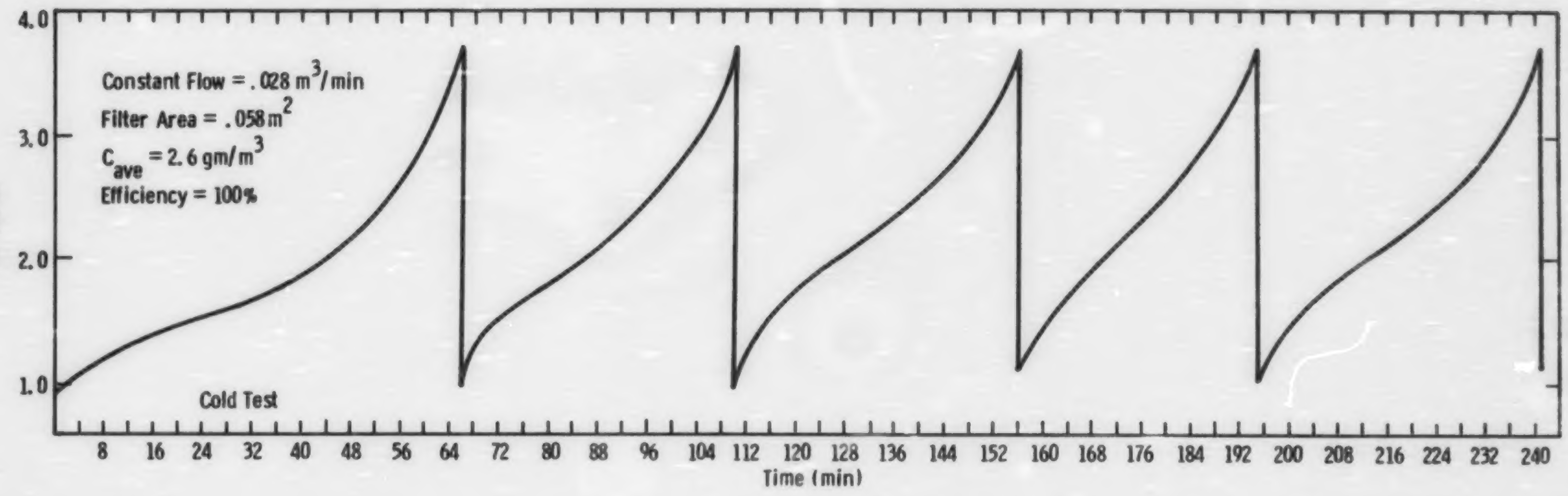

Fig. 30 — Pulsed purge = 137.9 KPa 3.0 seconds duration

4.5 LOW FLOW HIGH TEMPERATURE TESTS

Having made the decision to further investigate the properties of the thin walled, cross flow, honeycomb structures, it was necessary to construct an apparatus for hot bench scale experiments. The relatively few samples of Thermacomb available initially were of a size that was compatable with the roughly 5 cm cubes used in the screening test apparatus so it was decided to base the design of the hot low flow unit on this specimen size.

The first effort was directed toward the design of a filter holder and sealing system suitable for high temperature application. The design that evolved was similar in many respects to the screening test filter holder. A sketch of the device is shown in Figure 31. The inlet to the filter was up through a 3.8 cm square hole in the support plate. The actual filter element sat on a 0.64 cm groove around the inlet hole. The top retainer had a matching groove and through hole, however, a cylindrical containment was welded over the hole in the retaining plate and a tubing connection through the top plate of the jig was made. This arrangement allowed a cleaning pulse to be administered straight down the corrugations in which the collected dust accumulated. The cylindrical region was packed with 20 mesh alumina chips to distribute the pulse over the entire 3.8 by 3.8 cm area. The alumina chips were retained by a stainless steel screen over the hole. During filtration the cleaned gas emerged from two vertical sides of the Thermacomb and exited the filter jig through the outlet indicated in the sketch. During this period a valve on the central, dirty side line was shut preventing flow straight through. Cleaning was accomplished by pulsing either or both the dirty side of the filter and the clean side. The dust which had accumulated in the vertical channels of the filter was knocked down through the inlet hole and into a collection hopper.

A schematic of the test facility is shown in Figure 32. During the filtering mode of operation, dusty air flowed through a normally open solenoid valve V_1. Valves V_2 and V_8 were closed forcing the gas

Dwg. 1684B44

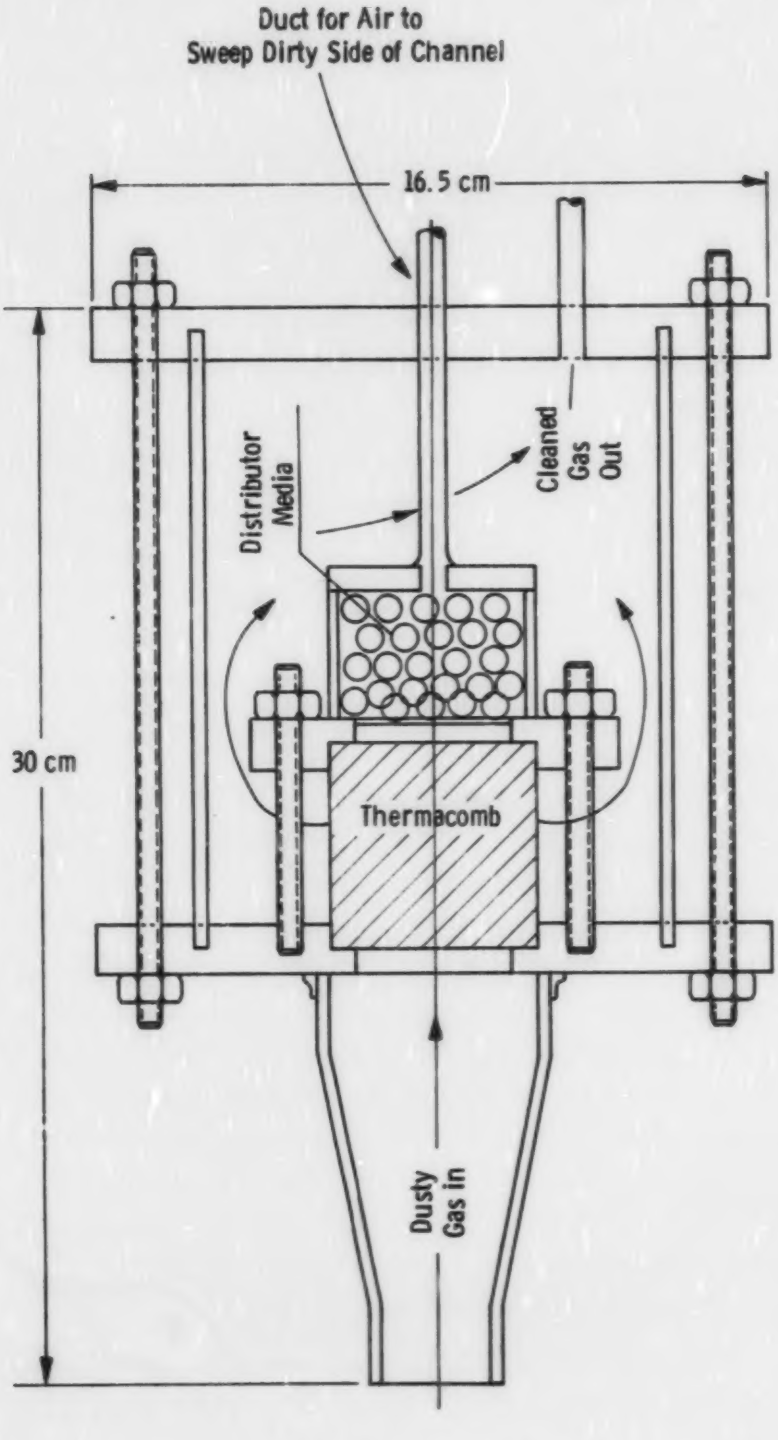
Duct for Air to Sweep Dirty Side of Channel
16.5 cm
Distributor Media
Cleaned Gas Out
30 cm
Thermacomb
Dusty Gas in

Fig. 31 — Hot thermacomb test jig

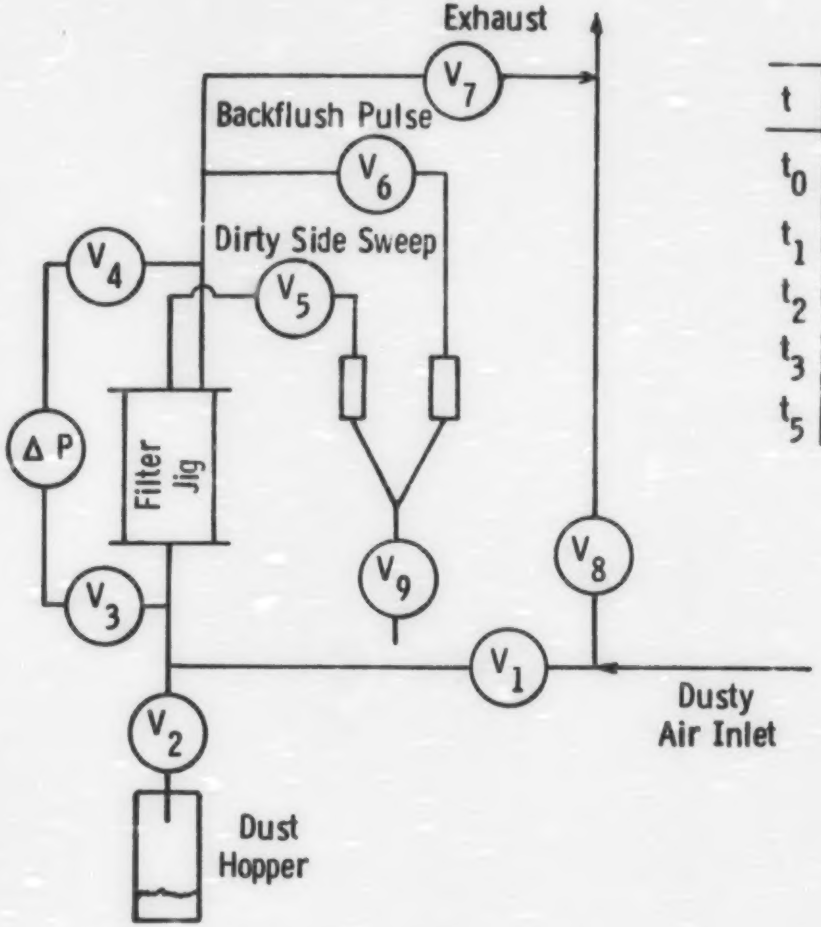
Exhaust
V_7
Backflush Pulse
V_6
Dirty Side Sweep
V_4
V_5
ΔP
Filter Jig
V_3
V_9
V_8
V_1
V_2
Dusty Air Inlet
Dust Hopper

Dwg. 6387A60

Cleaning Sequence

O – Open
C – Closed

t	V_1	V_2	V_3	V_4	V_5	V_6	V_7	V_8	V_9
t_0	O	C	O	O	C	C	O	C	C
t_1	C	O	C	C	C	C	C	O	C
t_2	C	O	C	C	O	O	C	O	C
t_3	C	O	C	C	C	C	C	O	O
t_5	O	C	O	O	C	C	O	C	C

Fig. 32 – Flow schematic and cleaning sequence for low flow-high temperature system

up into the filter jig and through the Thermacomb. The cleaned gas exited the system through V_7 into the house exhaust. During filtering V_3 and V_4 were open and the pressure drop across the filter was monitored by a Dwyer pressure gauge-switch. When the pressure drop reached the set point on the gauge the following sequence was initiated for cleaning. First V_3 and V_4 closed in order to isolate the gauge from the cleaning pulse. Valves V_1 and V_7 closed while V_8 and V_2 opened. This directed the dusty air supply into the by-pass leg and directly into the exhaust. Valve V_2 opened the dust hopper. Valves V_6 and V_5 could be opened allowing a high pressure cleaning pulse to vent into either the clean side of the filter holder or straight down the dirty side. When this was accomplished the entire sequence was reversed returning the system to its filtering mode. The final step was to repressurize the pulse holder with V_9 in preparation for the next cleaning cycle. Since this sequence had to be repeated hundreds of times a solid state automatic sequencer was designed and fabricated to step the valves through the proper sequence upon a signal from the pressure gauge-switch. This system worked very well since it allowed manual override at any point in the sequence, thus it gave the operator a great deal of flexibility for special operation while freeing him from tedious routine switching.

Heat was supplied to the system by placing the entire filter jig in a vertically mounted tube furnace which was 17.8 cm inside diameter by 38 cm long. In later tests it was discovered that internal Thermacomb temperatures were not nearly as high as the exit gas temperature because of air cooling and poor thermal conduction in the filter. This necessitated the installation of an additional tube furnace in the feed line between V_1 and V_2. This preheated the inlet air and eliminated the very poor temperature distribution in the filter element. The cleaned hot air was cooled by water cooled jackets around the exhaust piping. The cooled air flowed through a fixed resistance and by measuring the temperature and pressure drop at the resistance the flow rate was determined.

Dust was dispersed and fed to the system using a "Modified" Harvard dry dust dispenser. Some problems in feeding dust were experienced because of the relatively high back pressures experienced. This caused low suction at the ejector and poor dust feeding control. This problem was eliminated by placing the rotating dust dispenser in a pressurized containment. By maintaining the pressure at or slightly above the filtration pressure, fairly uniform trouble free dust feeding was achieved.

Photographs of the test assembly are presented in Figures 33 and 34.

It was anticipated that sealing the rigid honeycomb structures in the support and top retaining plates would be a problem. However, it was discovered that gaskets cut from fiber frax were ideal for sealing and cushioning the element in the stainless steel plates. Sealing problems were minimized by smoothing the edges of the filter element with a ceramic adhesive called Ceramabond. This material could be used to create an actual bond between the fiber frax and the element, however, this was not found to be necessary.

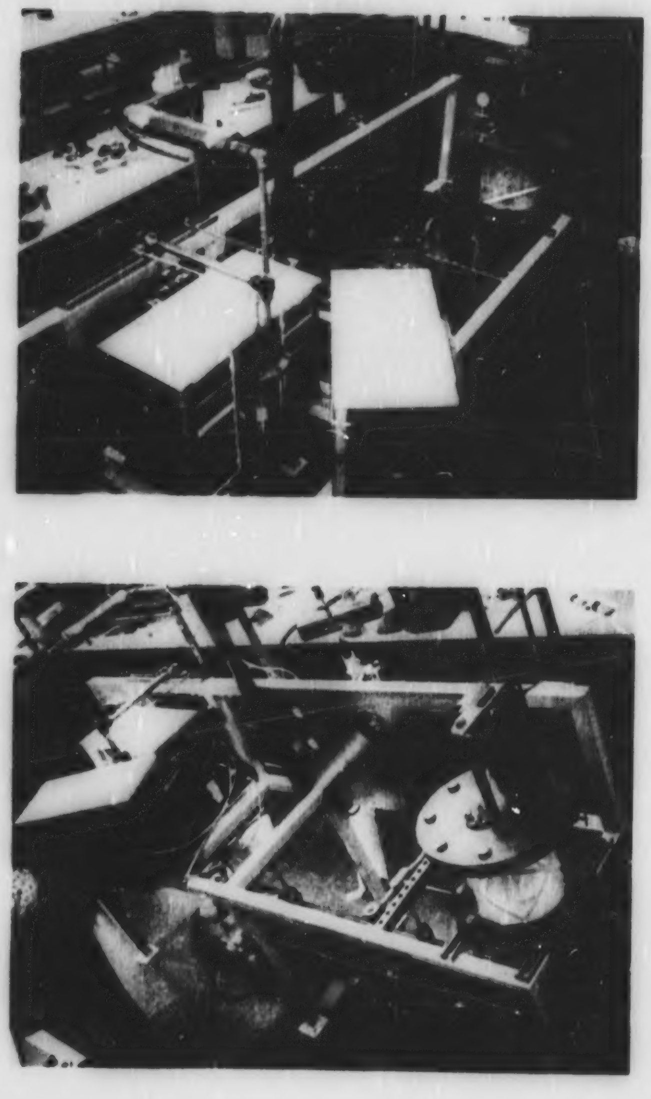

Fig. 33 - High temperature ceramic test facility

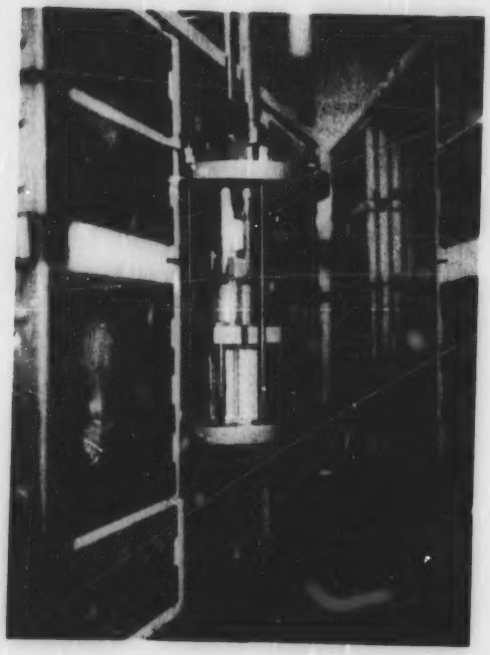

Figure 34. High temperature ceramic filter assembly.

Low Flow High Temperature Test Results

Completion of the fabrication of the low flow high temperature test apparatus was followed by several shakedown runs at ambient conditions to establish operating conditions and check equipment out.

A preliminary cold test was run with the 3M material at a flow rate of 0.072 m^3/min and an average concentration of 3.17 gm/m^3. Although the filter allowed no penetration, the initial pressure drop rose from 0.8 kPa in the first cycle to about 6.0 kPa in cycles 1 to 6. After 6 cycles, the initial pressure drop remained relatively constant. Subsequent tests at a lower flow rate (0.051 m^3/min) indicated that the initial pressure drop of 3.6 kPa did not increase with time. During these tests it was found that some problems existed when feeding dust in the low flow case because the ejector could not be run at full pressure. By putting in a by-pass which allowed some of the flow to be exhausted directly, the pressure in the ejector could be maintained and a low flow to the filter was also possible.

A series of hot runs were then undertaken, and during these preliminary hot runs two unexpected phenomena were observed. The first of these is demonstrated in Figure 35 which shows the filter performance at a flow of about 0.023 normal m^3/min (0.085 actual m^3/min at 1090°K). During this run no penetration of dust could be measured, and the initial pressure drop remained constant at about 3.6 kPa. This pressure drop was somewhat lower than expected based on previous experience. For a given ambient flow and pressure drop, one might expect a 2.5 fold increase in pressure drop due to viscosity effects and an additional 3.5 times increase due to the higher face velocity.

In the next series of tests another unexpected behavior was observed. The element was brought up to temperature with just the air flowing and with no dust being injected. The first cycle initial pressure drop was relatively low - see Figure 36. The subsequent initial pressure drops increased giving the appearance of very gradual blinding. However, if

Curve 687709-B

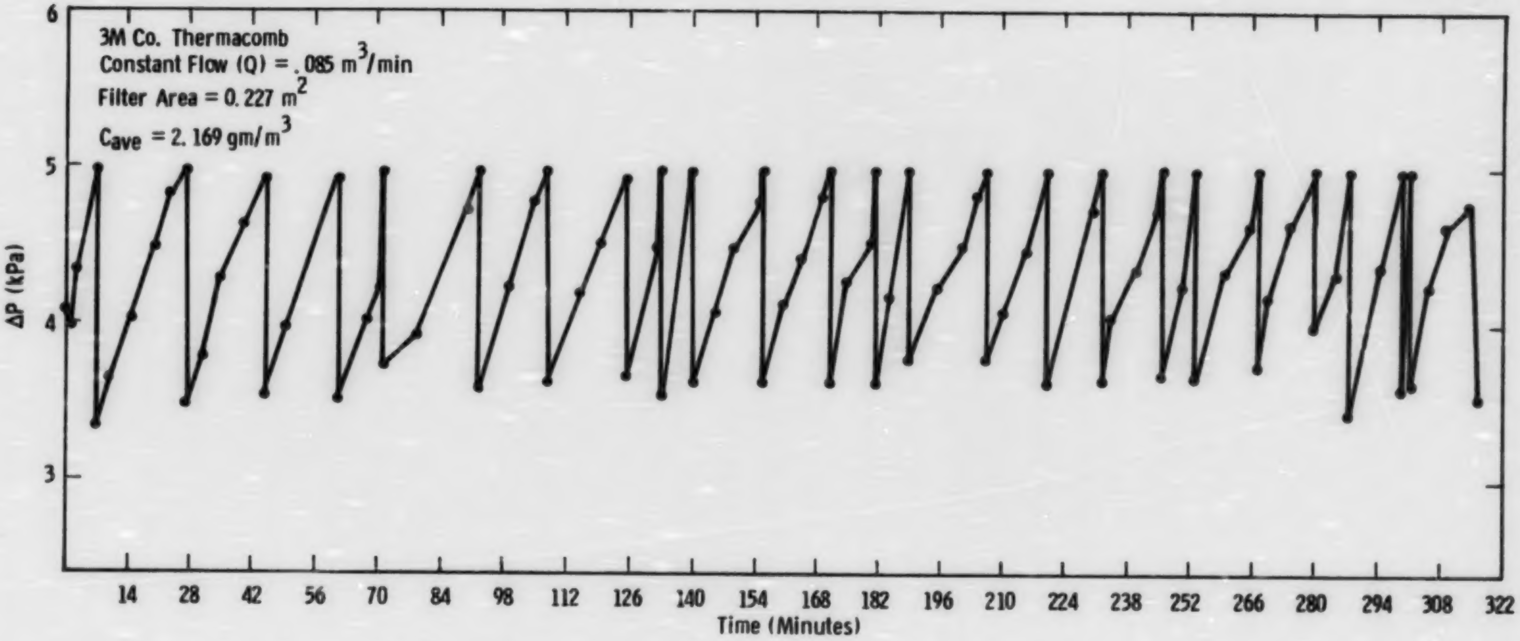

Fig.35- Pressure drop vs time at (1090° K) no penetration

the dust was shut off, and the unit was left hot with only the air on for an hour or so, the filter could be cleaned by normal back pulse and the low initial pressure drop regained. Figure 37 is the same filter run the day after the run shown in Figure 36. The mass flow rates in Figure 36 and 37 are the same, however, the test shown in Figure 37 was conducted at ambient temperatures. It can be noticed that the problem does not seem to exist at ambient conditions. The possibility of some chemical reaction between the limestone dust and the filter material was considered, but it is difficult to propose a suitable explanation for these observations. Representatives at 3M Company were consulsted and they could not offer any explanation for this behavior. This phenomena has been observed frequently throughout the entire test program and a satisfactory explanation has not been established.

During these preliminary hot tests a series of runs were made to explore the cleaning cycle. These tests indicate that over the range of conditions tried the cleaning cycle was relatively insensitive to length of pulse. Pulse times from 1 to 3 seconds were tried with pressures from .77 atm to 1.3 atm.

It was also discovered that if the pulse down the dirty side was administered second, it could lead to slightly poorer cleaning as evidenced by higher initial pressure drops. It is believed that the first pulse from the clean side knocks the cake loose from the wall and the bulk of the collected material out of the channels. When the second pulse is administered to the dirty side it merely compresses the remaining dust against the wall rather than sweeping it out of the filter.

The less than 100% collection efficiencies recorded in these tests were due to improper sealing of the specimen in the jig. When corrected no penetration was observed.

In attempt to discover the reason for the lower than expected pressure drop it was decided to check the internal temperature of the Thermacomb sample during a run.

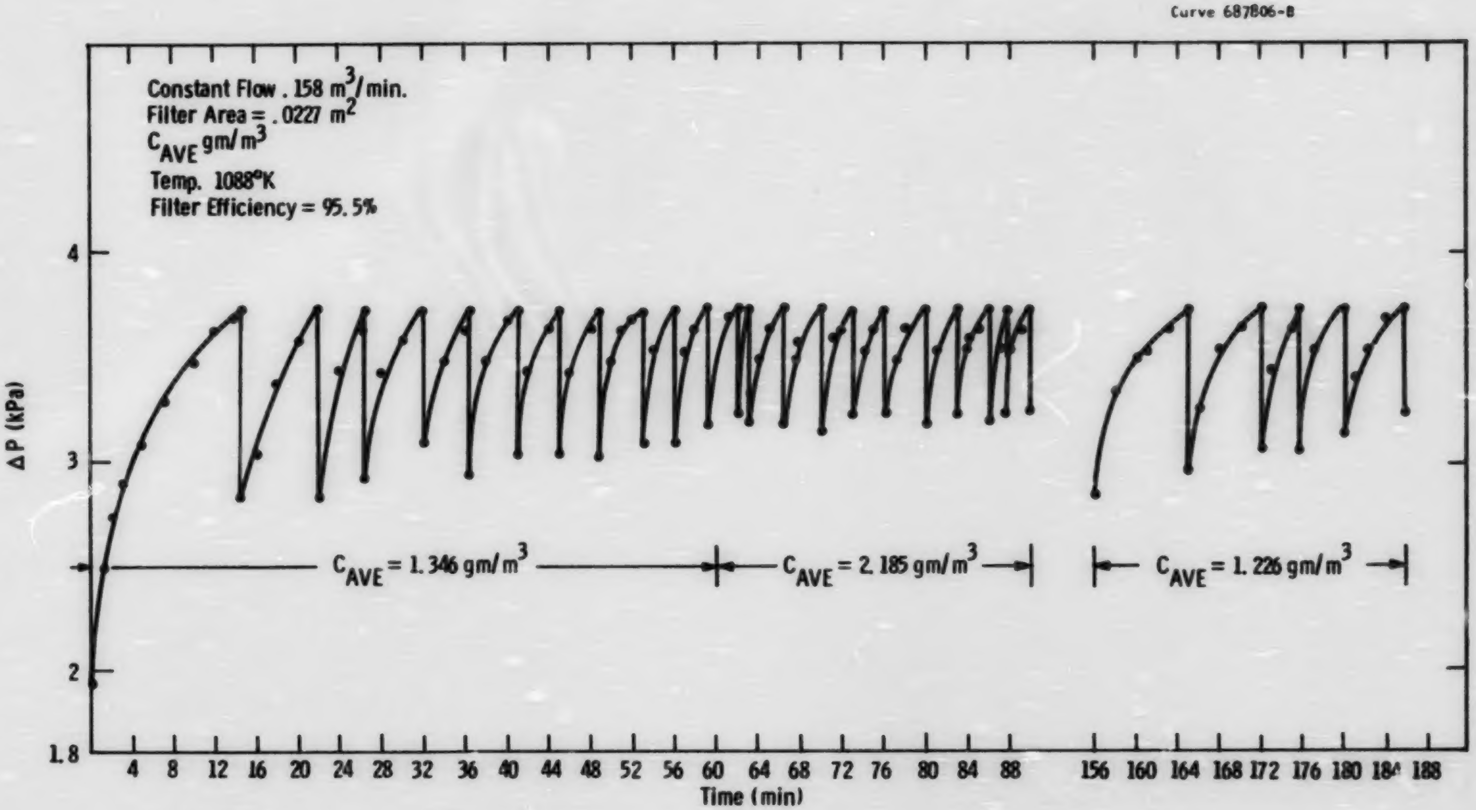

Fig. 36 — Hot thermacomb test

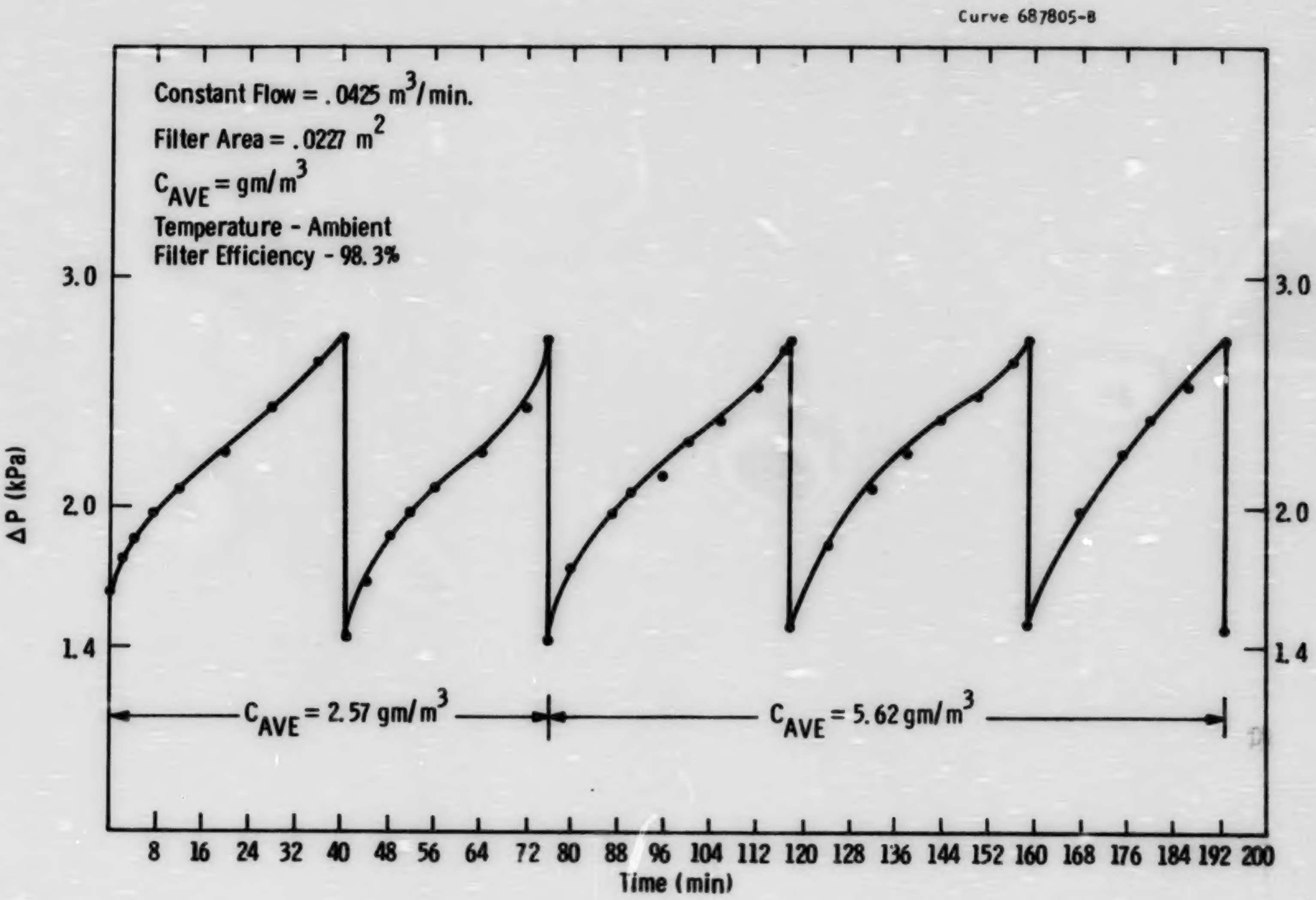

Fig. 37 — Ambient temperature test (thermacomb)

Previously it had been assumed that the operating temperature of the filter was the same as the gas exiting the filter jig, however, when this was checked by inserting a fine thermocouple into the Thermacomb it was discovered that portions of the interior of the Thermacomb were being maintained at about 525°C because of the materials low thermal conductivity. The only apparent solution to the problem was to preheat the air, however, because of constraints on the space available in the existing test apparatus only a space of about 1 m was available. Several electrical heating devices were tried, but because of the injected dust fouling equipment little success was achieved with in line heaters. Combustion of natural gas in the system seemed promising but it was anticipated that relatively complicated safety equipment would be required to prevent explosions. The scheme that was used, with reasonable success, simply consisted of a 70 cm ceramic tube in a muffle furnace. A concentric alumina tube was placed within the original tube to obtain an increase in heat transfer area with a minimum of obstruction to the dust. With this setup, gas temperatures exiting the preheating device could be raised from ambient to about 825°K and temperatures within the Thermacomb could be maintained at about 1000°K. These temperatures were for flow rates of approximately 30 normal liters/min. Two test runs were completed at these new conditions. The results of these runs are shown in Figures 38 and 39. During the second run, Figure 39, some problems were observed in the inlet sampler purge, so that the inlet loading measured is probably not accurate.

It was noted that increase in pressure drop was still not as great as would be expected. During heat-up, the mass flow rate of air was maintained at about 37 gm/min. At ambient temperatures the pressure drop across the filter was measured at about 1.25 kPa. At the final filter temperature of about 1000°K the pressure drop had only doubled to 2.5 kPa. It was noted that the filter was leaking during these runs, but it seems unlikely that this apparently small leak could reduce the pressure drop to the level observed. A more likely explanation, but yet unconfirmed, is that the apparent pore size is an increasing function of temperature.

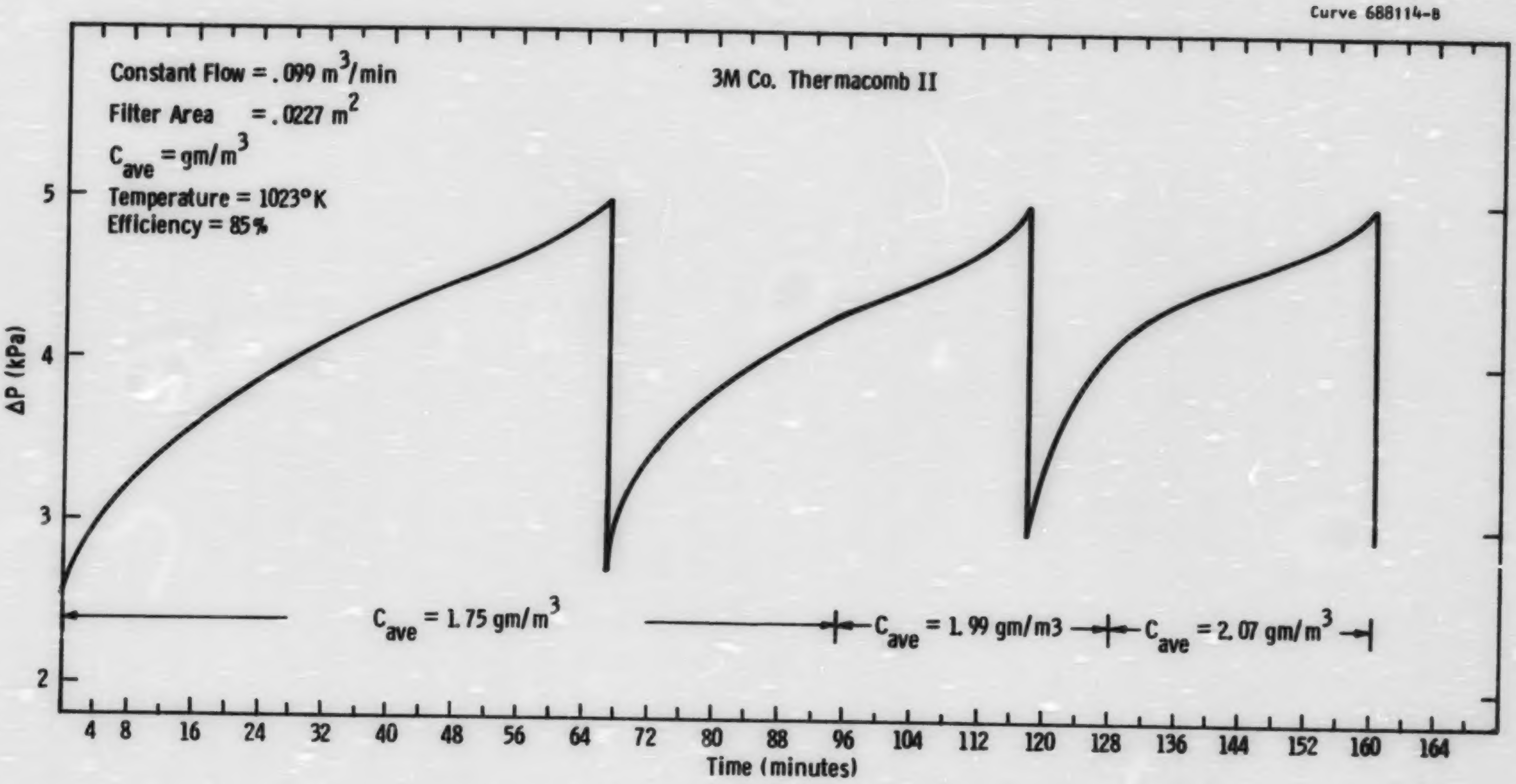

Fig. 38 — Hot thermacomb test

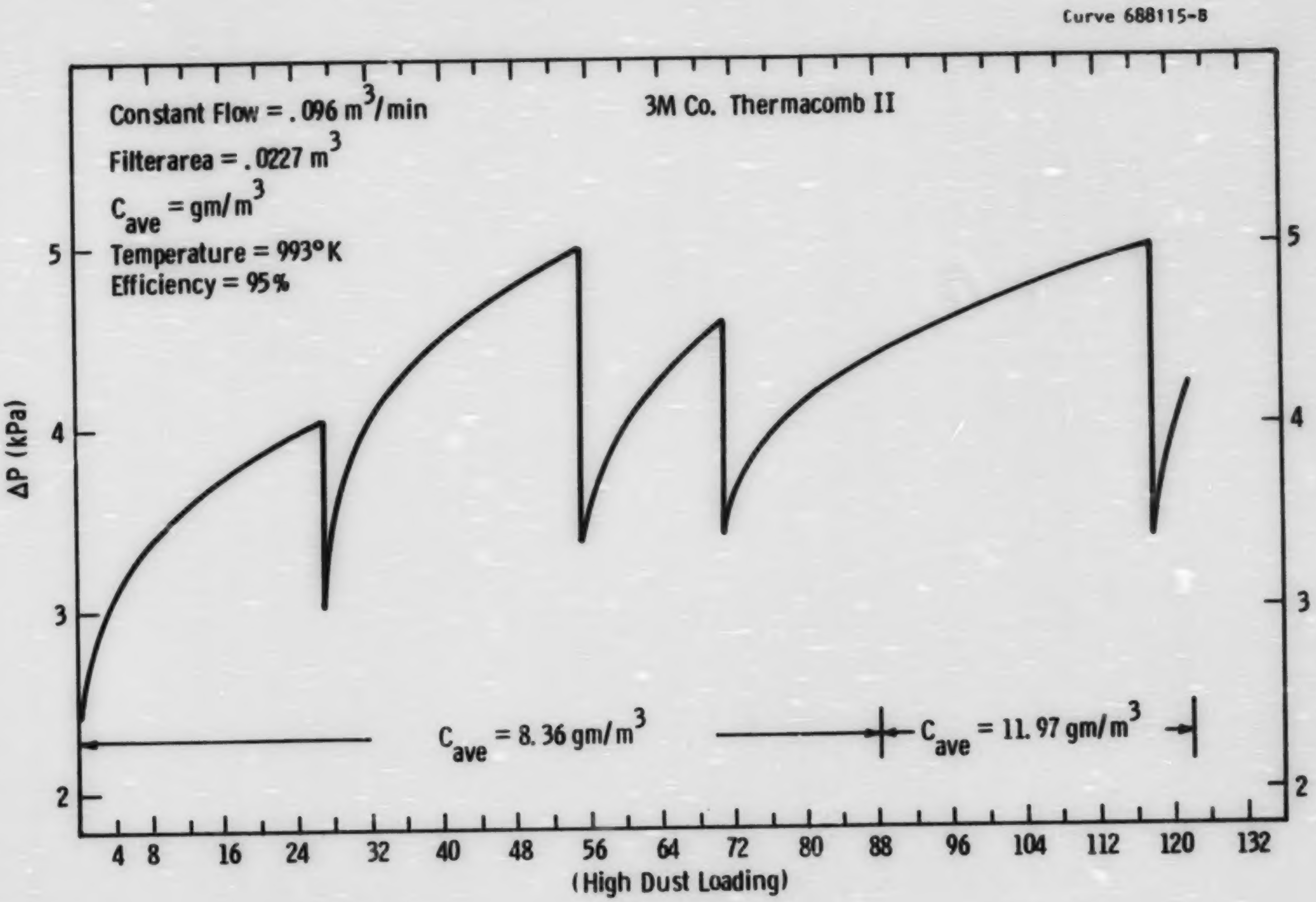

Fig. 39 — Hot thermacomb test

This specimen was removed from the test jig in order to cement the corrugations that were leaking. During this process the entire sample split along a barrier plane. It is suspected that this major break was due to the rather rough treatment required to open the jig. At this time it was observed that the filter material seemed more fragile than it had been. This caused some concern since a commercial application would require tens of thousands of hours of life without deterioration. Subsequent samples did not appear to suffer this loss of physical integrity, leading to the conclusion that it was most likely the severe treatment the sample received when dismounting it from the jig that caused the apparent weakness.

A new specimen was cut to size and mounted in the test jig. A series of three runs at constant mass flow rate, but different temperatures were carried to examine the effect of temperature on the filter performance.

The results of the constant mass flow at different temperature tests are shown in Figure 40 through 42. As can be noted from these data, the initial steady pressure drop increases from about 2.2 kPa to 2.8 kPa to 3.0 kPa as the test temperature increases from 633°K to 793°K to 983°K. One would expect an increase in pressure drop of about 1.41 times due to gas viscosity and an additional 1.24 times due to increased face velocity. This should raise the 2.2 kPa figure at 633°K to about 3.86 kPa at 983°K, instead of the observed 3.0 kPa. Technical representatives at 3M have agreed that the lower than expected pressure drops may be due to pore expansion at higher temperatures. Since there is apparently no penetration with the pores expanded, there may be some possibility of increasing the porosity of the filter material without loss of efficiency.

Having observed that both filtration efficiency and pressure drop characteristics remained excellent at high temperature, the next effort was directed toward better definition of the cleaning technique. It had previously been established that the second pulse down the dirty side

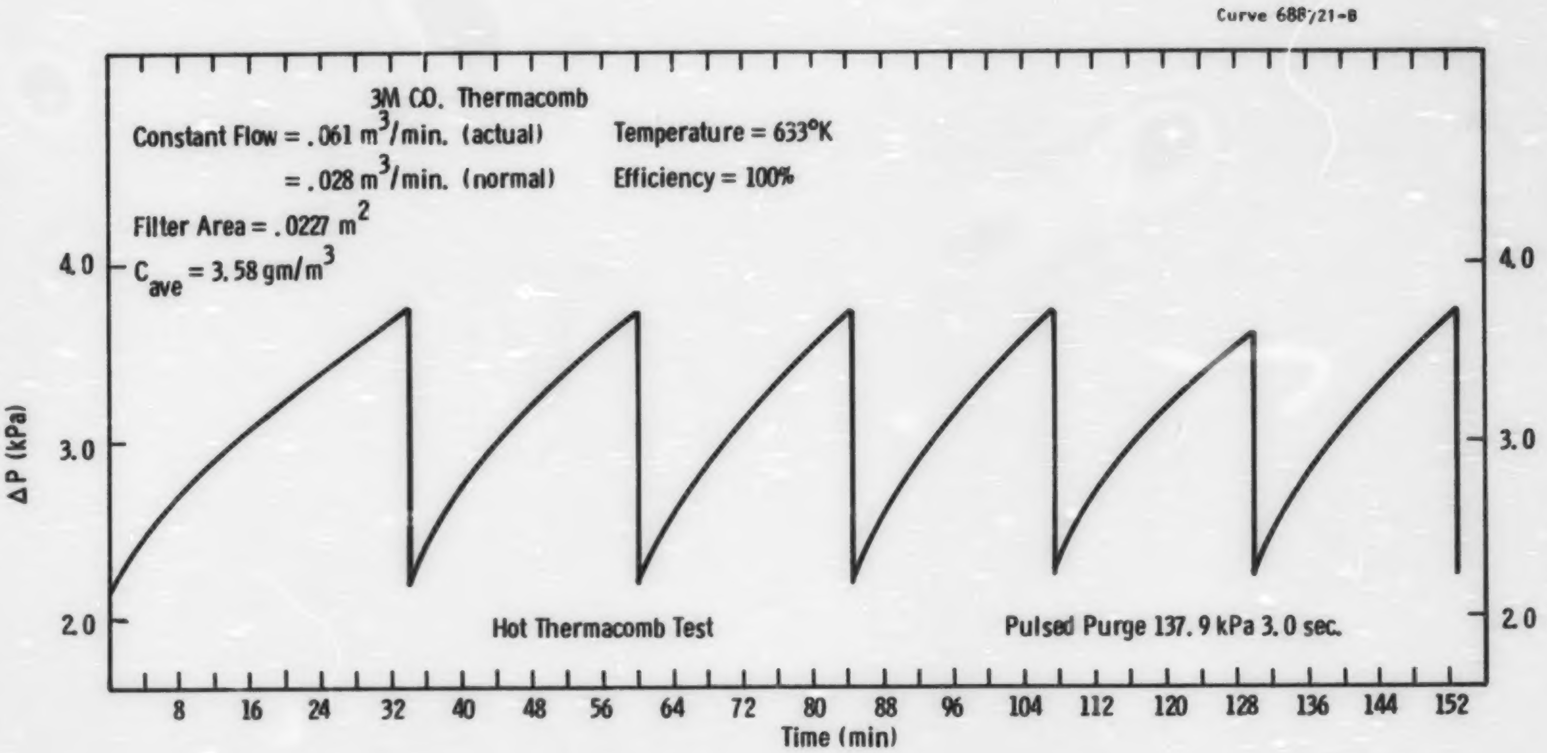

Fig. 40 — Therma comb filter test - constant flow

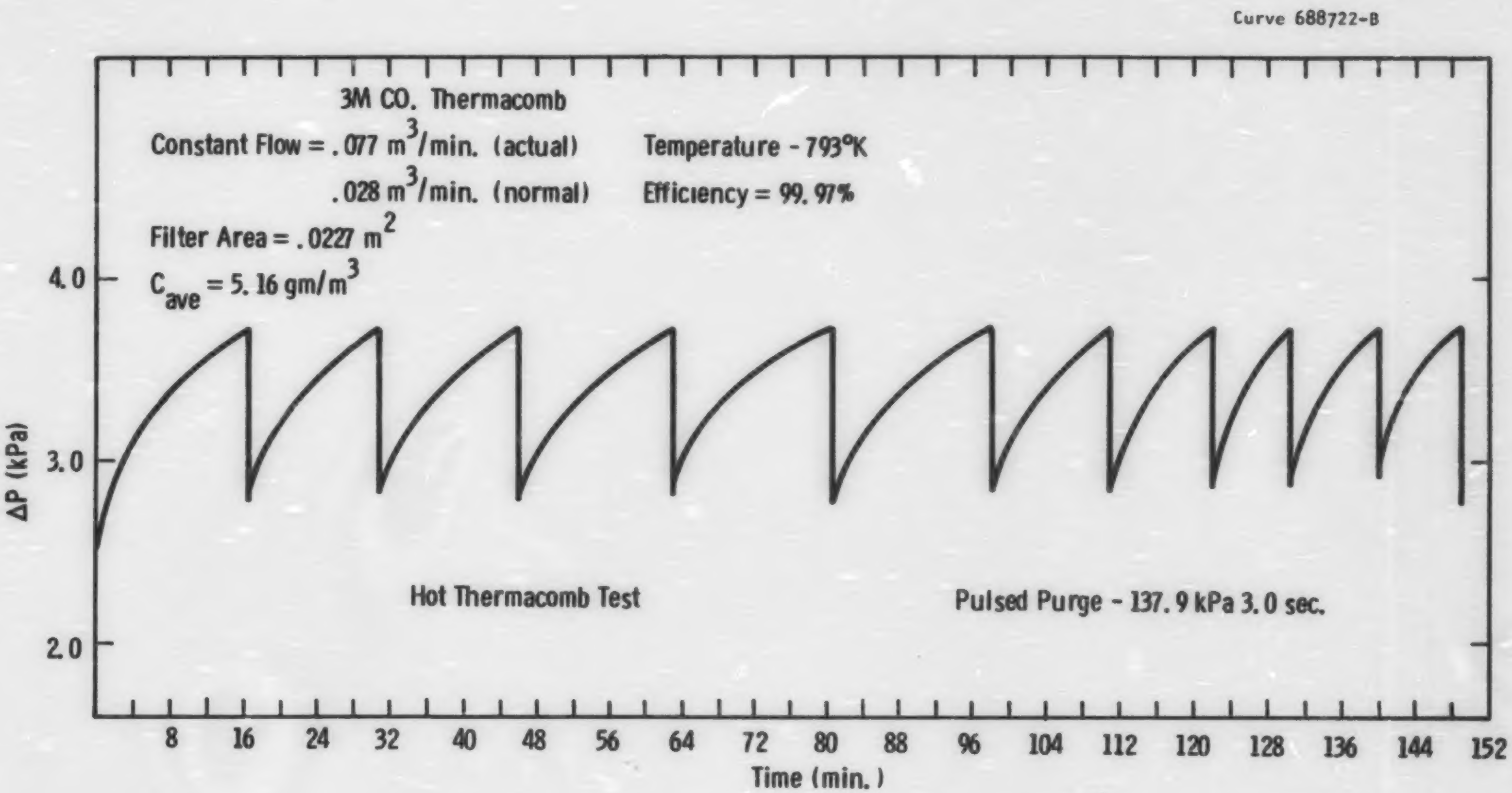

Fig. 41 — Therma comb filter test - constant flow

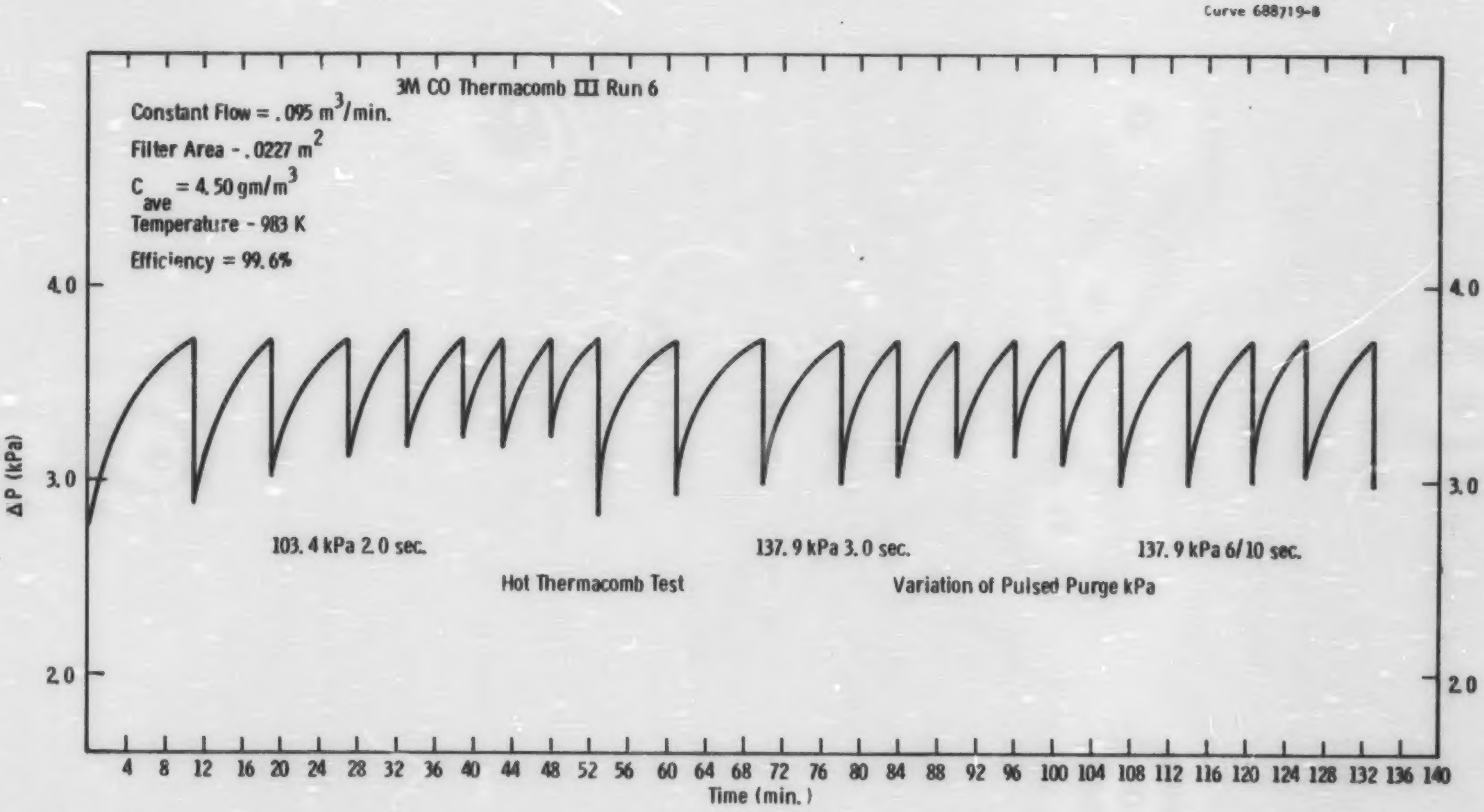

Fig. 42—Therma comb filter test-constant flow

did little or no good, so the remaining parameters to be examined were pulse duration and initial pulse pressure.

The initial run with a "standard" cleaning cycle is shown in Figure 43. The cleaning cycle used was an initial pulse pressure of 103 kPa from a .385 ℓ vessel. The pressure virtually instantaneously dropped to about 60 kPa for the remainder of the 0.6 sec pulse. As can be seen in Figure 43 there is a small increase in the initial steady pressure drop for this cleaning cycle. Some of this is because the element was new and had not yet been "conditioned". Figure 44 shows the effect of varying the initial pressure of a 0.6 sec pulse. The 69 kPa initial pressure dropped to a steady pressure of 34.5 kPa for the remainder of the 0.6 sec pulse and the 34.5 kPa pulse dropped to somewhat below 10 kPa. Figure 45 shows the result of a similar set of runs except that the pulse time was increased to 5 sec. from 0.6 sec. It can be seen from these data that the length of the pulse does not have much effect on the cleaning results. Figure 46 shows the data from another run in which the pulse time was reduced to 2 sec.

Later tests indicated that a slightly higher initial pulse pressure (138 kPa) gave somewhat more consistant cleaning than pulses of 103 kPa, Apparently, 103 kPa pulses are marginal for this system, as occasionally some deterioration in cleaning was observed. The performance of the higher pressure cleaning cycle is shown in Figure 47. With the initial pressure of 138 kPa a very stable cycle was maintained throughout the test. The negligible effect of pulse duration was confirmed by this test as there was no apparent difference between the 0.6 second pulse and the 3 second pulse.

Later in the program, after the W. R. Grace & Company material had been received and screened at ambient conditions, a hot test in the low flow facility was carried out.

The results of this experiment are shown in Figure 48. As the figure indicates this material performs at least as well as the 3M Thermacomb material giving 100% efficiency and comparable pressure

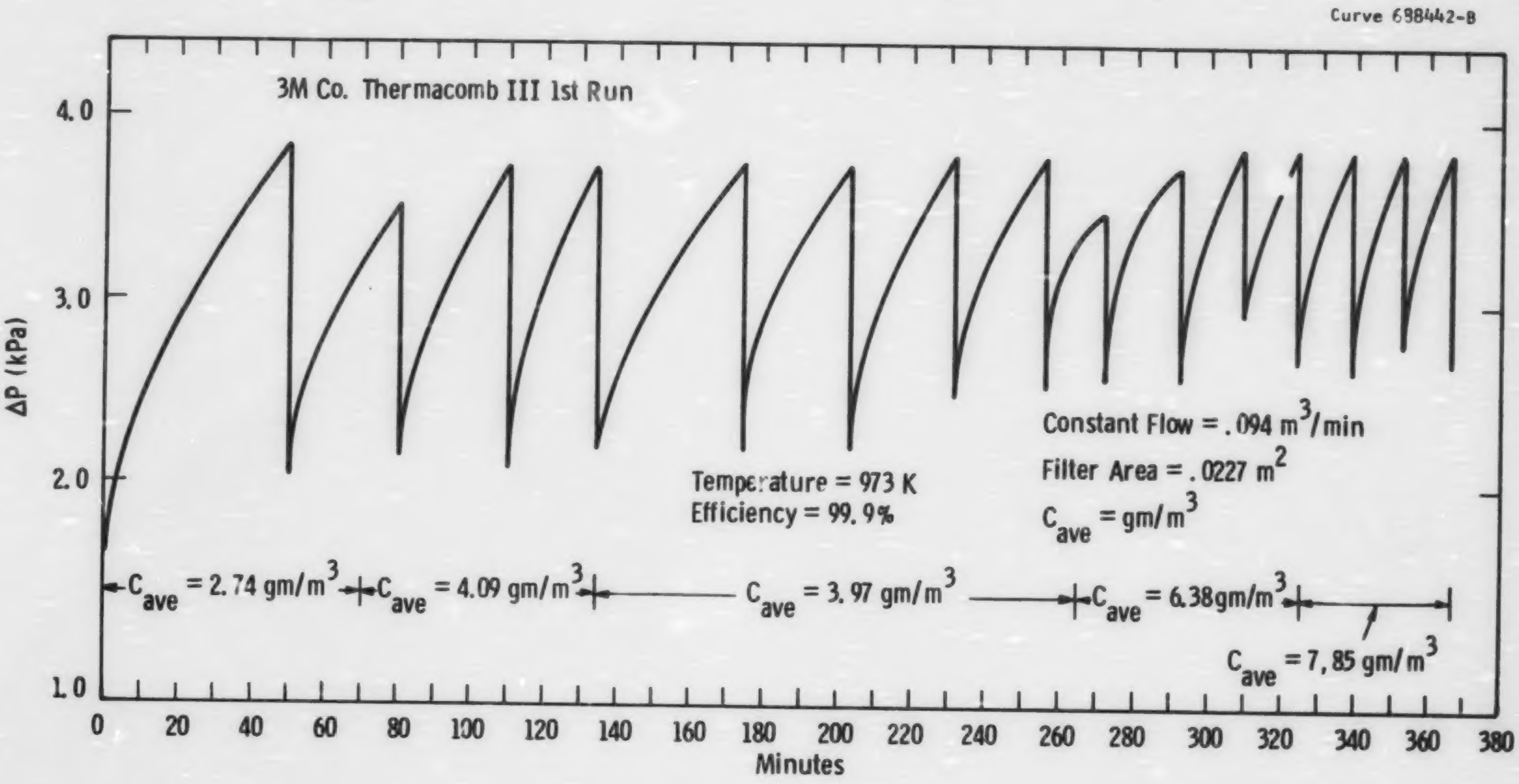

Fig. 43 – Hot thermacomb test (high dust loading)

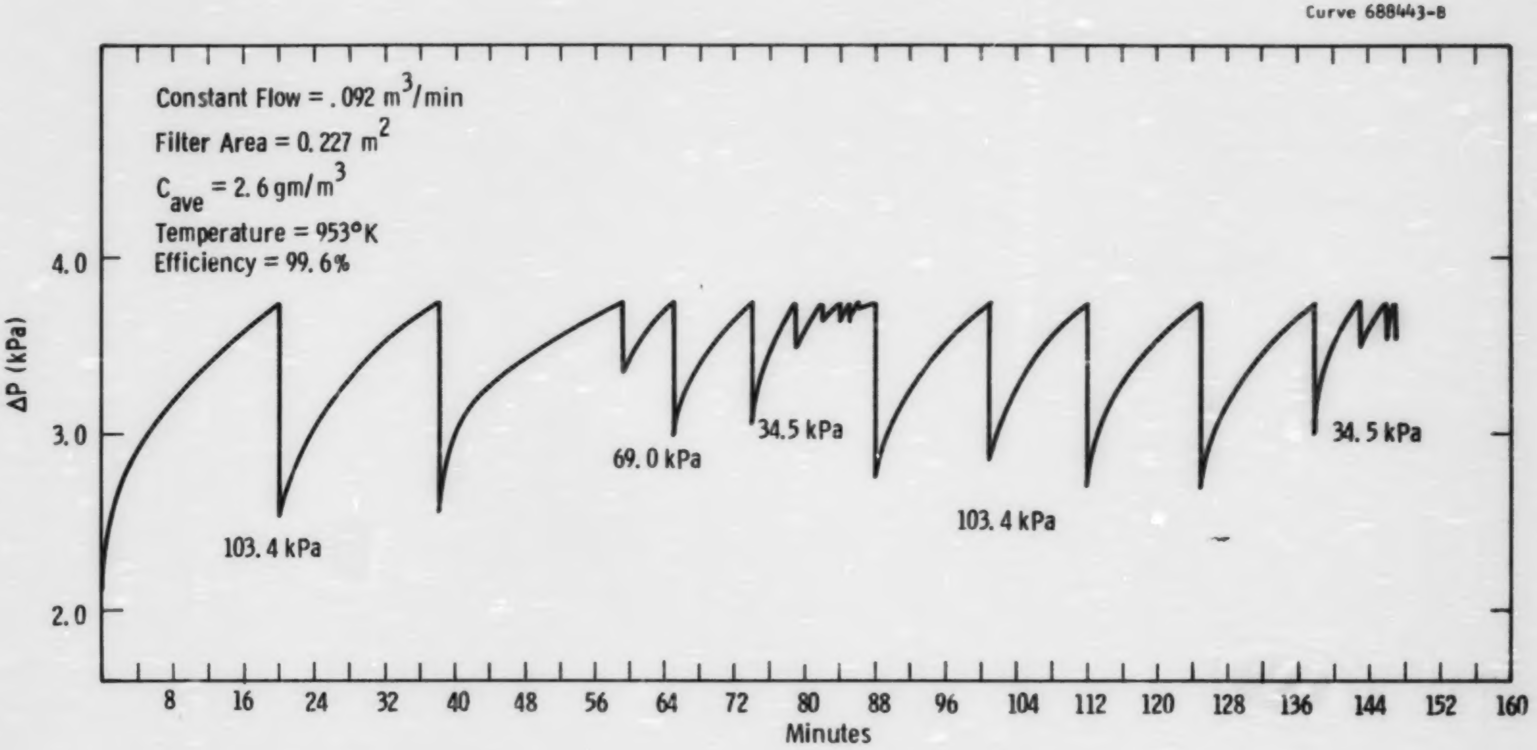

Fig. 44 — Hot thermacomb test

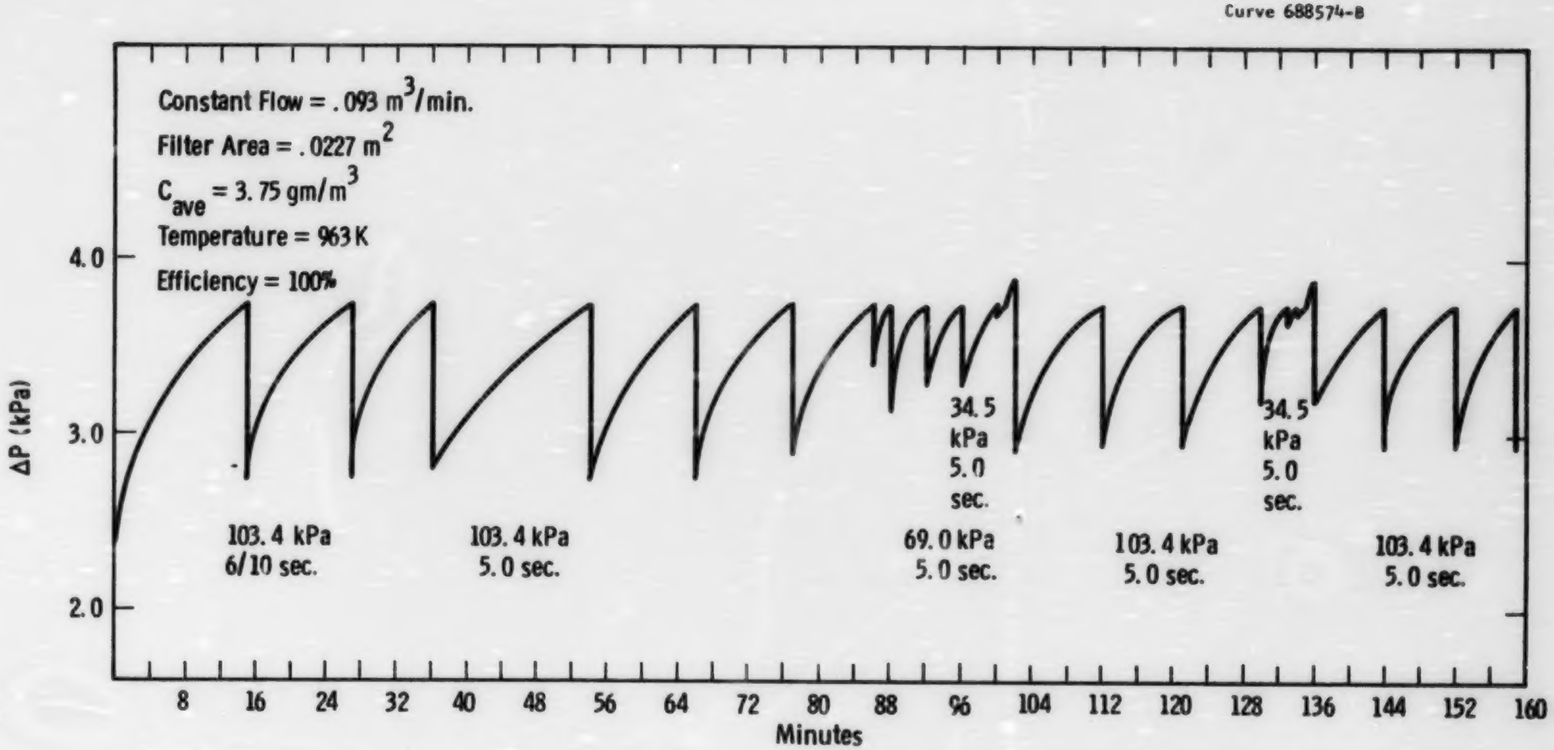

Fig. 45—Hot thermacomb test

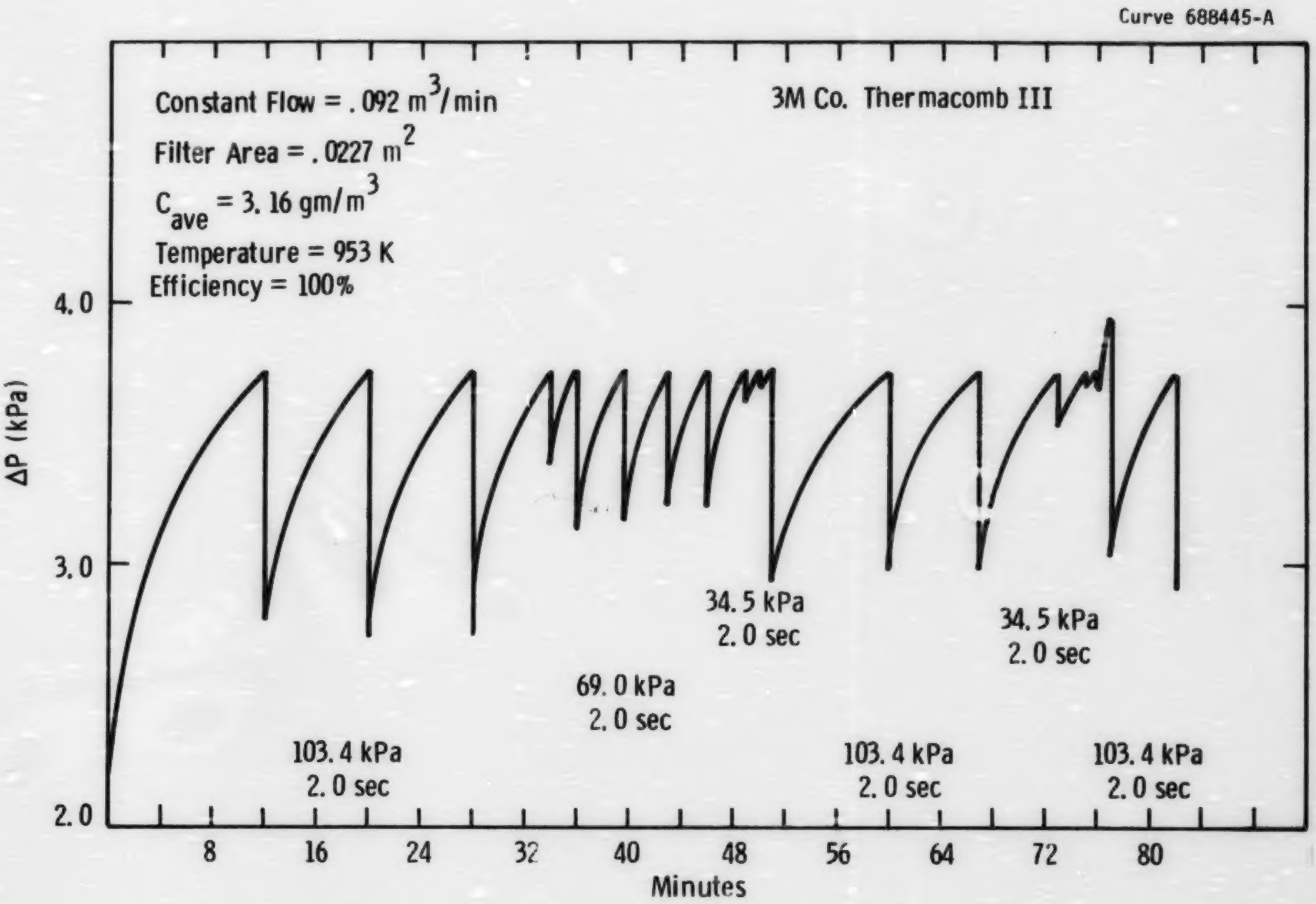

Fig. 46— Hot thermacomb test variation of pulsed purge kPa

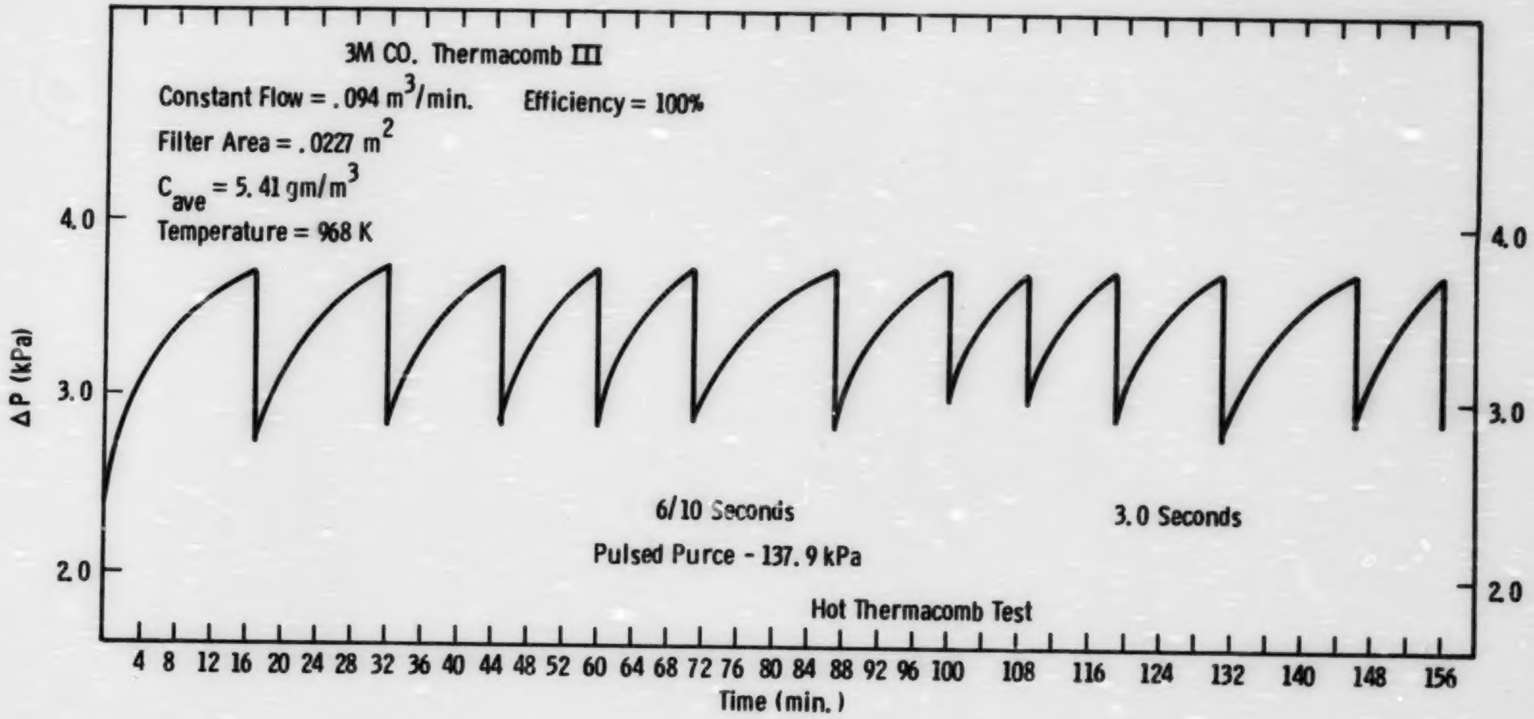
Curve 688720-B

Fig. 47 — Therma comb filter test-pulse times

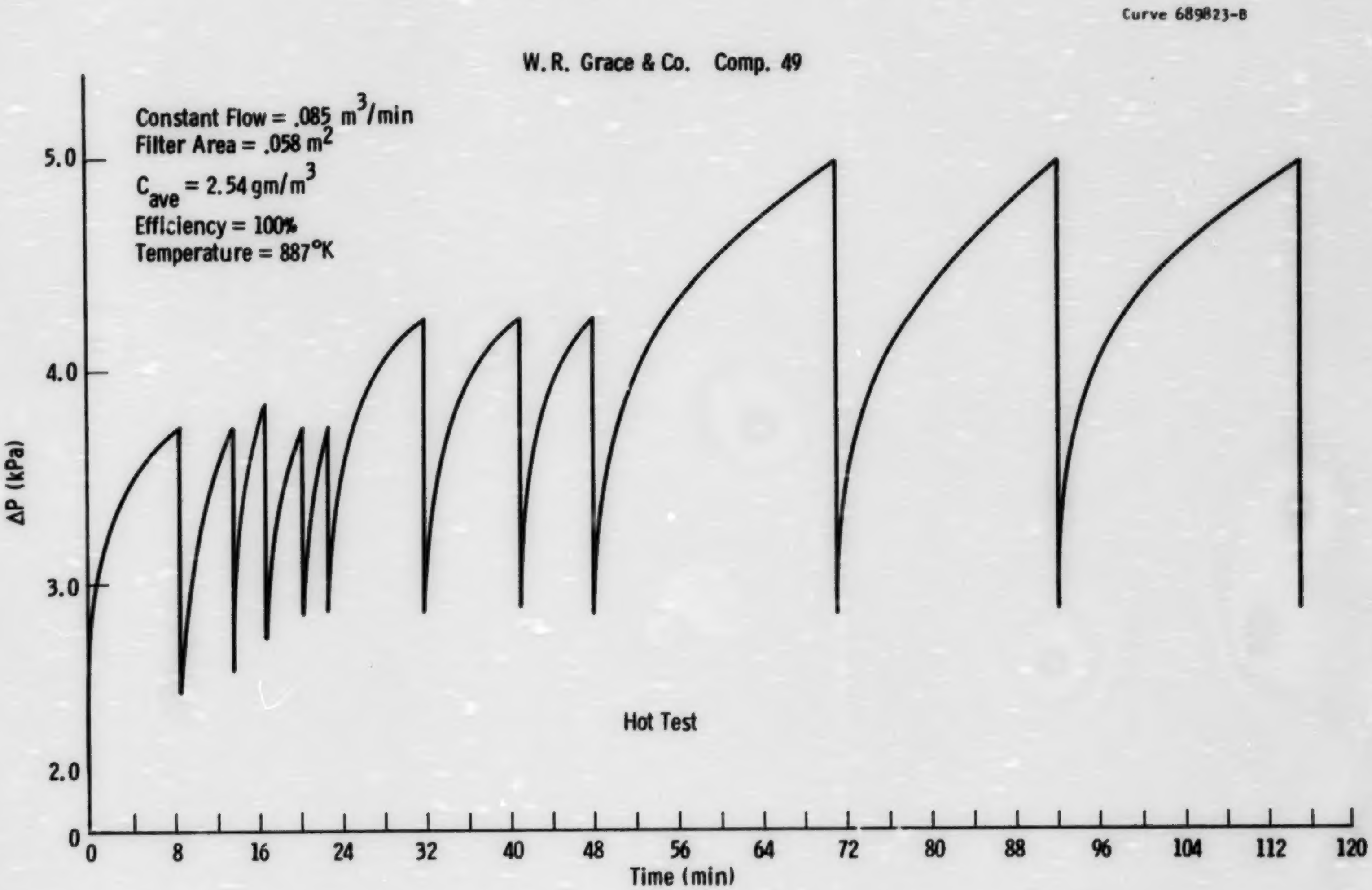

Fig. 48— Hot low flow test of W. R. Grace & Co. ceramic filter

drop-flow characteristics. The cleaning cycle consisted of a single 138 kPa pulse from a 0.385 ℓ vessel for 1 second. The pulse was directed to the clean side of the filter. A very stable, relatively low initial pressure drop was maintained with this cycle even as the filter was loaded with larger and larger amounts of dust. The W. R. Grace & Company material in this configuration seems to be less fragile than the Thermacomb and easier to handle.

At the time of this test, work on the high flow hot unit with the large Thermacomb filters was underway so no further testing of this material in the hot, low flow apparatus was possible.

4.6 HIGH FLOW HIGH TEMPERATURE TESTS

The initial tests on the hot-low flow bench facility were promising so efforts to carry out hot tests on a larger scale were initiated as early as possible since the major goal of the Phase II effort was the demonstration of hot gas filtration at a reasonable scale. Because of constraints on time it was necessary to modify an existing facility for the high flow tests.

The most appropriate available apparatus was a device previously used in hot granular bed filtration studies. This facility had a flow capacity of approximately 15 m^3/min at temperatures up to 1100°K and at ambient pressure. The containment vessel had straight sides about 0.6 m in height and a diameter of 1.1 m outside with a conical top and bottom. The vessel and piping arrangement are shown in Figure 49. By proper arrangement of the four, 10 cm slide valves flow could be directed either down through the vessel when filtering or up through the bed when backwashing the granular bed filter. The granular bed was supported by a perforated distributor plate sealed between the vessel flanges. Air was supplied to the system by a 1.0 kg/sec compressor and this air was heated by an in-line material gas combustor. Dust could be fed to the system in either of two ways. One method was to feed a relatively coarse, easy flowing limestone powder to a Sturtevant fluid energy mill via a hopper and controlled vibrating trough. The fluid energy mill would grind the dust to the desired size and disperse it into the air stream from the compressor. The second method was to use a pre-ground test dust and inject and disperse it using a device similar to the one used in the bench scale work, but larger. This second option proved to be the easier to control and was used in all testing.

The system was equipped with a combustible gas analyzer which shut the apparatus down automatically if a combustible mixture was sensed in the vessel. The vessel was also equipped with a vent pipe and a 35 kPa rupture disk to prevent over pressure in the vessel.

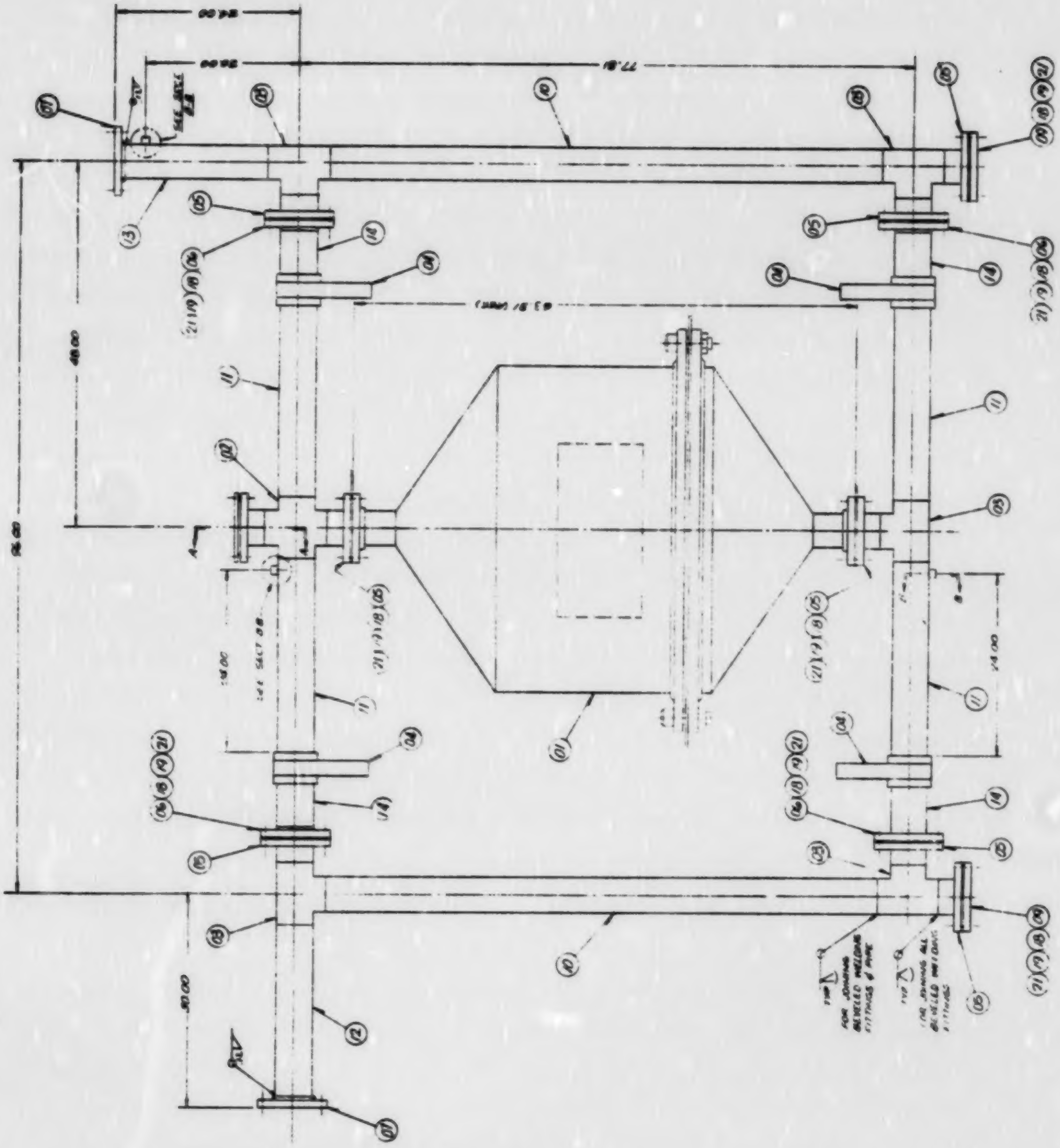
24.00
24.00
77.81
48.00
56.00
30.00
14.00
FOR JOINING BEVELED WELDING FITTINGS & PIPE

Figure 49. Hot high flow test facility.

Several modifications were required to enable this system to be used for testing the ceramic filters. The major problem centered around provisions for blowing back the filter elements since this required pressures in excess of two atmospheres which was more than the vessel or distributor plate could withstand at temperature. The solution to this difficulty involved isolating each of the 15 cm cubes of Thermacomb in a "hat" like container on a new support plate. This support plate accommodated seven of these modules each enclosing a 15 cm cube of Thermacomb. The arrangement of the Thermacomb filter and one hot module is shown in Figure 50. This arrangement allowed high pressure pulses to be directed to the clean side of the filter since only a small area of the support plate was pressurized. It also allowed individual elements to be pulsed independently. The major problem associated with this configuration was the method of closing the hat while a pulse was being administered. The simple sliding mechanism shown in Figure 50 was adopted since it was anticipated that the closure would not need to be tight, but that it would only be required to direct most of the pulse through the filter. Provisions for opening and closing the slides were made using rigid mechanical linkage which could be operated manually from the vessel exterior. Preliminary hot testing revealed that the support plate warped upon heating causing the linkages to bind and become inoperative. This problem was overcome by welding an 0.32 cm diameter wire rope to each slide. The ropes were extended out through Conax fittings in access doors at opposite sides of the vessel. This allowed individual slides to be pulled open or pulled closed regardless of support plate warpage.

The blow back system simply consisted of a pressure vessel with the same volume as a hat. A group of seven solenoid valves allowed the vessel to be vented to any of the seven elements mounted on the support plate. This arrangement only allowed the clean side of the filter to be pulsed since bench scale tests indicated that the dirty side pulse was not effective. In later tests it was necessary to try a pulse from the dirty side in order to improve cleaning. A schematic of this modification is shown in Figure 51.

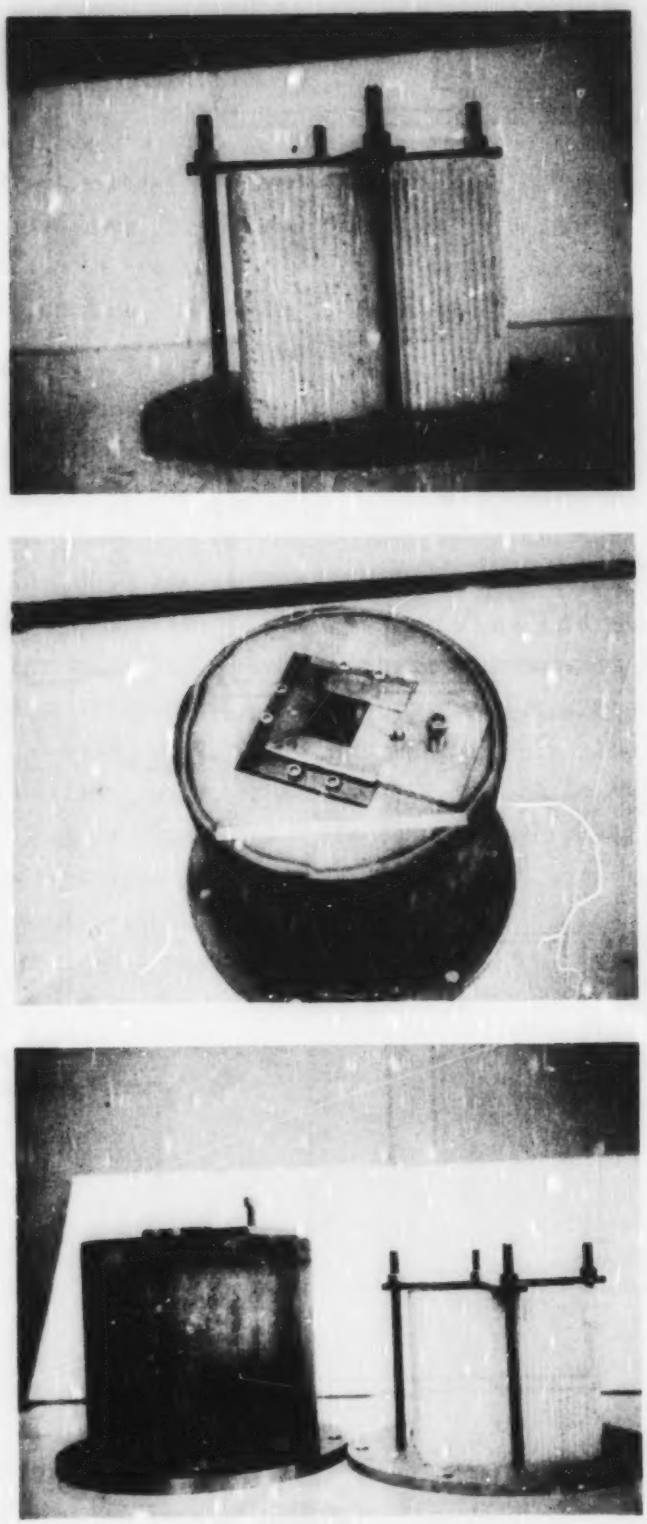

Figure 50. 6 inch ThermaComb
test assembly.

Dwg. 1690805

FILTER BLOW BACK SYSTEM

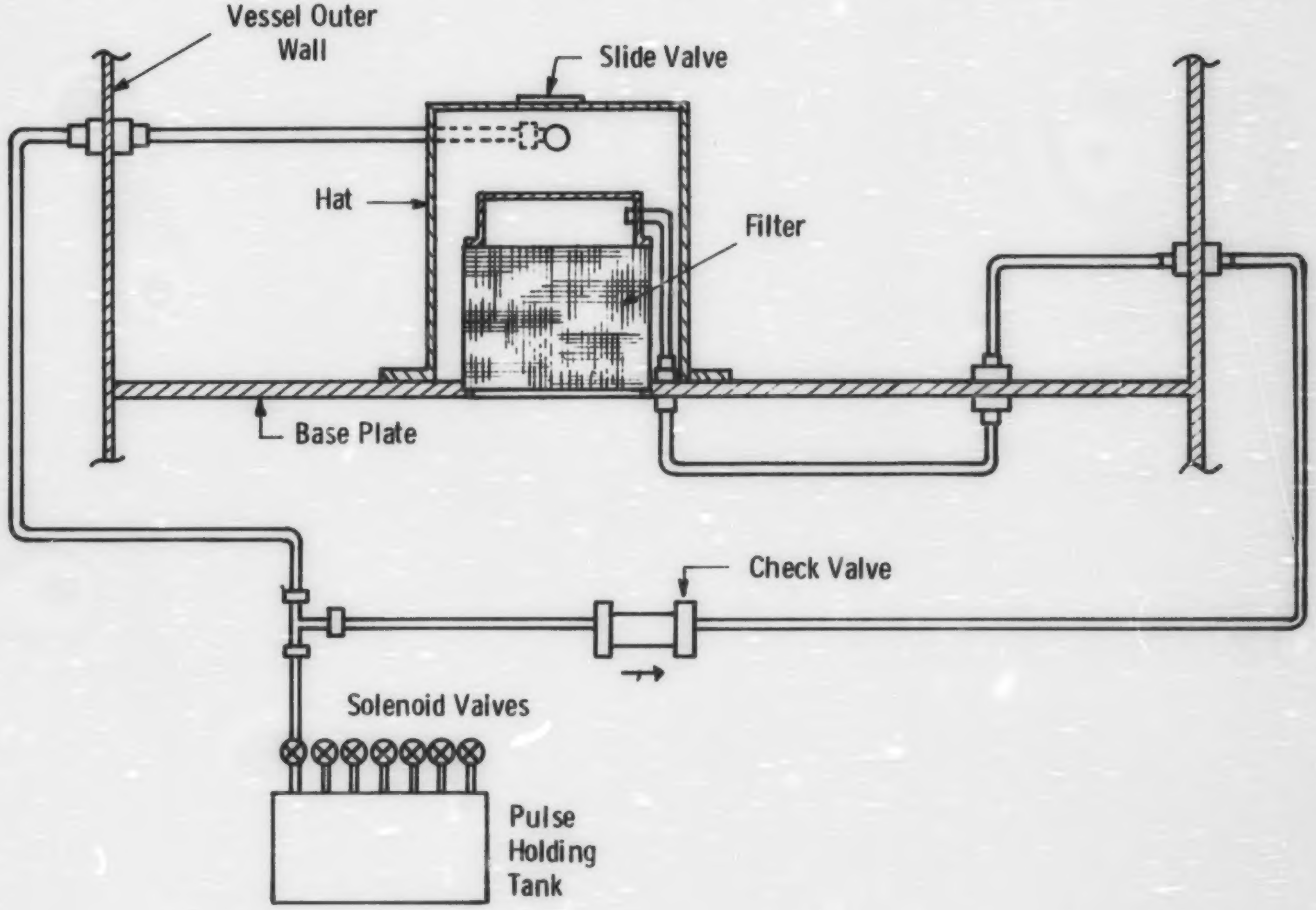
Vessel Outer Wall
Slide Valve
Hat
Filter
Base Plate
Check Valve
Solenoid Valves
Pulse Holding Tank

Fig. 51– Schematic of pulsing modification

Figure 52 is a schematic of the entire test facility. Figure 53 is a photograph showing the vessel, major piping, sampling ovens and blow back pulse tank and lines. Figure 54 is a photograph of the filter modules mounted on the support plate. One hat and blow back tube have been removed to show the manner in which the Thermacomb elements were mounted.

In summary, the operation of the high flow high temperature system was planned to proceed in the manner described below. The filtering mode began as the hot dust laden gas flowed from the natural gas combustor down the left leg of vertical piping and into the bottom of the vessel (refer to Figure 52). Flow was maintained in this direction by closure of slide valve #2 while valve #1 was maintained in the open position. The dirty gas flowed up through the support plate, was filtered in the Thermacomb, exited the hat and finally escaped the system through slide valve #1. The cleaning cycle began by opening valve #2 and closing valve #1 which allowed the dirty gas to by-pass the entire filter system. The slides on each hat were then pulled closed and a back wash pulse was administered to each filter. The dust that had been accumulated in the filter was knocked down through the conical bottom of the vessel and was swept out of the system by the by-pass stream. This procedure was then reversed and the filtering mode of operation was re-entered.

Dwg. 1688B02

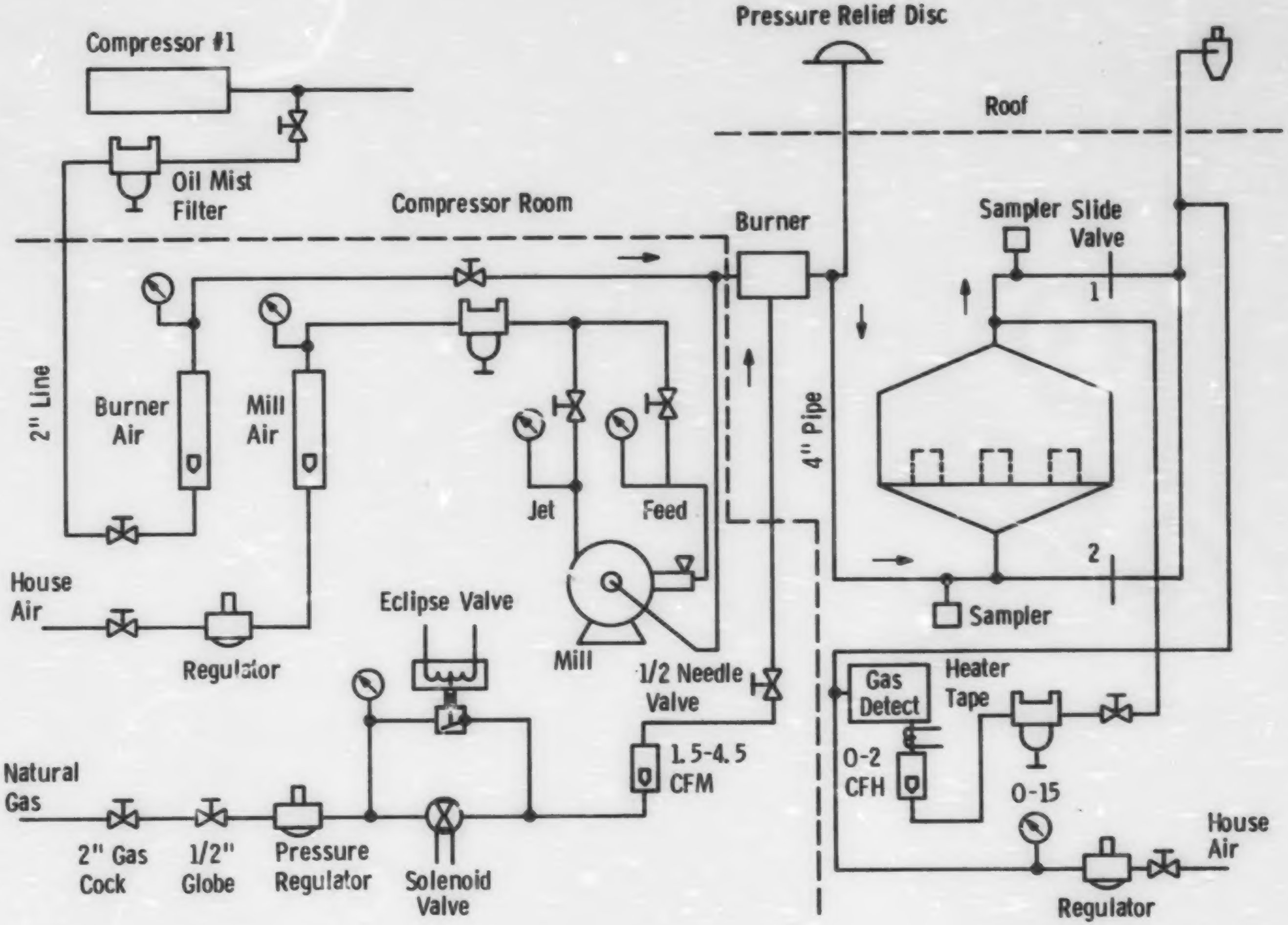
Pressure Relief Disc
Compressor #1
Roof
Oil Mist
Filter
Compressor Room
Burner
Sampler Slide
Valve
1
2
2" Line
Burner
Air
Mill
Air
Jet
Feed
4" Pipe
Sampler
House
Air
Regulator
Eclipse Valve
Mill
1/2 Needle
Valve
Gas
Detect
Heater
Tape
1.5-4.5
CFM
0-2
CFH
0-15
Natural
Gas
2" Gas
Cock
1/2"
Globe
Pressure
Regulator
Solenoid
Valve
House
Air
Regulator

Fig. 52 — High temperature high flow test facility

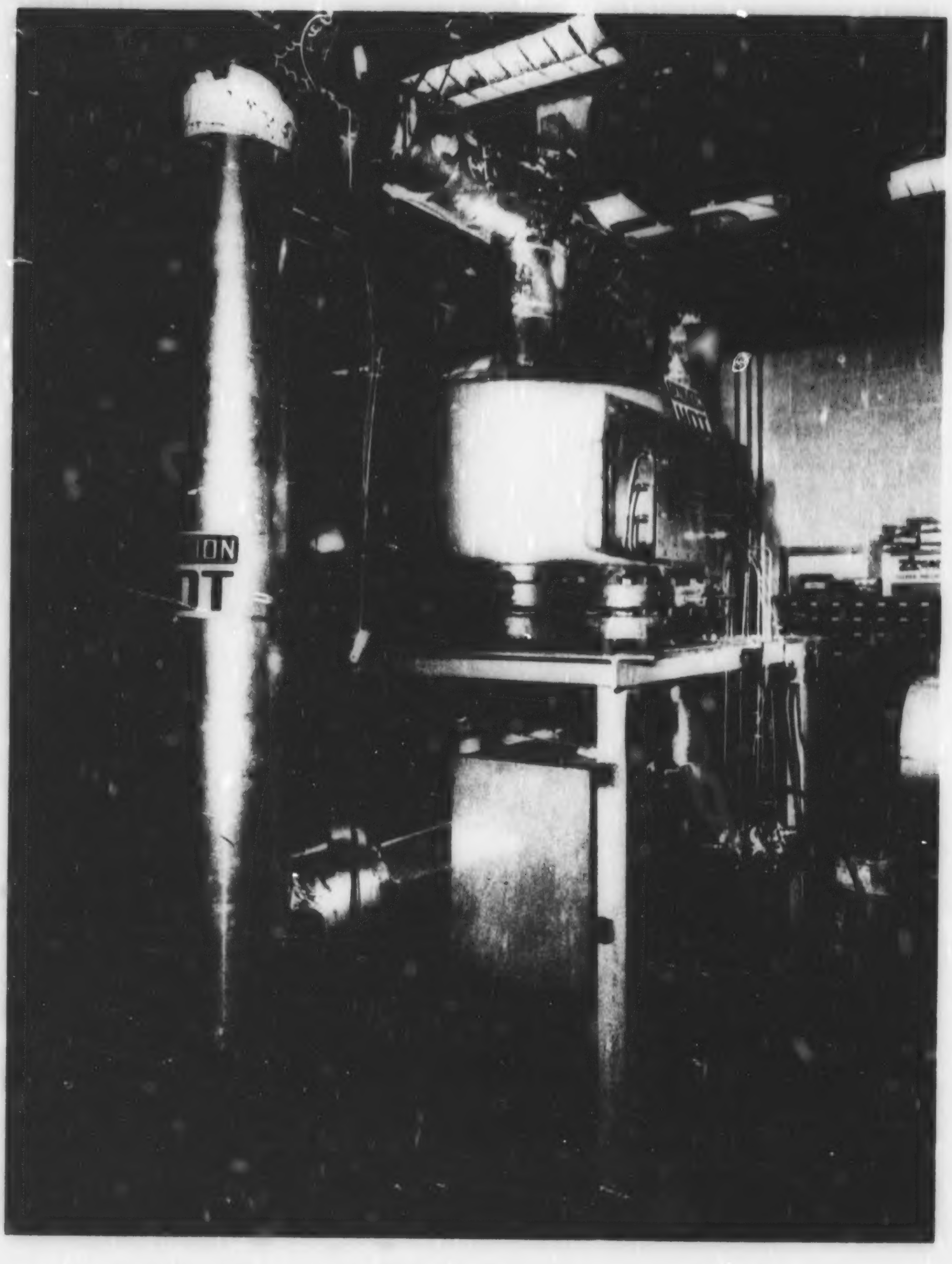

Figure 53. High temperature ceramic test facility.

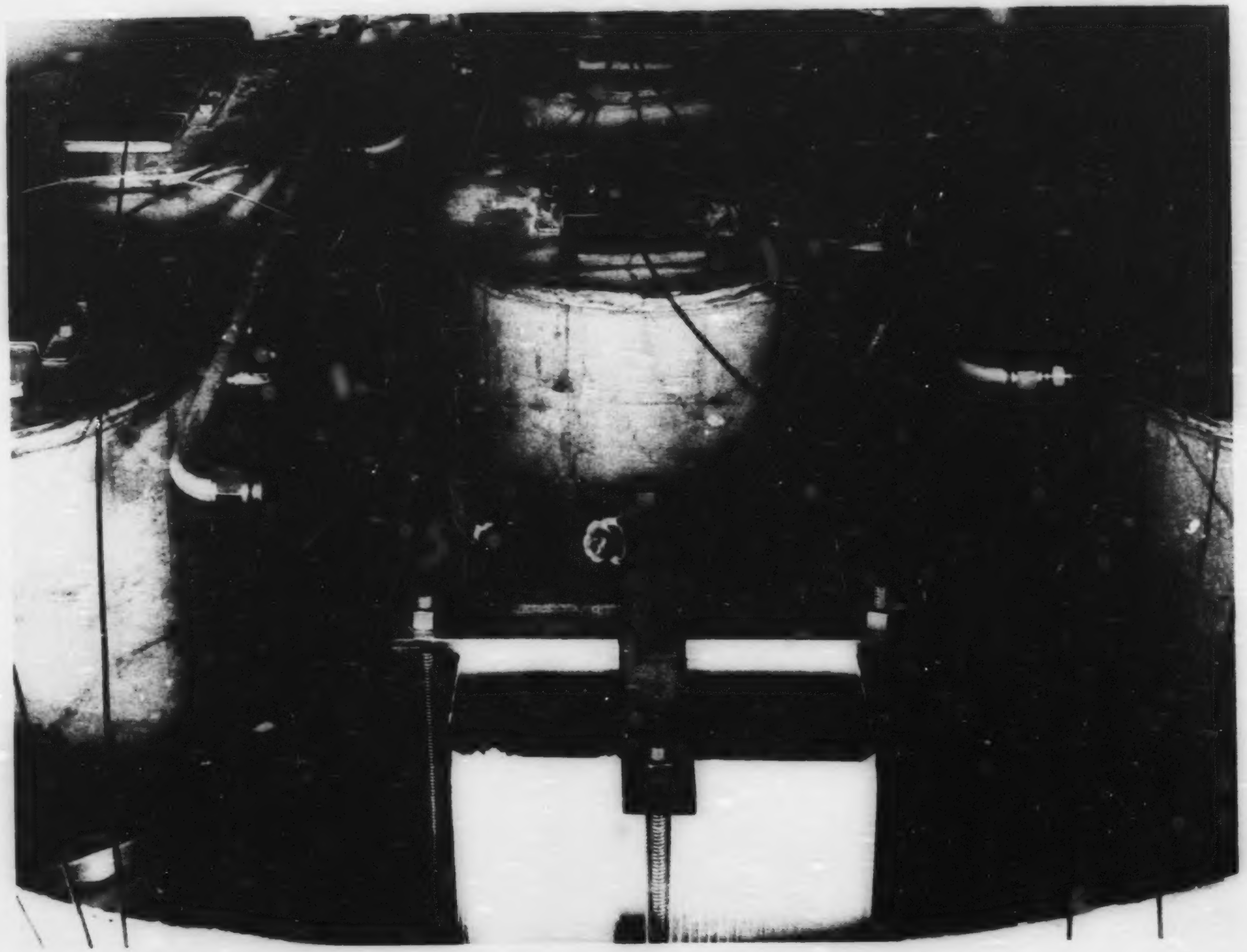

Figure 54. Detail of ceramic filter assembly.

High Flow High Temperature Results

Upon completion of the mechanical alterations and required installations, a series of four preliminary runs were made in the high flow unit which were as follows: (1) cool (95°C) and clean, (2) hot (610°C) and clean to test mechanism for opening and closing the slides, (3) cool and dirty to try dust injection system and pulse back cleaning system and (4) a hot dirty test. During the first test, the pressure drop rose linearly from 0 to 1.14 kPa as the flow increased from 0 to 3.14 m^3/min. There probably was some accumulation of dust from the piping in the filter during the run. The second test demonstrated that the stainless steel ropes work well. The third test was run at 3.64 m^3/min with dust injected. The pressure drop rose from an initial 1.49 kPa to 2.07 kPa over a period of 110 minute with a dust loading of 0.48 gm/m^3. The filters were then back flushed with a pulse from a 8.9 liter vessel charged to a pressure of 3.4 atm. The volume of this vessel is approximately the same as the filter hat. The initial steady pressure drop after being flushed was 1.89 kPa, which then rose to 2.49 kPa over a period of 65 minutes. The elements were then back flushed and the initial steady pressure drop returned to 1.92 kPa.

After this test a larger dust injection system was installed in an attempt to deliver more dust and shorten cycle times. A hot (615°C) test was initiated after this modification. The initial pressure drop was 5.03 kPa and increased to 5.22 kPa in 10 minutes with a dust loading of 0.1 gm/m^3, and a flow of 9.15 m^3/min. There is some doubt about the accuracy of the dust concentration measurement for this run as it should have been considerably higher. When the filters were subjected to the 3.4 atm pulse for cleaning the pressure drop only decreased from 5.22 kPa to 4.98 kPa. There was an obvious leak so the test was terminated at this point. Inspection of the filters indicated that they were not packed in a sufficient amount of fiber frax to make a good seal with the stainless steel support plate. It was also observed that the bottom of the filters had accumulated a lot of dust which had not been removed by the cleaning cycle being used.

The problem of leaks at the support plate seal was overcome by simply increasing the thickness of the fiber frax gasket in the support plate. This allowed more fiber frax to be compressed into the edge surfaces of the Thermacomb and formed a dust tight seal quite simply.

During a preliminary check of the sealing improvement it was noted that the back flush cleaning did not return the initial steady pressure drop to a constant value, rather it increased in slow but steady fashion as shown in Figure 55. There were a couple of plausible explanations for this observed behavior. The first is that most of the dust is never expelled from the filte elements during the cleaning pulse, and the residual dust in the filter increases continuously until sufficient blockage to stop testing has occurred. A second possibility is that as one filter is pulsed the expelled dust is blown into the surrounding filters. A third possibility is that the dust is expelled from the filter to the vessel walls and does not get blown out of the vessel into the bypass stream. Then, when the device is returned from the cleaning mode to the filtering mode, the once collected dust is blown back into the filters.

A series of tests were run at compressor outlet temperature in an attempt to discern which circumstance accounted for the observed increase in initial steady pressure drop. In the first test the filters were run until the initial steady pressure drop increased from about 3.5 kPa to about 5 kPa. One filter element was removed and it was noted that the bottom surface had accumulated a considerable amount of dust, and that the open area had been greatly reduced. Then three elements were given back flushes of varying intensity and removed in sequence. There was an observable increase in dust removal as the initial pressure of the pulse was increased. It was noted that the bottom of the element that was subjected to the highest pressure pulse, appeared to be in a condition similar to the samples from the hot, low flow unit where cleaning was successful. Figures 56 and 57 show how the bottom of the filter surface changed with increasing pulse pressure over the range from 0 to 552 kPa.

Curve 689703-A

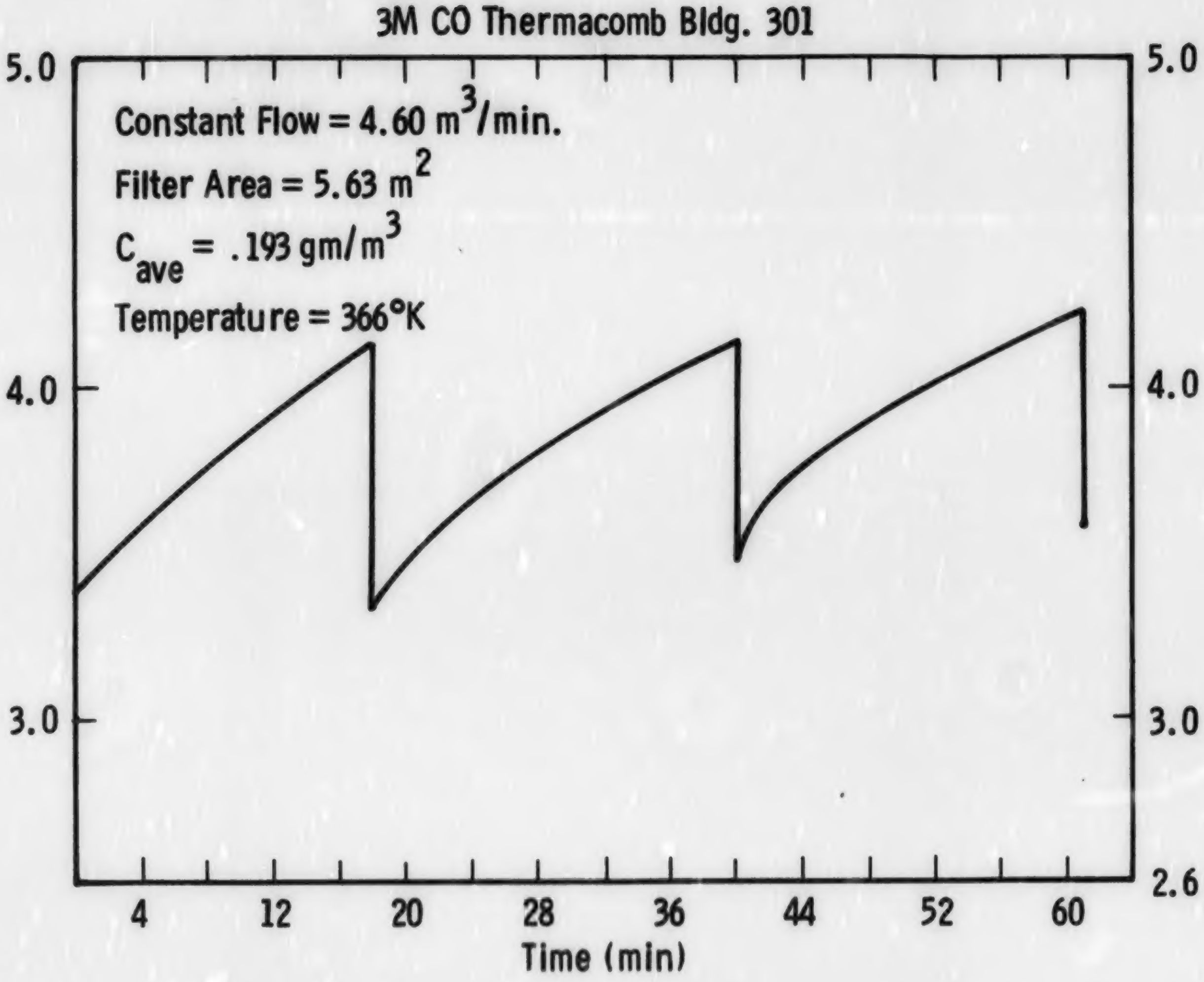

Fig. 55—High flow test starting with clean filters

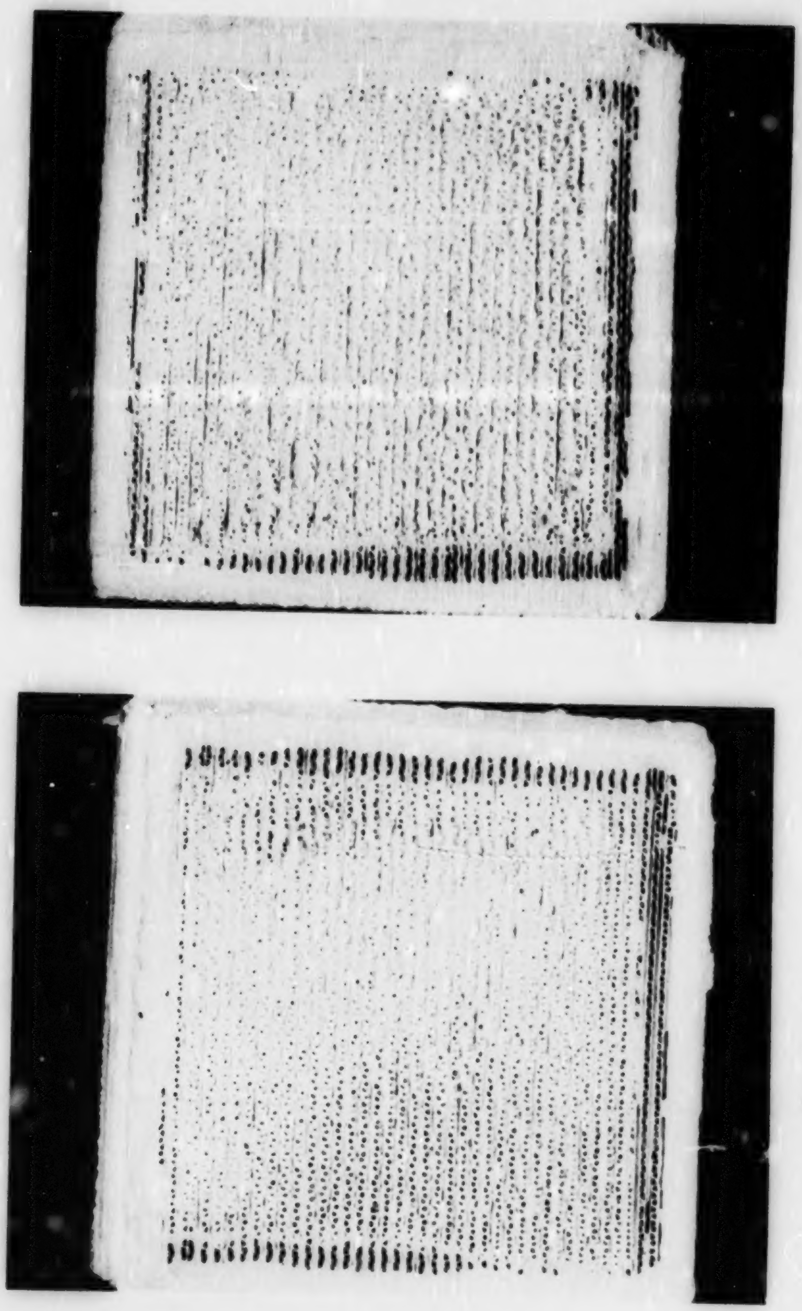

No Pulse

172 kPa Pulse

Figure 56. Pulse intensity tests.

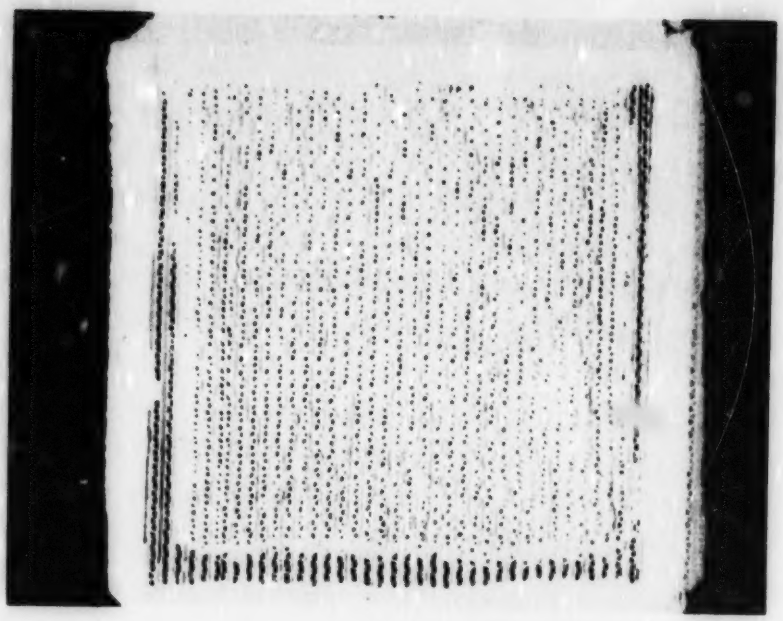

345 kPa Pulse

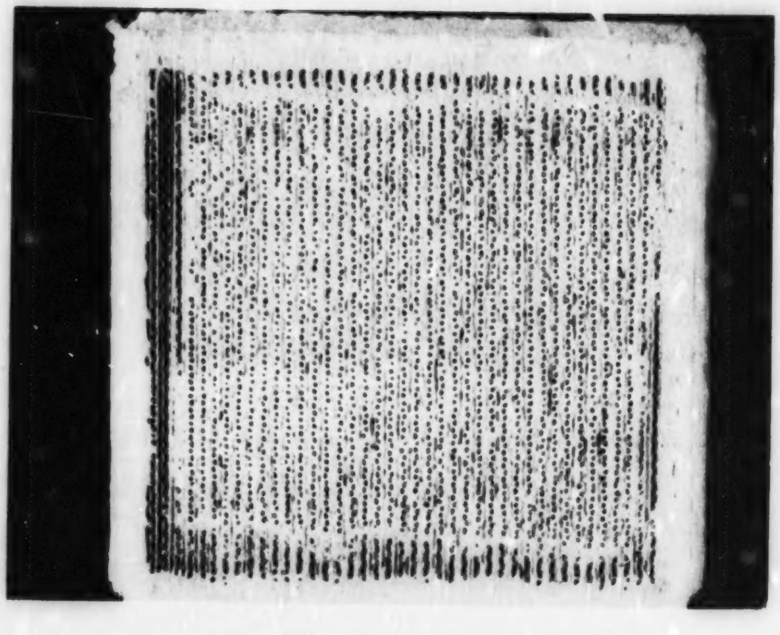

552 kPa Pulse

Figure 57. Pulse intensity tests.

All of the elements were then vacuumed clean as was the conical wall of the vessel. The elements were then reinstalled and tested again. The initial steady pressure drop decreased from the previous value of about 5 kPa to 3.0 kPa, but it rose steadily again with each cycle as is shown in Figure 58. This indicated that immediate entrainment of accumulated dust on the vessel wall was probably not the problem since there had not been enough time to accumulate much dust in the vessel. In subsequent tests designed to prevent the possibility of blowing dust from the element being cleaned directly into the others, the element being cleaned was given a quick pulse followed by flow of clean air to all the other elements. This did not reduce the initial steady pressure drop. The compressors were shut down to eliminate the by-pass flow during cleaning, but this did not help either.

In spite of the relatively clean appearance, the problem was apparently a failure to get the dust out of the element with the pulse being used, and not a problem of reintrainment of collected dust.

At this point it was decided to attempt to get better cleaning by one of two methods. The first attempt was to reduce the length of the dirty corrugations by sawing the cubs in half. It was hypothesized that due to the high aspect ratio there may have been difficulty in forcing all the dirt from one channel out the relatively small triangular opening. The second option to be investigated consisted of administering a pulse directly down the dirty side to sweep the bulk of material out of the filter prior to the clean side pulse. The option to do this had been included in the low flow rig, but since it had proved unnecessary in the small facility no easy continuous way to give the dirty side pulse existed in the original high flow unit design.

The first method was relatively easy to check. This was accomplished by removing all of the elements and sawing them in half, reducing the dirty side channel length from 15 cm to 7.5 cm. After the cubes were cut in half, and the edges re-sealed with ceramic cement,

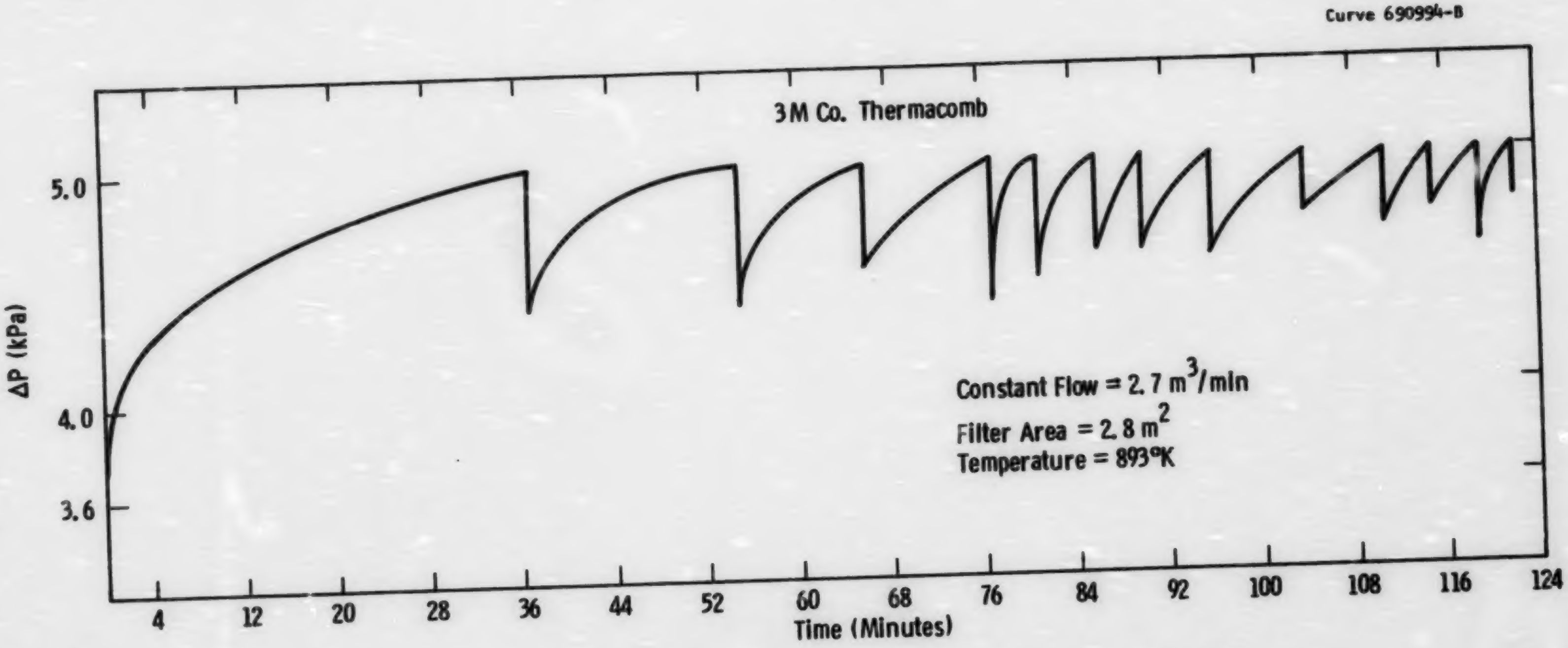

Fig. 66— Hot thermacomb test with cleaning pulse to clean and dirty sides

they were replaced in the support plate and tested at compressor outlet temperature. The initial pressure drop was quite low (about 2.5 kPa at a face velocity of 1.64 m/min) but the initial pressure drop rose rapidly indicating a continued failure to completely clean the Thermacomb material (Figure 59). A subsequent test at a lower face velocity (1.1 m/min) was conducted with similar results. It was noted that when the elements were cut in half, the upper half of the filters were almost completely plugged with dust that had not been removed by the cleaning methods used.

Not having achieved satisfactory results by halving the element length, it was decided to try the concept of administering a dirty side pulse to the smaller elements. This idea was tested by the following sequence:

(1) Load filters with dust
(2) Remove hats
(3) Remove top filter retaining plate and fiber frax
(4) Replace hat
(5) Pulse
(6) Remove hat
(7) Replace filter retaining plate and fiber frax
(8) Replace hat
(9) Continue filtering

This method was used on the initial cleaning cycle of a test run at compressor outlet temperature and a relatively low face velocity of 0.93 m/min. Figure 60 summarizes the result of this run. There were 20 cycles during this test and the cleaning remained adequate as is reflected in the constant initial pressure drop of about 3 kPa. No penetration of dust could be detected throughout this test. Having observed some success in a cold run, it was decided to continue at temperature. The first of three such runs was carried out at 953°K with a face velocity of 1.72 m/min. At these conditions the filter performance was relatively good although a gradual increase in initial pressure drop was observed. The data from this run are shown in

Cu-ve 6900998

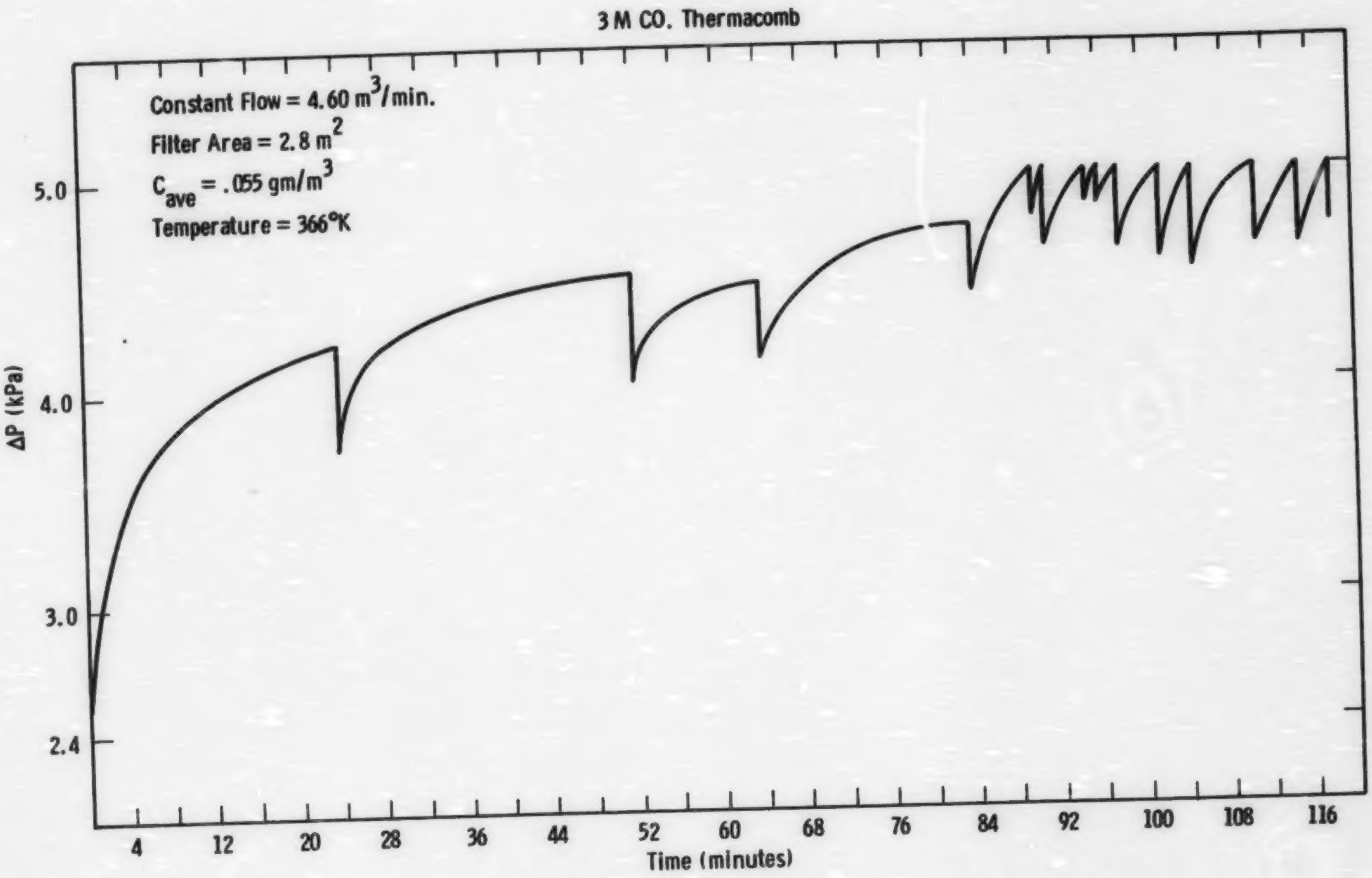

Fig. 59—Initial test with Thermacomb cut in half

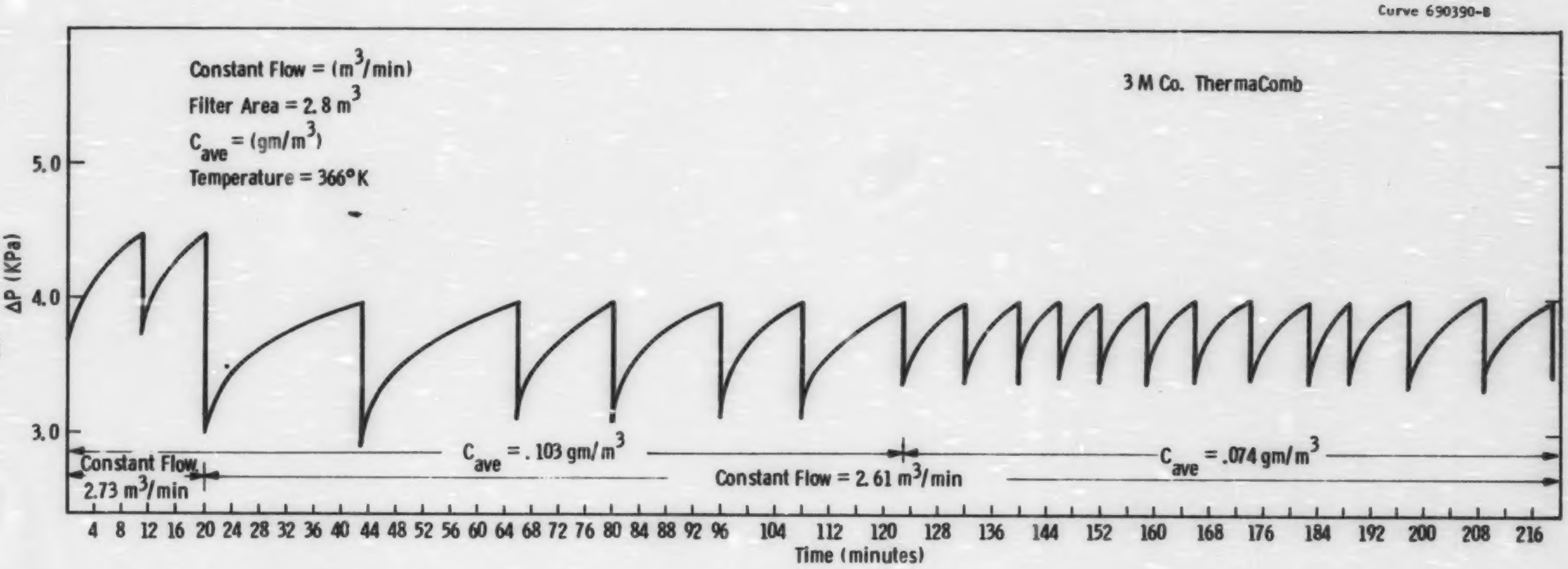

Fig. 60—Manual dirty side pulse test

Figure 61. The subsequent run was merely a continuation of this test to determine if the gradual increase in initial pressure drop would persist. As Figure 62 indicates, it did so a decision was made shut down and repeat the dirty side pulse procedure. Having done this the initial pressure drop returned to the original value of about 7 kPa for a couple of cycles, but the initial pressure drop increased rapidly during subsequent cycles indicating progressive blockage of the filter. These results are shown in Figure 63.

At this time the equipment which allowed repeated pulsing of the dirty and clean sides of the filter was returned from the machine shop. This modified blow back system (Figure 51) was designed for simultaneous pulsing of both the clean and dirty sides of the filter but, by capping off the appropriate line, either side could be pulsed alone or in sequence. The system was checked out during a cold (compressor outlet temperature) run. Mechanically, everything checked out, but the 150 min. test (shown in Figure 64), showed a definite increase in initial pressure drop indicating incomplete cleaning. Since cold tests are always suspect, due to problems with compressor oil in the air, a hot run was conducted next. During this run, the first few cycles started at fairly low pressure drops, but this pressure drop increased rapidly from about 4.5 kPa to 6.2 kPa at a face velocity of 1.38 m/min and 973°K. The pressure drop and cycle time then seemed to level out and remained constant. These data are presented in Figure 65.

These preliminary tests with the modified simultaneous pulse were followed by a series of experiments which were to investigate the options offered by the modified blow back system. These runs were all carried out at the relatively low face velocity of about 1 m/min. Figure 66 shows the "base" case, which is a simultaneous pulsing of both dirty and clean sides. Due to a problem with the outlet sampler no overall efficiency was obtained for this run. It can be seen that a fairly stable cycle has been established after four or five cycles. The following day an identical run was attempted in order to verify

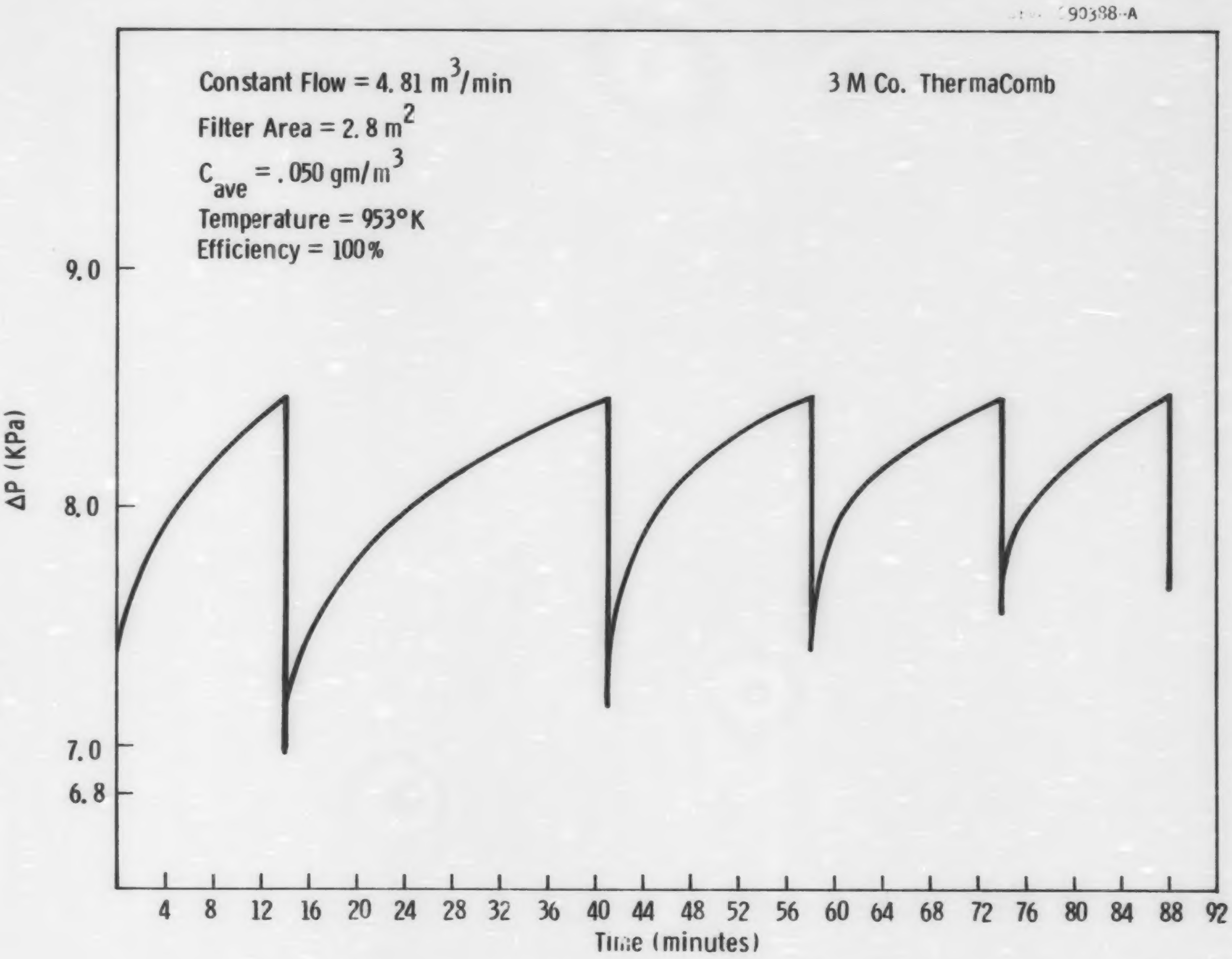

Fig. 61—Hot test with initial dirty side pulse

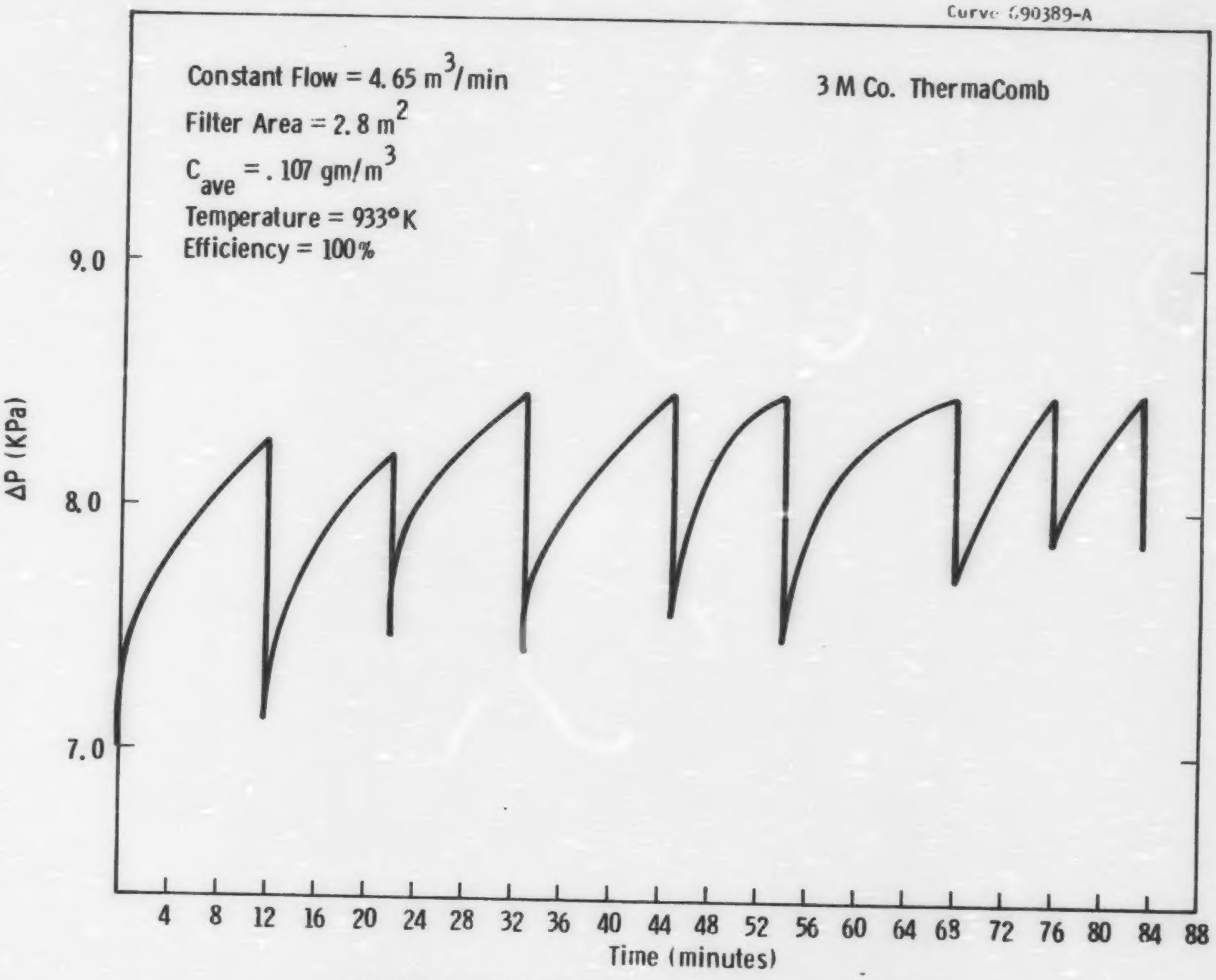

Fig. 62—Hot test with initial dirty side pulsed continued

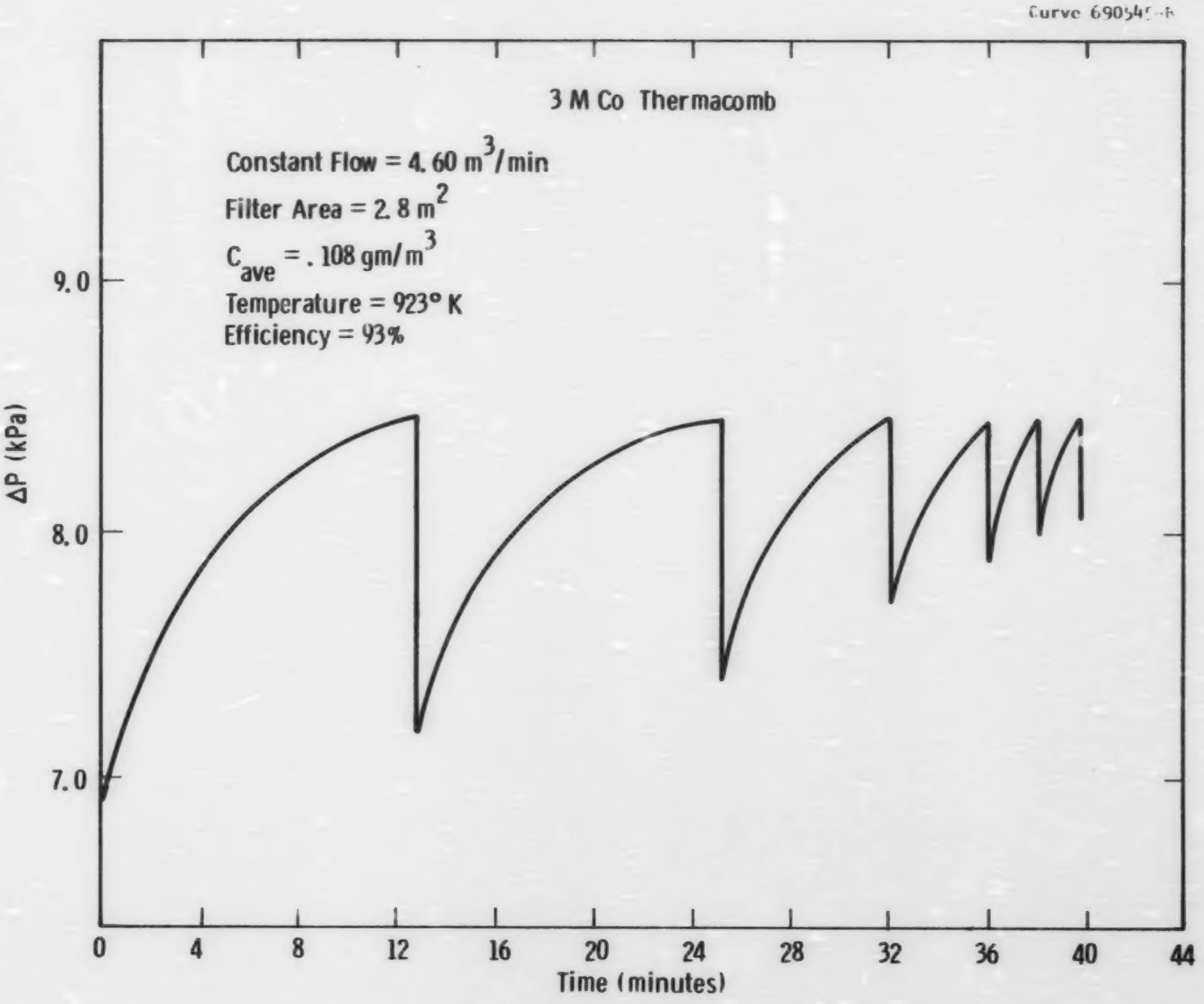

Fig. 63— Hot high flow test after individual dirty and clean pulses

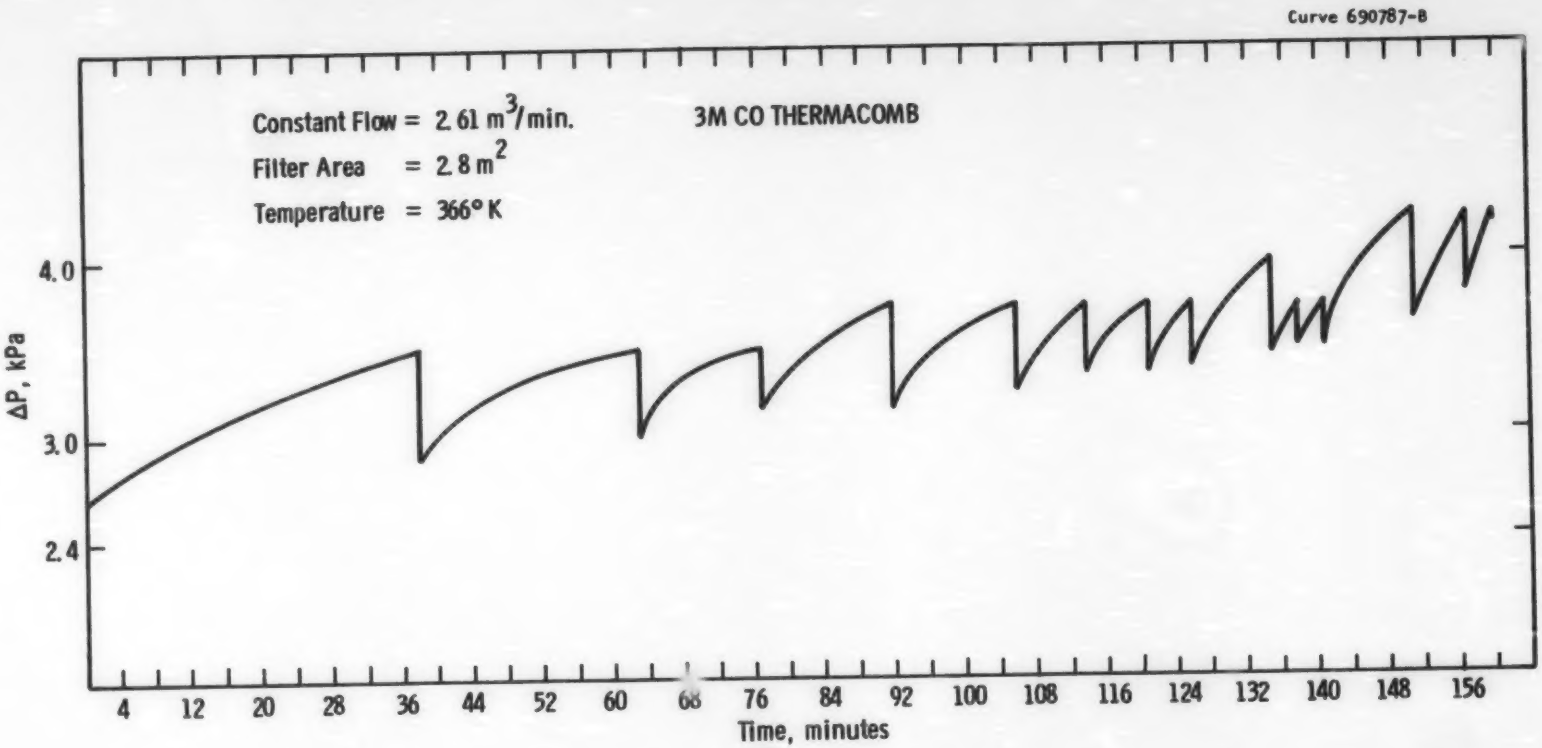

Fig. 64 — Cold test with modified pulse

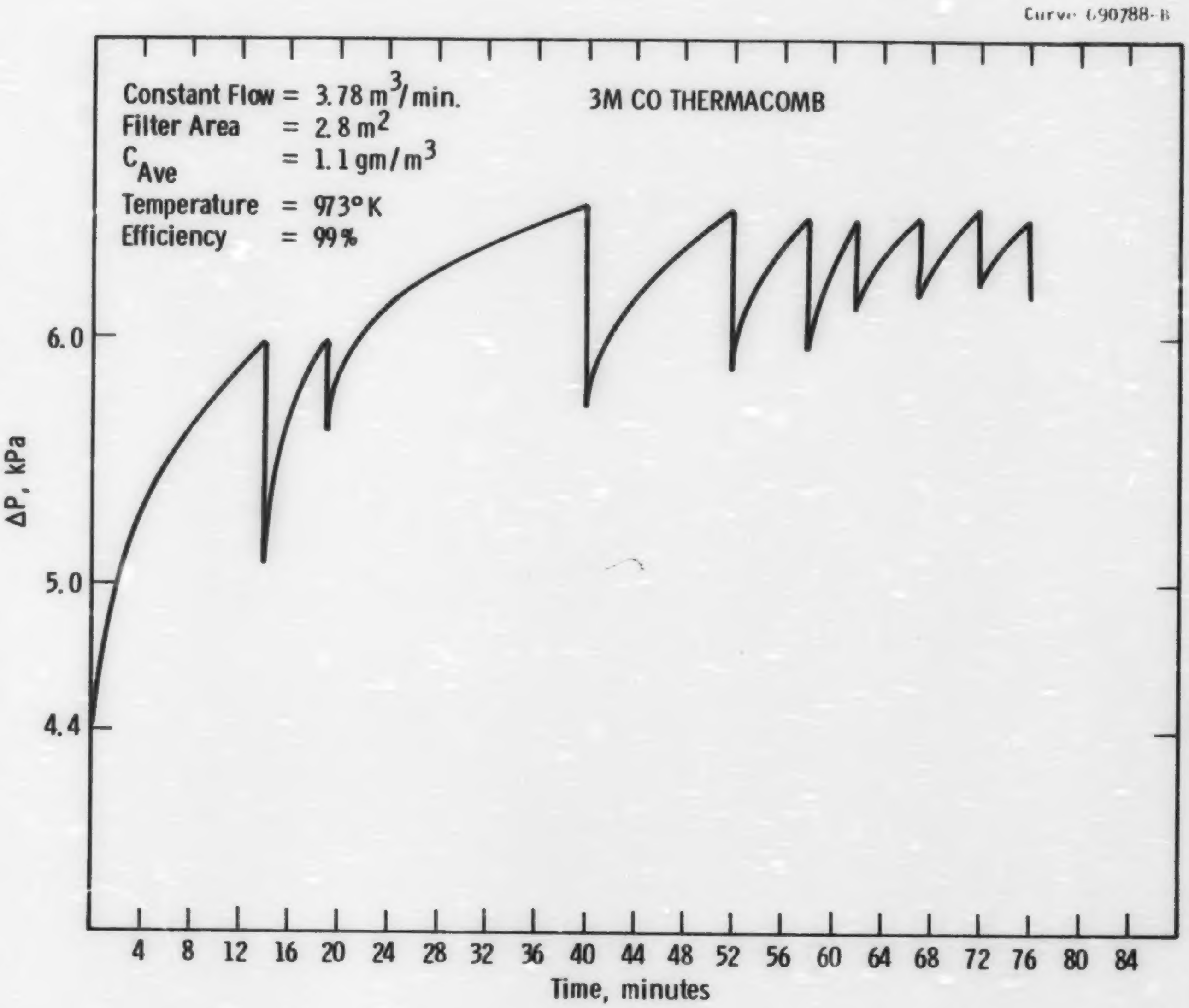

Fig. 65 — Hot test with modified pulse

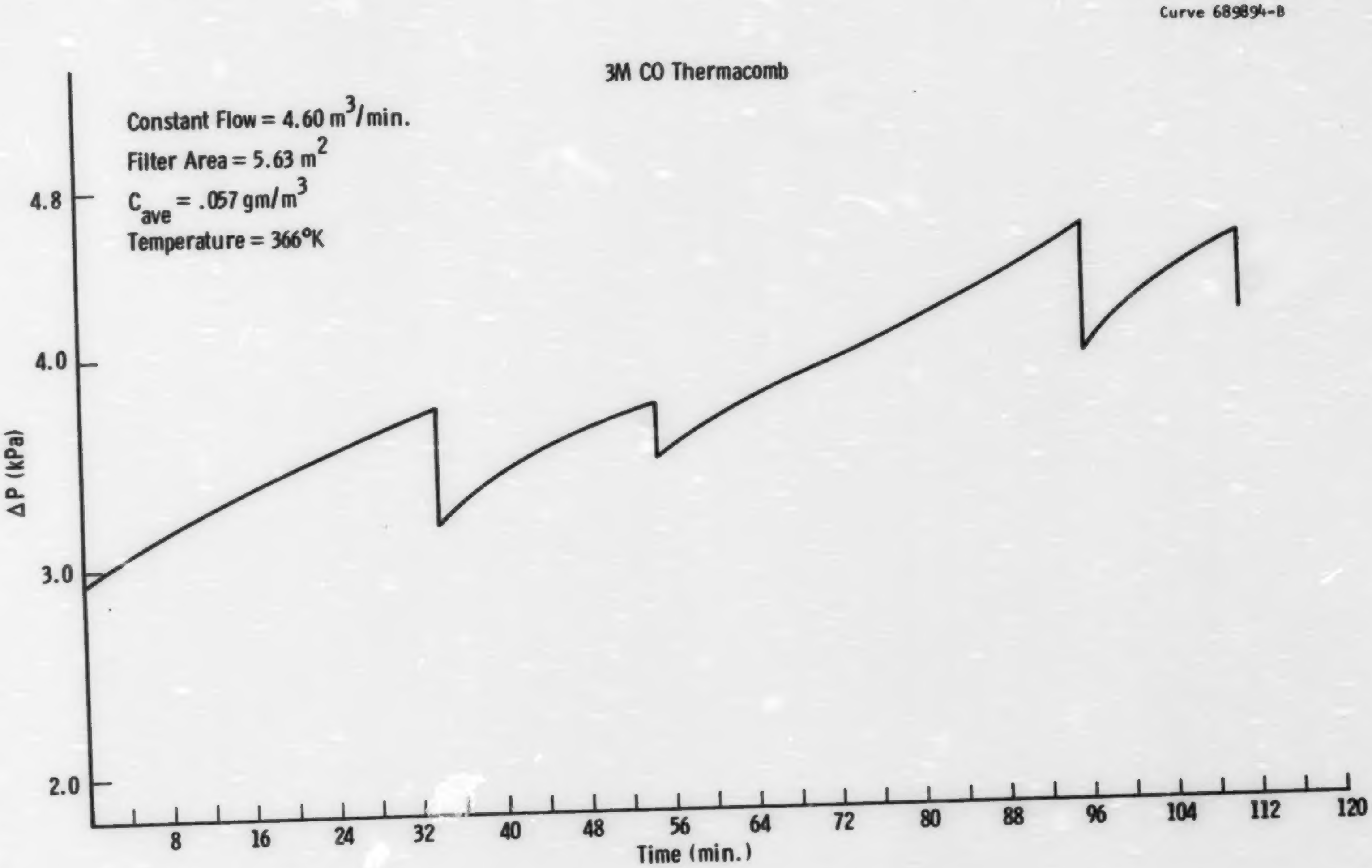

Fig. 58 — Filters and vessel precleaned

the long term stability of the cycle established. During this run a recurrent problem arose with the modified pulse system. Due to unequal thermal expansion in the vertical line supplying the dirty side pulse, and the retaining studs there was a tendency for the filter element to be lifted on one side. When this occurred a leak would result. If it was not anticipated fairly large pieces of the fiber frax gasket could be blown out by the pulse and this would result in large leaks as demonstrated by the data shown in Figure 67. Figure 68 shows the result of a run after the major leak had been repaired. It is not certain how much of the penetration measured was due to contamination of the clean side of the vessel and piping by the previous run. After an initial operating period of about 45 min. an apparently stable cycle had been established with the initial pressure drop at about 7 kPa and rising to 7.5 kPa over a 20 min. period. The next two runs were conducted to establish what effect variations from the combined side pulse would have. Figure 69 shows a test in which a stable or slightly increasing pressure drop cycle was established using the standard combined pulse. At the point labeled 1 a standard combined pulse was immediately followed by a pulse that was forced entirely down the dirty side. This additional pulse recovered a full 0.4 kPa in pressure drop, lowering the initial pressure drop to a point below all but the first cycle. During the next cycle a combined pulse returned the pressure drop from 7.5 kPa to only about 7.0 kPa, but when this was followed by a pulse directed entirely down the clean side the pressure drop returned to its previous low value of about 6.2 kPa. A subsequent test was performed to examine this phenomena and the results are presented in Figure 70. As is indicated by these data, a repeatable decrease in initial pressure drop can be realized by virtually any combination of the combined, clean or dirty pulse options. A stable cycle between pressure drops 6.5 and 7.5 kPa was maintained throughout the test with no evidence of the usual gradual blocking of the filter.

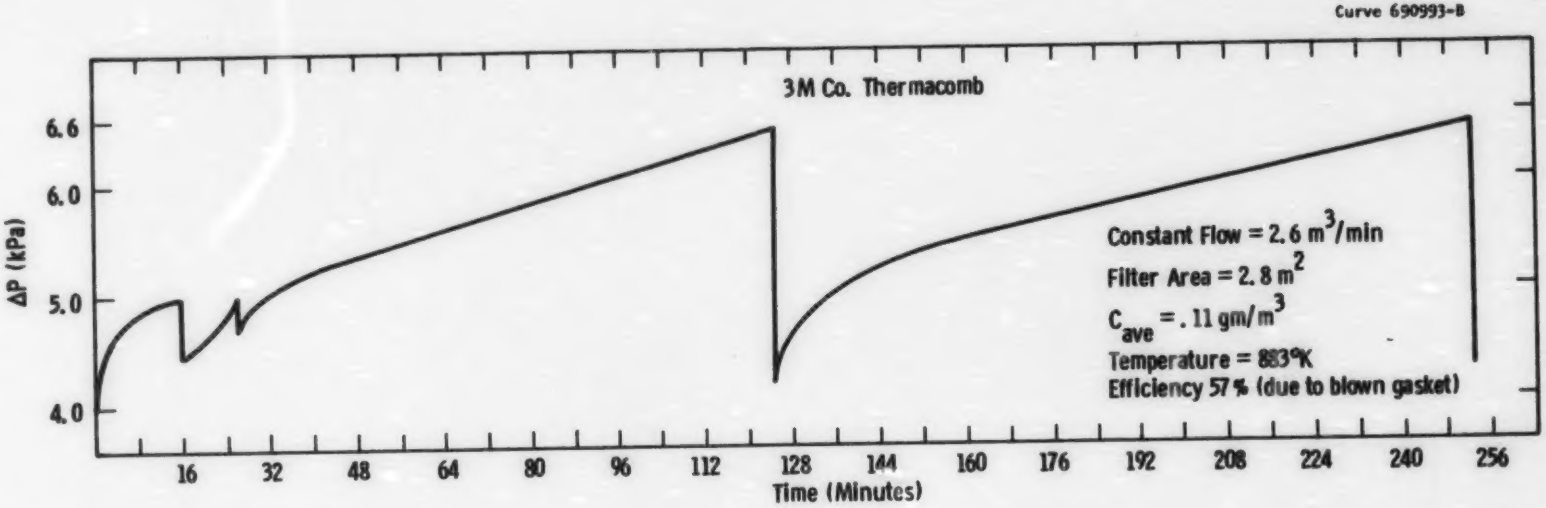

Fig. 67 – Hot thermacomb test with cleaning pulse to clean and dirty sides

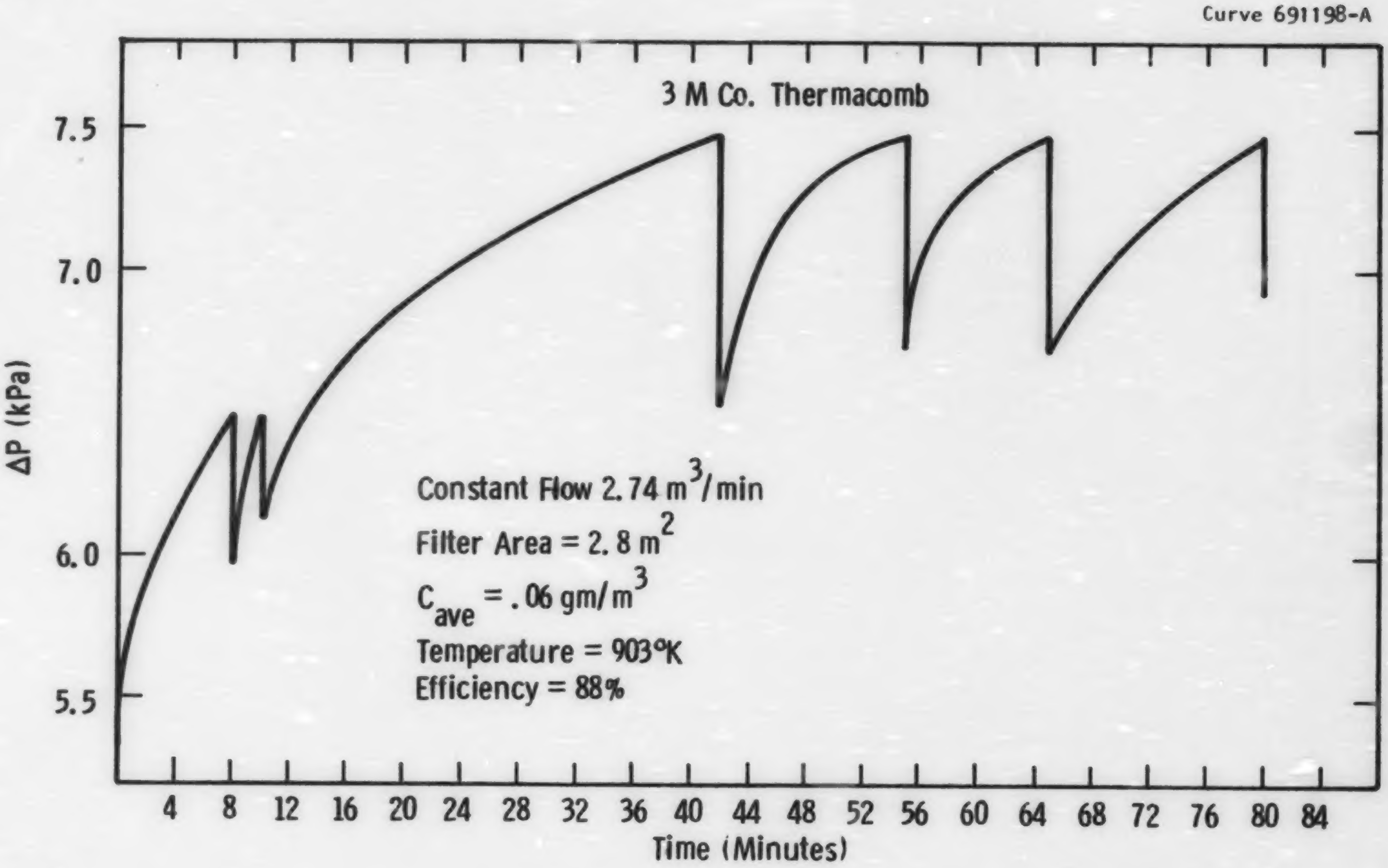

Fig. 68 — Hot thermacomb test with combined pulse

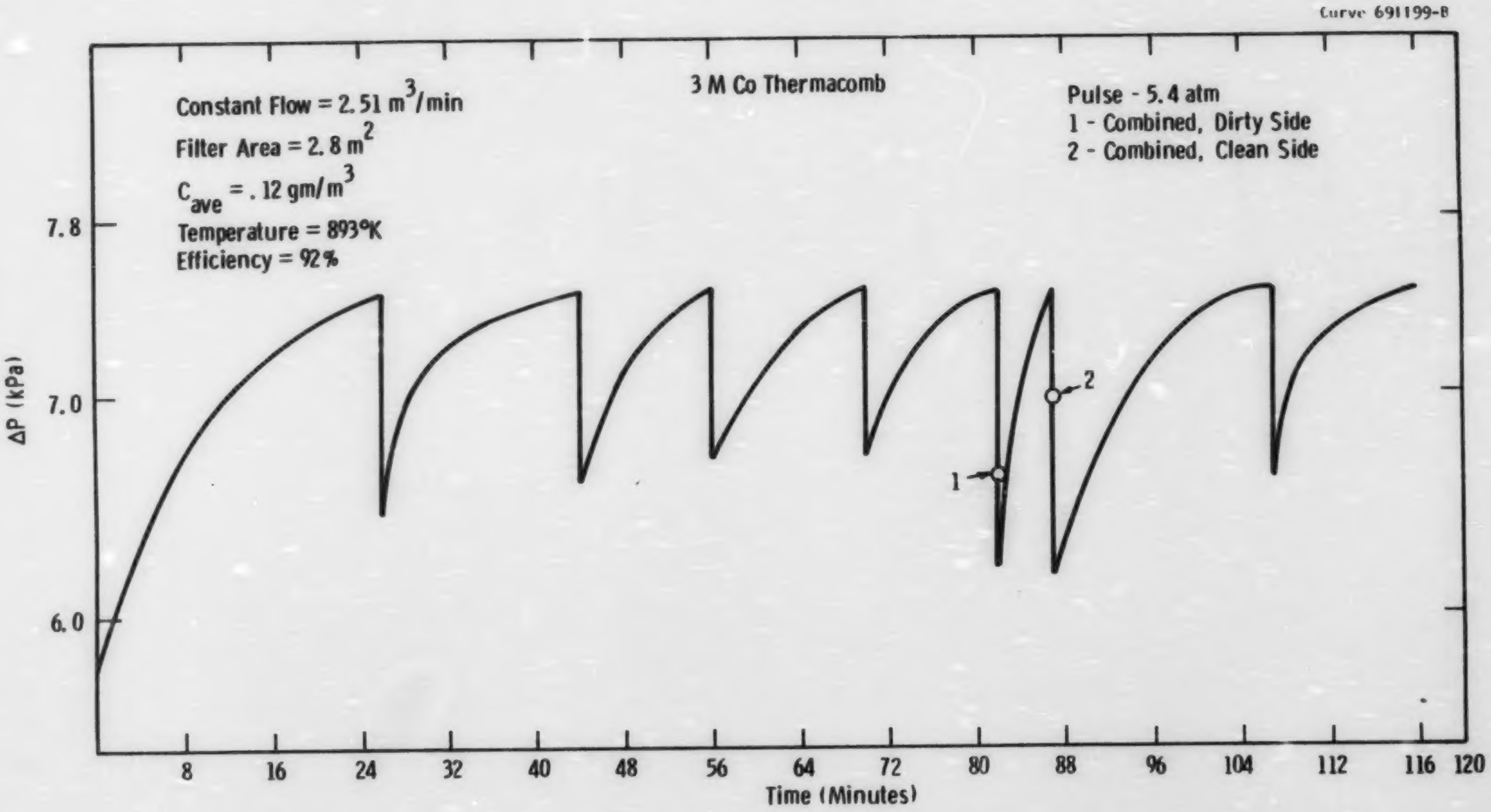

Fig. 69 — Hot thermacomb test with pulse variations

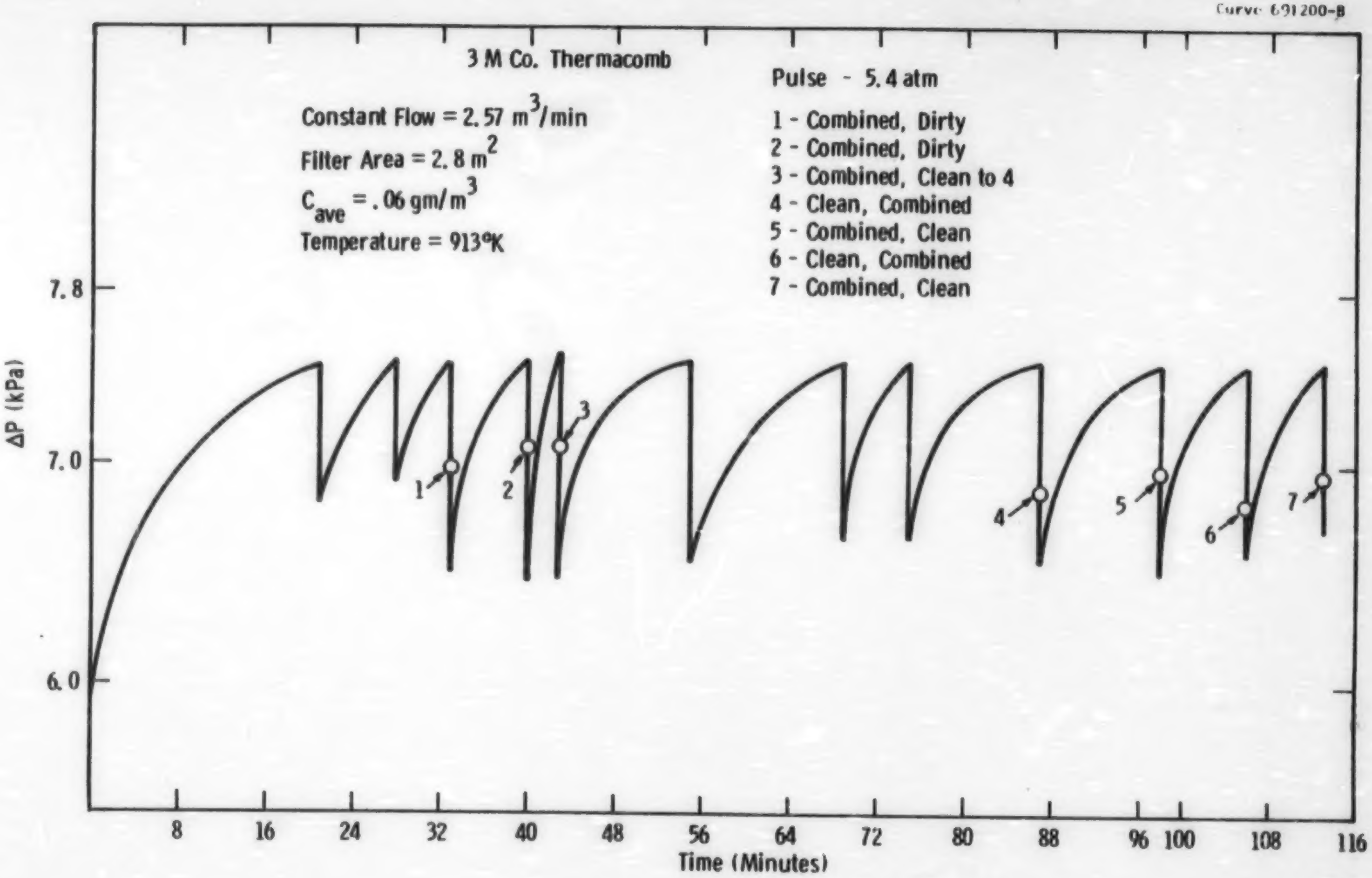

Fig. 70 — Hot thermacomb test with pulse variation

A final test on the high flow unit with the 3M Thermacomb was performed using only a clean side pulse initially. At a face velocity of 0.96 m/min the cycle was somewhat irregular and appeared to be climbing. On the tenth cycle the clean side pulse was followed by a combination pulse to both sides. As is indicated in Figure 71, this reduced the pressure drop as had been observed in previous tests. A continuation of this test was prevented by a complete failure in one of the element's seals which resulted in gross leakage.

Very late in the program 7 cubes of the W. R. Grace & Company material were obtained. There was only time to install them and perform preliminary tests on them using the original clean side pulse only on the full 15 cm thick elements. The results of the three runs accomplished are summarized in Figures 72 and 73. It can be seen from these data that there was a very gradual increase in the initial pressure drop over the test period, however, it is believed that a combination of pulses would be at least as effective in preventing residual pressure drop buildup in this material as it was for the Thermacomb.

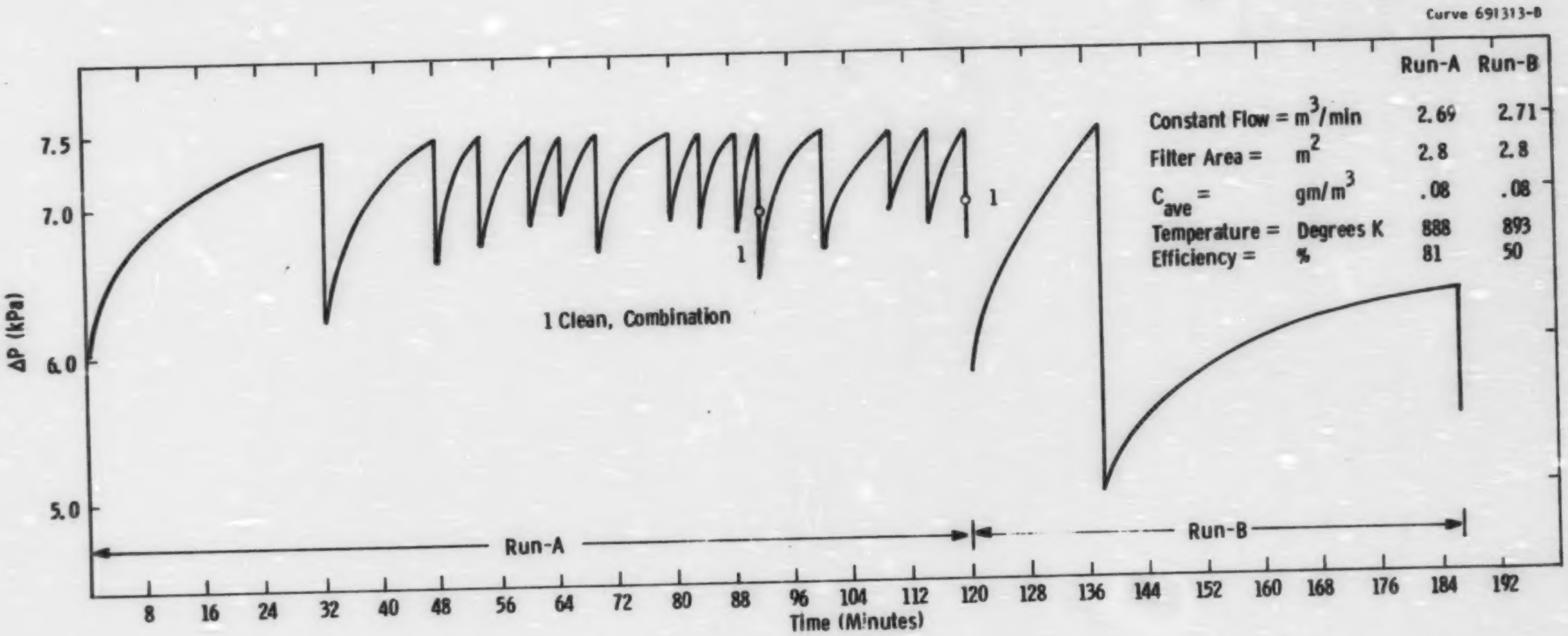

Fig. 71—Final hot test with thermacomb

Curve 691311-8

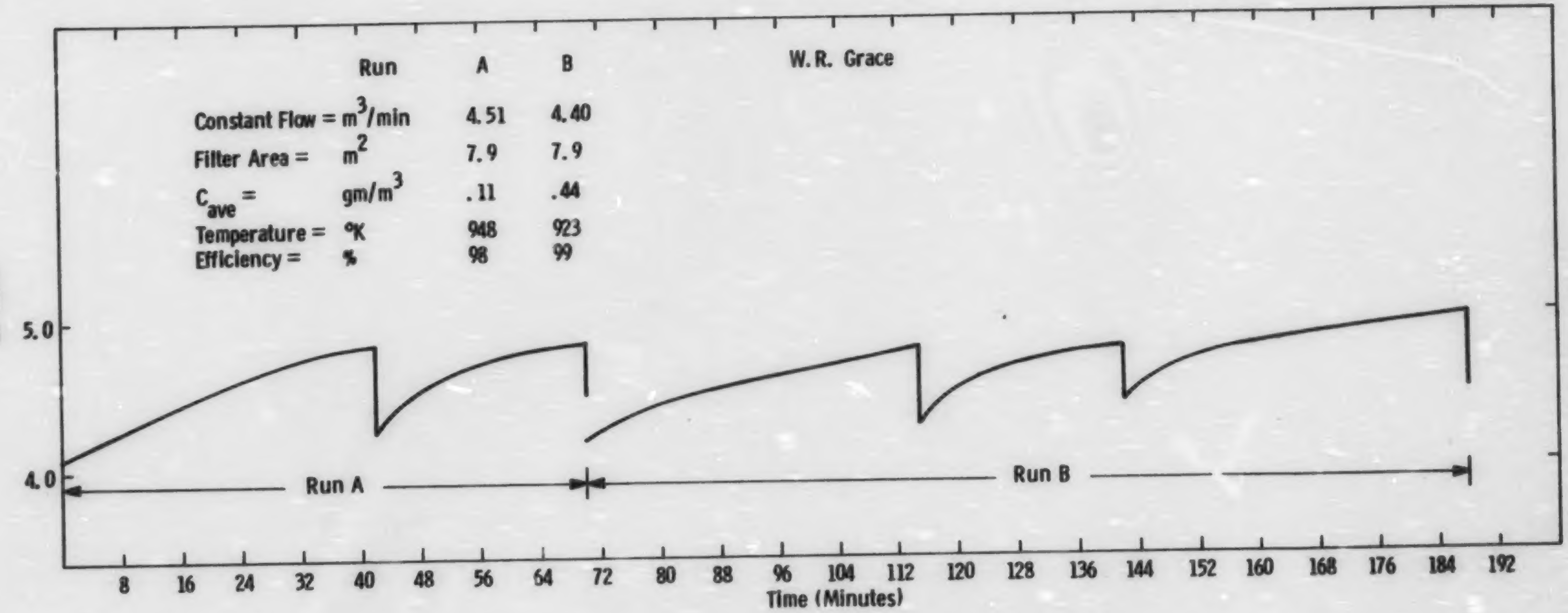

Fig. 72—Initial hot test with 15 cm cube of W. R. Grace material

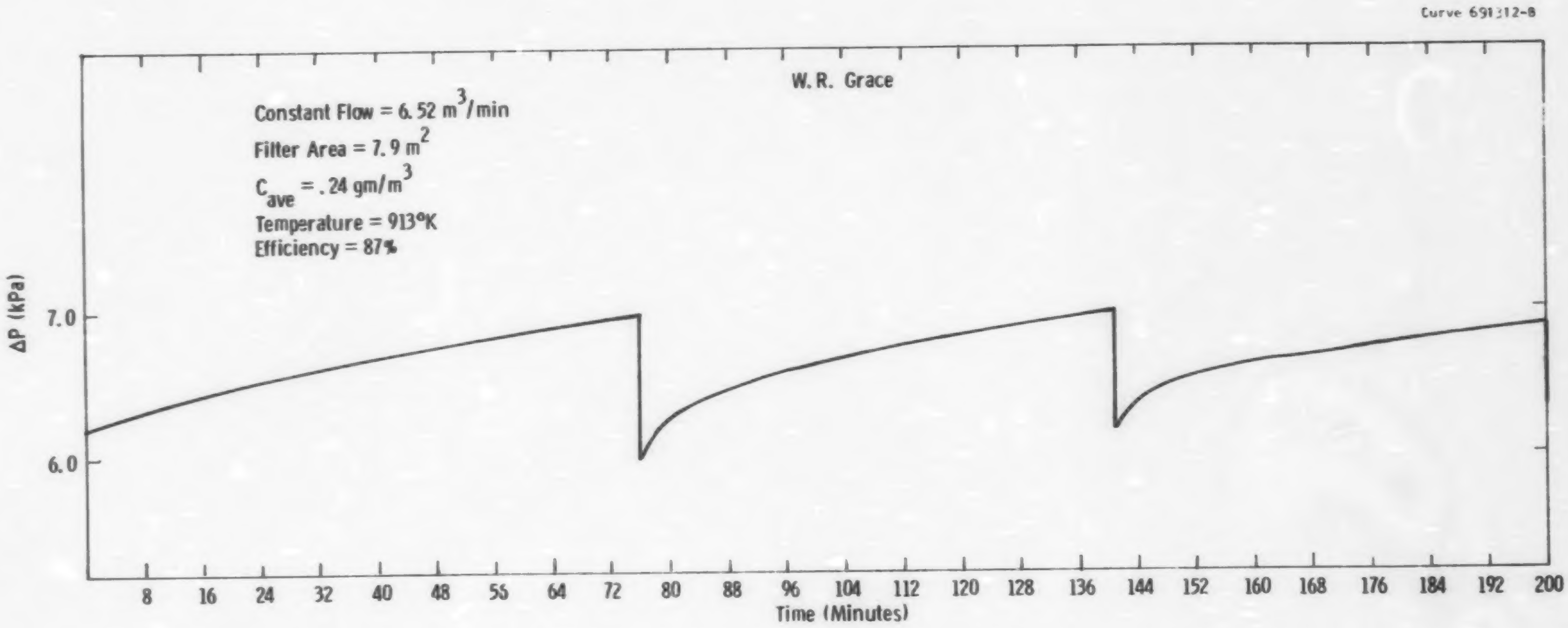

Fig. 73—Hot test with 15 cm cube of W. R. Grace material

4.7 COMMERCIAL AND ECONOMIC ASSESSMENT

Objectives. One of the major objectives of this task was to use the experimental data available from the high and low flow tests to estimate operating parameters for a commercial application. This data on face velocity, pressure drop, physical dimensions of filter elements, efficiency and cleaning requirements would be used to generate a conceptual design of a module of ceramic filter apparatus suitable for large scale application. Finally, this conceptual design was to be costed out and compared with other high temperature fine particulate removal devices.

Discussion. It has become apparent that the experimental work with the high and low test units have not advanced to the stage where all of the operating parameters necessary for a commercial design are at hand. This is especially true with respect to filter element fabrication alternatives and cleaning technique. Other problems such as the nature of the ash in actual use have not been addressed. Recent experiments with granular bed filters at the Exxon mini plant(4) have shown that this can be an important consideration. In spite of uncertainties, it is possible to proceed with at least a rough conceptual design, with current estimates of performance.

The basis for this design was taken to be a 150 MWe low BTU coal gasification plant. The coal gasification application was chosen since it is generally considered a more difficult task to clean hot, reducing fuel gases than cleaning hot flue gas from application such as a pressurized fluidized bed combustion. The size chosen is large enough to be representative of a commercial unit, as most equipment for a larger facility would be composed of modules, and data for the 150 MWe plant were available. The important plant parameters are summarized as follows:

Plant Size	150 MWe
Temperature	870°C
Pressure	10 atm
Flow	1900 actual m^3/min

Dust to Last Stage	
Loading	0.5 gm/m^3
Size	100% < 10μ

Using these inputs, the ceramic filter module shown in Figure 74 has been offered as a rough conceptual design for a commercial scale application.

Operation of the unit is as follows: The dirty gas enters the four modules at the bottom of the pressure vessel through the inlet manifold. The dust laden gas then flows up into the square enclosures that support the filter elements and out through the filter elements into the blow back enclosure, and out the cleaned gas manifold. Periodically, as the pressure drop across a module rises, the module is isolated from the outlet manifold by a slide valve. A pulse of cleaned gas is then introduced on the clean side of the filter elements knocking the accumulated dust out of the elements and down into the hopper where it is periodically lock hoppered out of the system. It is anticipated that one module can be cleaned while the other three modules remain in the filtering mode. Assumptions that have been made regarding the filter elements and their performance are:

Face Velocity	1-1.5 m/min
Max. Filter Thickness	15 cm
Overall Efficiency	99+ %
Pressure Drop	5-10 kPa
Cleaning Cycle Time	60-90 min.
Cleaning Pulse Gas Requirement	0.2 kg/min @ 12 atm

The estimate for face velocity is based on the latest data from the hot, high flow unit where the most stable operation was achieved at similar velocities. Earlier operation with the low flow unit has indicated that good performance can be achieved at velocities 3 or 4 times the 1-1.5 m/min range, however, to be conservative the lower range has been used in sizing the unit. The assumption of a maximum filter element thickness of 15 cm is based on the increase in cleaning

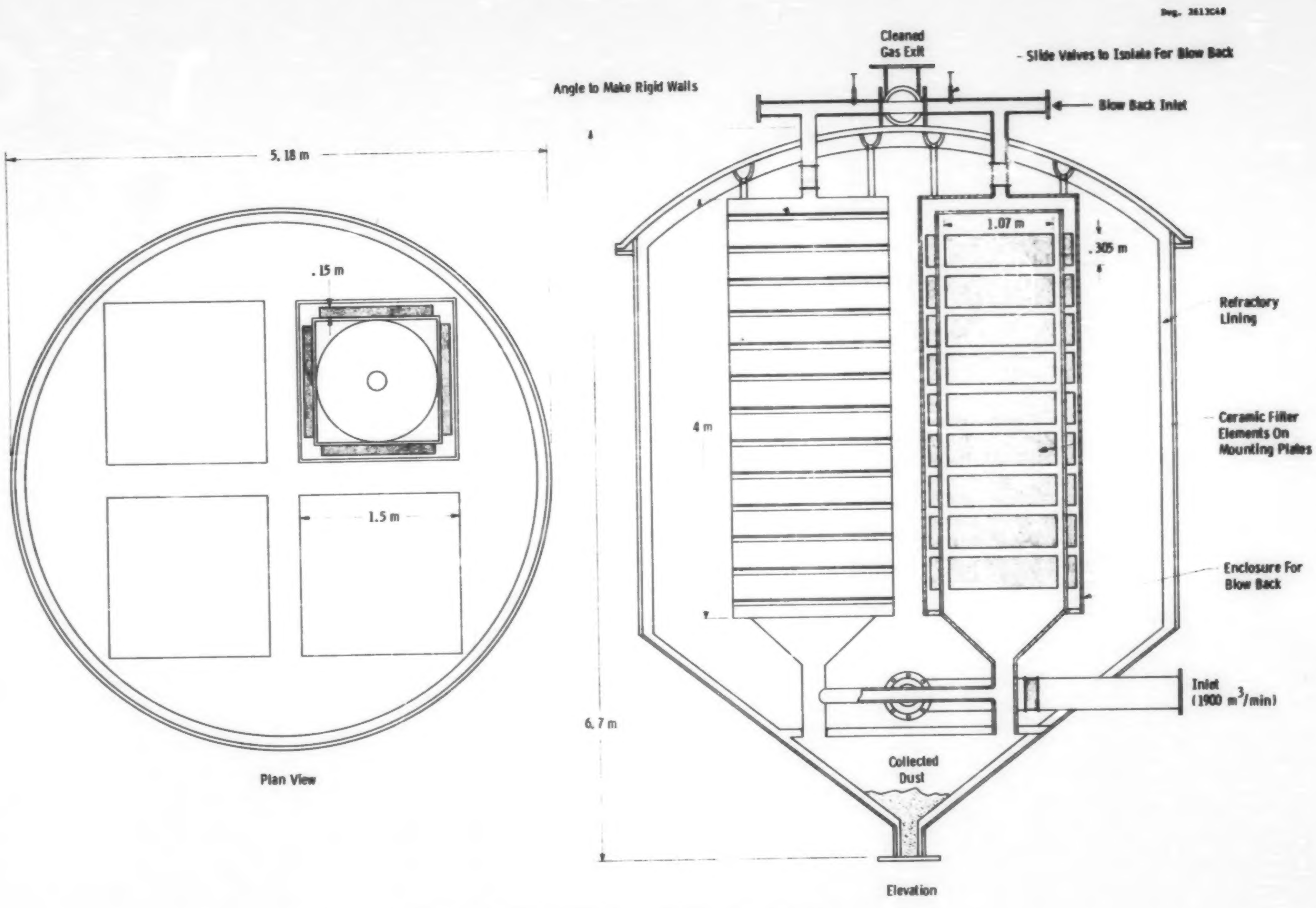
Dwg. 2613C48
Cleaned Gas Exit
- Slide Valves to Isolate For Blow Back
Angle to Make Rigid Walls
Blow Back Inlet
5, 18 m
.15 m
1.5 m
Plan View
1.07 m
.305 m
Refractory Lining
4 m
Ceramic Filter Elements On Mounting Plates
Enclosure For Blow Back
Inlet (1900 m³/min)
6, 7 m
Collected Dust
Elevation

Fig. 74 – Sketch of possible arrangement for commercial use of ceramic filters

problems observed in going from the low flow unit to the high flow unit. Improved corrugation sizing and filter porosity along with better pulsing techniques should increase this maximum thickness. The estimate of overall efficiency and pressure drop are based on experimental observations from both high and low flow tests. The estimate of cleaning cycle time depends on the expected concentration of dust to the filter. It has been assumed that two stages of mechanical collectors have reduced the projected loading from the bed of about 35 gm/m^3 to 0.5 gm/m^3 at the filter with only the sub 10μ fraction remaining. The cleaning cycle time data varied a great deal between the high and low flow units. The high flow unit had typical cycle times of 10-20 min. with loadings of about 0.1 gm/m^3 and face velocity of 1-2 m/min, but the low flow unit had similar cycle times with loading of 2-5 gm/m^3 and velocities of 2.4 m/min. The low flow unit typically operated between 2 and 5 kPa while operation with the high flow unit was usually in the 6-9 kPa range. These observations may be explained by assuming that some of the high flow filter channels were not cleaned and were unavilable filter area. For estimation of the cycle time, it has been assumed that the filter performance will be similar to the low flow unit. Using a 10 min. cycle with 2 gm/m^3 loading at a face velocity of 2 m/min would lead to an estimate of a 40 min. cycle time for the commercial application. If the other end of the range is used, 20 min. cycle, 5 gm/m^3 and 4 m/min, a cycle time of 400 min. is obtained. The cycle time chosen (60-90 min.) corresponds to a conservative estimate. The cleaned gas requirement for pulsing the filters was scaled up to maintain the same ratio of flow to filter area.

The vessel size is on the order of 6.7 m tall and 5.18 m diameter with an elipsoidal head, 3 m straight sides and a hemispherical bottom rather than the conical shape indicated in the sketch. Metal thickness for the head and sides would be about 5 cm and the bottom would be about one-half this. This vessel would also require about 15 cm of refractory lining in order to maintain suitable metal temperatures.

The valves required for the pulsing sequence do not need to be tight seal valves since they are only required to direct most of the pulse to the intended module. The valves should not, therefore, be a high cost item. The filter element modules are shown in a square configuration to minimize filter element mounting and sealing problems. It may be feasible and desirable to consider cylindrical mounting structures in the future. A major cost item in the ceramic filter system is the mounting plate-pulse containment structure. Anticipating possible corrosion problems in the reducing fuel gas atmosphere it was assumed that the material chosen for these support plates will have to be something like Haynes 188, which makes these components very costly. For oxidizing atmospheres, such as for fluidized bed combustion, the cost of this material will be substantially less.

The device chosen to compare the performance and cost with is a granular bed filter since this is about the only other high temperature fine particle device currently available. Ducon has done considerable development work with granular bed filters and is currently testing a device for pressurized fluidized bed combustion application. Since some data on the cost of elements for the Ducon filter are available, this particular device has been chosen for comparison with the ceramic filter.

The process assumptions used in the ceramic filter system were enumerated previously, while those assumed for the granular bed filter system are described below:

Filter Type	Ducon cylindrical
Face Velocity	15.24 m/min
Elements/Unit Plan Area	4 elements/m^2
Overall Efficiency	98+ %
Pressure Drop	20-35 kPa

In this estimate it has been assumed that the maximum pressure vessel diameter that is practical is about 7.5 m diameter. If more plan area is required multiple modular units would be constructed.

On the basis of these assumptions the granular bed filter system would be composed of two modules, each handling about 950 m^3/min of low Btu fuel gas from the 150 MWe coal gasification plant. Each module would be a 7.6 m diameter refractory lined pressure vessel with an ellipsoidal head and hemispherical bottom and a 3.05 m straight section. Each vessel would house about 170 elements fabricated from Haynes 188.

Since the Ducon granular bed filter is in a much more advanced stage of development, it is likely that this device could be costed out in greater detail than the proposed ceramic filter system, however, as the ECAS study(5) has shown wide variations in the estimated cost of this equipment exist. The approach taken here has been to estimate the costs of the major components of each system using a consistent basis.

Since the systems have several similar features, which have been costed at the same degree of detail, the results should be comparable if not correct on an absolute basis. The results given will be adequate as order of magnitude equipment costs and more accurate as relative costs.

The results of the cost comparison are presented in Table 19. Pressure vessel costs have been estimated using a factor of 4.63$/kg for large field erected vessels. Scrap and nozzles were estimated at 10%. Refractory lining costs were based on suppliers previous quotes on similar applications. The Ducon filter element cost was based on an estimate of 400$/element for production quantities. This estimate from Ducon was based on stainless steel construction and has been scaled up to 1400$/element to reflect the additional materials and labor costs associated with using Haynes 188 at 17.62$/kg. The ceramic filter element costs are small as estimated by the 3M Company at 3531$/$m^3$. However, the materials costs for the retaining plate and blow back enclosure are large since it has been assumed that these would have to be fabricated from a material like Haynes 188. The valving and blow back equipment for the systems represent a relatively small portion of the total cost of the equipment. It has been assumed that high pressure steam will be used for the granular bed filter blow back system rather than cleaned fuel gas. The ceramic filter system has assumed that the cleaning gas will be taken from the filter exit stream and compressed from 10 to 12 atm and held in a 7.25 m^3 vessel for pulsing.

These estimates indicate that the granular bed filter could cost about three times as much as the ceramic filter system. The largest cost in the granular bed filter system arises from pressure vessel construction. It may be feasible to crowd the elements into tighter spacing and to run them at higher face velocities and reduce the cost of the pressure vessel. Because the ceramic filter system has a high surface to volume ratio the containment vessel costs are relatively lower. The cost of the high alloy retaining plates and pulse containment for the ceramic filter system would be reduced substantially if more conventional materials of construction could be used. This could be an important consideration in using the ceramic filter system in an oxidizing atmosphere such as one encounters in fluidized bed combustion. In these cases the amount of gas to be cleaned per unit mass of coal burned increases by a factor of about 3 over gasification, but more conventional materials can be used for the retainer, so the costs of this stage of particulate removal equipment will not increase in proportion to the gas flow.

On the basis of this admittedly crude cost comparison it appears that the ceramic filter system is worthy further examination.

Table 20

Ceramic Filter and Granular Bed Filter Costs

	Granular Bed Filter	Ceramic Filter
Pressure Vessel(s)		
Steel costs	867,514	162,171
Refractory lining	124,404	33,561
Filter Element	470,400	25,200
Retainer	--	247,849
Back Flush Equipment		
Valves	45,000	40,000
Piping	15,000	15,000
Installation	20,000	5,000
Booster compressor	--	8,880
Pulse holding tank	--	23,007
	$1,542,318	$560,668

REFERENCES

1. T. R. Wilshaw, J. Am. Cer. Soc., 51, (1968), p. 111.

2. Poe, G. G., R. M. Evans, W. S. Bonnett, and L. R. Waterland, "Evaluation of Ceramic Membrane Filters as a Control for Fine Particulate," Final Report, EPA Contract 68-02-1313.

3. Ciliberti, D. F. and B. W. Lancaster, Modified "Harvard" Dry Dust Disperser, Rev. Sci. Instrum., Vol. 46, No. 7, July 1975.

4. Bertrand, R. R., et al., "A Regenerative Limestone Process for Fluidized Bed Coal Combustion and Desulfurization," Monthly Reports 80-88, EPA Contract 68-02-1312.

5. Beecher, D. T., et al., "Energy Conversion Alternatives Studies," Westinghouse Phase II Final Report Prepared for NASA Lewis Research Center, Contract NAS 3-19407 (1976).